The Institute of Paper Chemistry

Appleton, Wisconsin

Doctor's Dissertation

Mechanisms of Alkaline Glycosidic Bond Cleavage in 1,5-Anhydro-4-O-β-Mannopyranosyl-D-Mannitol

Margaret Esther Henderson

June, 1986

MECHANISMS OF ALKALINE GLYCOSIDIC BOND CLEAVAGE IN 1,5-ANHYDRO-4-O-β-MANNOPYRANOSYL-D-MANNITOL

A thesis submitted by

Margaret Esther Henderson

B.A. (Chemistry) 1980, Smith College

M.S. 1982, Lawrence University

in partial fulfillment of the requirements
of The Institute of Paper Chemistry
for the degree of Doctor of Philosophy
from Lawrence University,
Appleton, Wisconsin

June, 1986

TABLE OF CONTENTS

SUMMARY

To further investigate reaction mechanisms which could be responsible for glycosidic bond cleavage in cellulose model compounds and cellulose under alkaline pulping conditions, the degradation of 1,5-anhydro-4-O-β-mannopyranosyl-D-mannitol (1,5-anhydromannobiitol) was studied.

Degradation of 1,5-anhydromannobiitol in liquors enriched with ^{18}O showed that, depending on the reaction conditions, 70-85% of the cleavage occurred at the glycosyl-oxygen bond while the remaining 15-30% took place at the oxygen-aglycon bond. Two products, 1,5-anhydro-D-mannitol (70-82%) and 1,5-anhydro-D-iditol (0-8%), were found. A series of ^{18}O-incorporation studies showed that 3-5% of the 1,5-anhydro-D-mannitol and 100% of the 1,5-anhydro-D-iditol came from the cleavage of the oxygen-aglycon bond. Depending on the reaction conditions, 0-30% (molar basis) of the aglycon failed to form detectable products.

Kinetic studies of 1,5-anhydromannobiitol were conducted at a variety of temperatures, hydroxide concentrations, and ionic strengths. Apparent thermodynamic functions of activation were calculated from the temperature series. The glycosyl-oxygen bond cleavage had enthalpy and entropy values of 35.3 kcal/mole and -4.3 cal/mole-°K, respectively. The enthalpy value for the oxygen-aglycon bond cleavage was 39.7 ± 8 kcal/mole, and the entropy was +3.28 ± 2 cal/mole-°K.

Neither glycosyl-oxygen nor oxygen-aglycon cleavage was accelerated by the addition of hydrosulfide ion (SH^-), which has been shown to be a stronger nucleophile than hydroxide (OH^-) at 170°C. A fivefold increase in the ionic strength of the medium caused an 11% increase in the rate of glycosyl-oxygen bond cleavage and an 82% increase in the rate of oxygen-aglycon bond cleavage. Varying the hydroxide concentration while holding the ionic strength constant

showed that both bond cleavages exhibit a strong positive dependence on hydroxide concentration. Methylating the hydroxyl groups in 1,5-anhydro-4-O-β-manno-pyranosyl-D-mannitol totally stopped cleavage at the glycosyl-oxygen bond and reduced the rate of oxygen-aglycon bond cleavage by a factor of 17.

The above results suggest that the glycosyl-oxygen bond is cleaved primarily by a neighboring group-type mechanism in which the conjugate base of OH-2 attacks at C-1 and displaces the ring oxygen [S_N1cB(2')-ro]. Some S_N1-type reaction may be occurring simultaneously. The oxygen-aglycon bond appears to cleave via a mixed S_N1cB(3)/S_N1 mechanism.

INTRODUCTION

ORIGIN OF THE PROBLEM

High temperature alkaline pulping processes, widely used in the papermaking industry, degrade cellulose and other wood polysaccharides at the same time they remove lignin. Up to 10% of the cellulose and 40-70% of the hemicelluloses are lost.[1,2] The degree of polymerization of the cellulose can be decreased by a factor of 3 or more,[1,3,4] resulting in lower pulp viscosity. Because carbohydrate degradation decreases pulp yield and viscosity and hence has negative economic consequences for the pulp and paper industry, it has been studied extensively.

Two major mechanisms of carbohydrate degradation have been identified; glycosidic bond cleavage and peeling. Peeling is the stepwise removal of sugar units from the reducing end of a polysaccharide chain. It occurs at low temperatures and is thought to be responsible for a significant proportion of the yield losses, particularly those which occur during the heat-up portion of the cook. Peeling can be terminated by either chemical or physical stopping reactions. In chemical stopping, the reducing end group rearranges to form an alkali stable group.[5] In physical stopping, the polymer chain peels until the reducing end group reaches the edge of a crystallite and becomes physically inaccessible to the hydroxide ions.[6] Thus peeling does not continue unchecked throughout the whole pulping time. Peeling has been reviewed by several authors.[7-10]

In contrast, glycosidic bond cleavage results in scission of the cellulose or hemicellulose chain at any glycosidic linkage along its length. This type of degradation is generally thought to require temperatures above 140°C and is

primarily responsible for the losses in pulp viscosity.[4,11] Each chain cleavage also creates a new reducing end from which peeling can begin. It has been estimated that another 40-65 glucose units peel from each new site before a stopping reaction occurs.[12] Therefore chain cleavage can also contribute to yield loss.

In order to minimize or eliminate chain cleavage in existing pulping systems or to design better new pulping systems, a basic mechanistic understanding of the reactions of chain cleavage is necessary. Many studies have been directed toward this goal. Comprehensive reviews of these studies have recently been published.[9,11,13,14] Therefore, only the most pertinent ones will be briefly discussed here.

BACKGROUND

Investigating the mechanisms of alkaline glycosidic bond cleavage in cellulose itself is complicated by the simultaneous occurrence of peeling, the presence of physical effects, and the multitude of possible reaction sites and products. Most studies have therefore used model compounds to investigate the mechanisms of glycosidic bond cleavage.

Alkaline Degradation of Aryl Glycosides

Studies of aryl glycosides have shown that, in general, those having a free hydroxyl group on C-2 which is trans to the glycosidic bond react much faster than those whose C-2 hydroxyl group is either cis to the glycosidic bond or blocked by a derivative.[15-17] In addition, glycosides having this trans-1,2 configuration and a hydroxymethyl group at C-5 cis to the glycosidic bond produce the corresponding 1,6-anhydride in most cases.[15] These observations led McCloskey and Coleman[18] to propose that aryl glycosides degrade via an $S_N1cB(2)$*

*Unimolecular nucleophilic substitution with neighboring group assistance from the conjugate base of OH-2.

mechanism, as shown in Fig. 1. In this mechanism, the compound must assume a conformation such that the C-1 and C-2 substituents are antiperiplanar. The hydroxyl group at C-2 then ionizes and displaces the oxygen-aglycon group from C-1, forming a 1,2-epoxide. If the C-6 hydroxyl group is axial, it can open this 1,2-epoxide ring to give a 1,6-anhydride.

Further support for this mechanism comes from some recent work by Kyosaka, Murata, and Tanaka.[19] They showed that phenyl α-mannopyranosides (trans-1,2) hydrolyzed 100 to 1000 times faster than their corresponding phenyl β-mannopyranosides (cis-1,2). In addition, phenyl α-D-mannopyranoside degraded much faster than phenyl β-D-glucopyranoside even though both have a trans-1,2 configuration. The authors suggest that this difference in reactivity is due to the fact that phenyl α-D-mannopyranoside does not have to change to its least stable conformation to achieve the necessary antiperiplanar relationship between OH-2 and the glycosidic bond.

The $S_N1cB(2)$ pathway is not, however, the only route via which aryl glycosides can degrade. Some phenyl glycosides which have the cis-1,2 configuration still degrade in alkali at 100°C. Both phenyl α-D-galactopyranoside and phenyl β-D-mannopyranoside yielded significant amounts of 1,6-anhydro-D-galactosan and 1,6-anhydro-β-D-mannopyranose, respectively,[15,20] although somewhat more slowly than their trans-1,2 analogs. Phenyl α-D-glucopyranoside is quite stable in alkali at 100°C, but does degrade at 170°C. Investigators have suggested that this compound degrades by an $S_N1cB(6)$* mechanism.[21]

*Unimolecular nucleophilic substitution with neighboring group assistance from the conjugate base of OH-6.

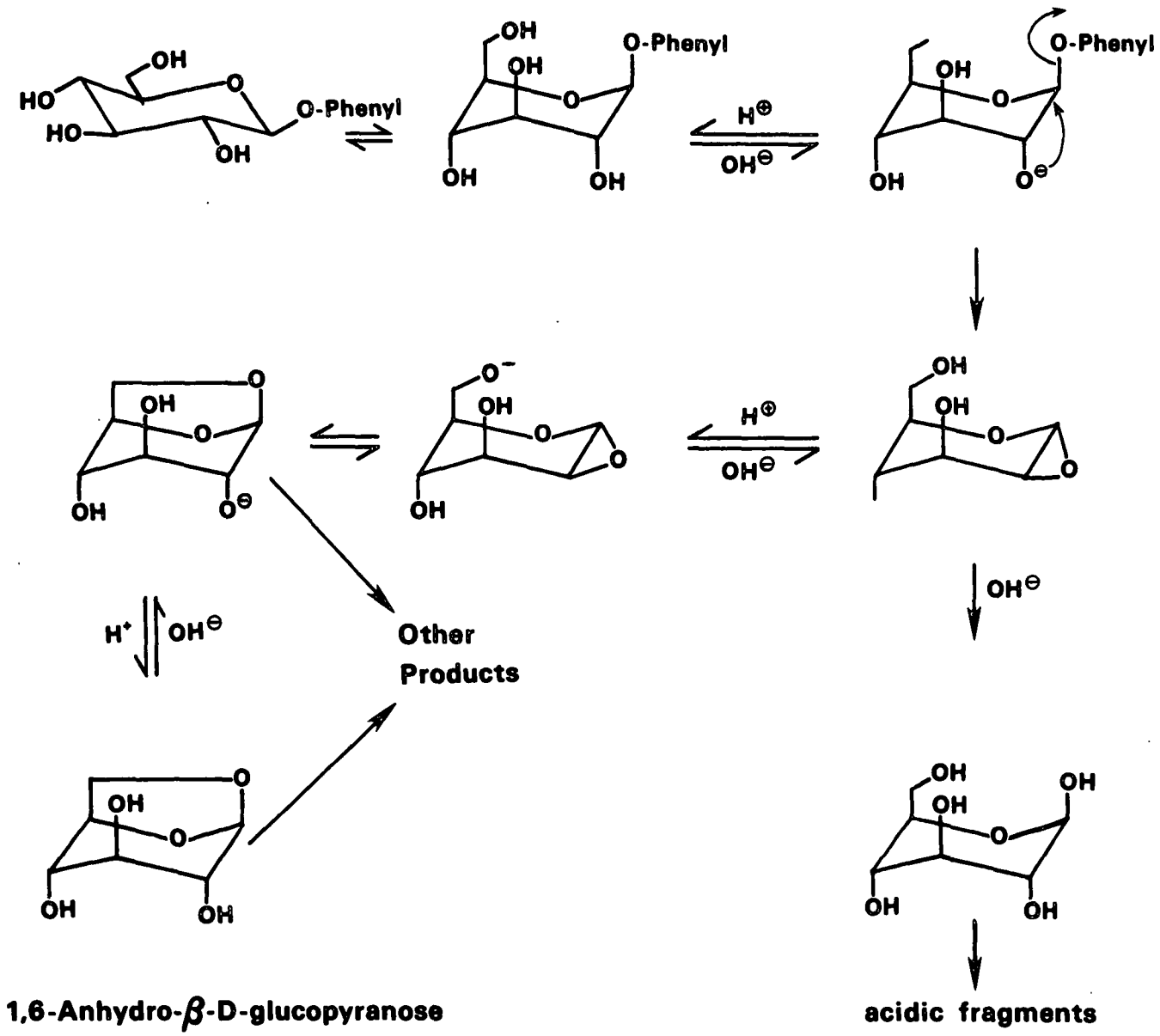

1,6-Anhydro-β-D-glucopyranose

acidic fragments

Figure 1. Degradation of phenyl β-D-glucopyranoside via the $S_N1cB(2)$ mechanism.[18,25,26]

Thus it appears that the $S_N1cB(2)$ mechanism is an important pathway for aryl glycoside degradation, but that there are other, competing mechanisms with just slightly higher free energies of activation.

Alkaline Degradation of Alkyl Glycosides

Early studies of methyl glycosides showed that, like the aryl glycosides, compounds having a trans-1,2 relationship between the OH-2 and glycosidic bond reacted significantly faster than their cis-1,2 analogs.[22] This led to the suggestion that the $S_N1cB(2)$ mechanism might also be important in the alkaline degradation of these compounds. Lindberg et al.[23] noted, however, that methyl glycosides with a cis-1,2 configuration or with a trans-1,2 configuration, but with OH-2 etherified, still hydrolyzed at significant rates. This indicated that reaction routes other than the $S_N1cB(2)$ mechanism also exist.

The alkaline degradations of methyl α- and β-D-glucopyranoside have been studied in more detail.[24,25,26] The overall degradation rates and postulated mechanisms for these compounds are shown in Table 1. The rate constants for the degradation of these three compounds are of the same order of magnitude. Methyl α- and methyl 2-O-methyl-β-D-glucopyranosides do react more slowly than methyl β-D-glucopyranoside, but the difference is only a factor of four. Due to the fact that only 18-30% of the methyl β-D-glucopyranoside degraded to 1,6-anhydro-β-D-glucopyranose (levoglucosan), Nault[24] concluded that the glucoside degraded by a mixed mechanism rather than a pure $S_N1cB(2)$ one. This work clearly illustrates that there are mechanisms other than $S_N1cB(2)$ which play an important role in the degradation of alkyl glycosides.

Table 1. Degradation of methyl glucopyranosides in 2.5M NaOH at 170°C.

Compound	$k_r \times 10^6$, sec^{-1}	Mechanism	Reference
Methyl-α-D-glucopyranoside	0.69	S_N2[a]	25, 26
Methyl-β-D-glucopyranoside	2.62	$S_N1cB(2)$ & S_N1[b] or S_N2	24
Methyl 2-O-methyl-β-D-glucopyranoside	0.71	S_N2	24

[a]Bimolecular nucleophilic substitution.[27]
[b]Unimolecular nucleophilic substitution.

Alkaline Degradation of Disaccharides

It is likely that there are significant differences between the glycosidic bonds in the simple aryl and alkyl glycoside models and those in polysaccharides. Simkovic et al.[28] studied the alkaline degradation of methyl β-D-glucopyranoside, methyl β-D-cellobioside, and methyl β-D-cellotrioside and found that the alkali sensitivity of the glycosidic bonds increased throughout this series. Earlier, Best and Green[29] reported that the interior glucosyl-glucosyl bond in methyl β-D-cellobioside reacted five times faster than the glucosyl-methyl bond. Investigators have therefore studied glycosidic bond cleavage in disaccharides in order to better approximate the reactions occurring in cellulose and other polysaccharides.

One study was made of disaccharide alditols; cellobiitol, lactitol, and maltitol.[30] All three compounds hydrolyzed at comparable rates. Based on the products, Lindberg postulated that cleavage was occurring at the glucosyl-oxygen bond by a mixed $S_N1cB(2')$ and S_N2 mechanism, and at the oxygen-aglycon bond via both S_N2 and $S_N1cB(1)$ pathways. The $S_N1cB(1)$ mechanism proposed by Lindberg is shown in Fig. 2.

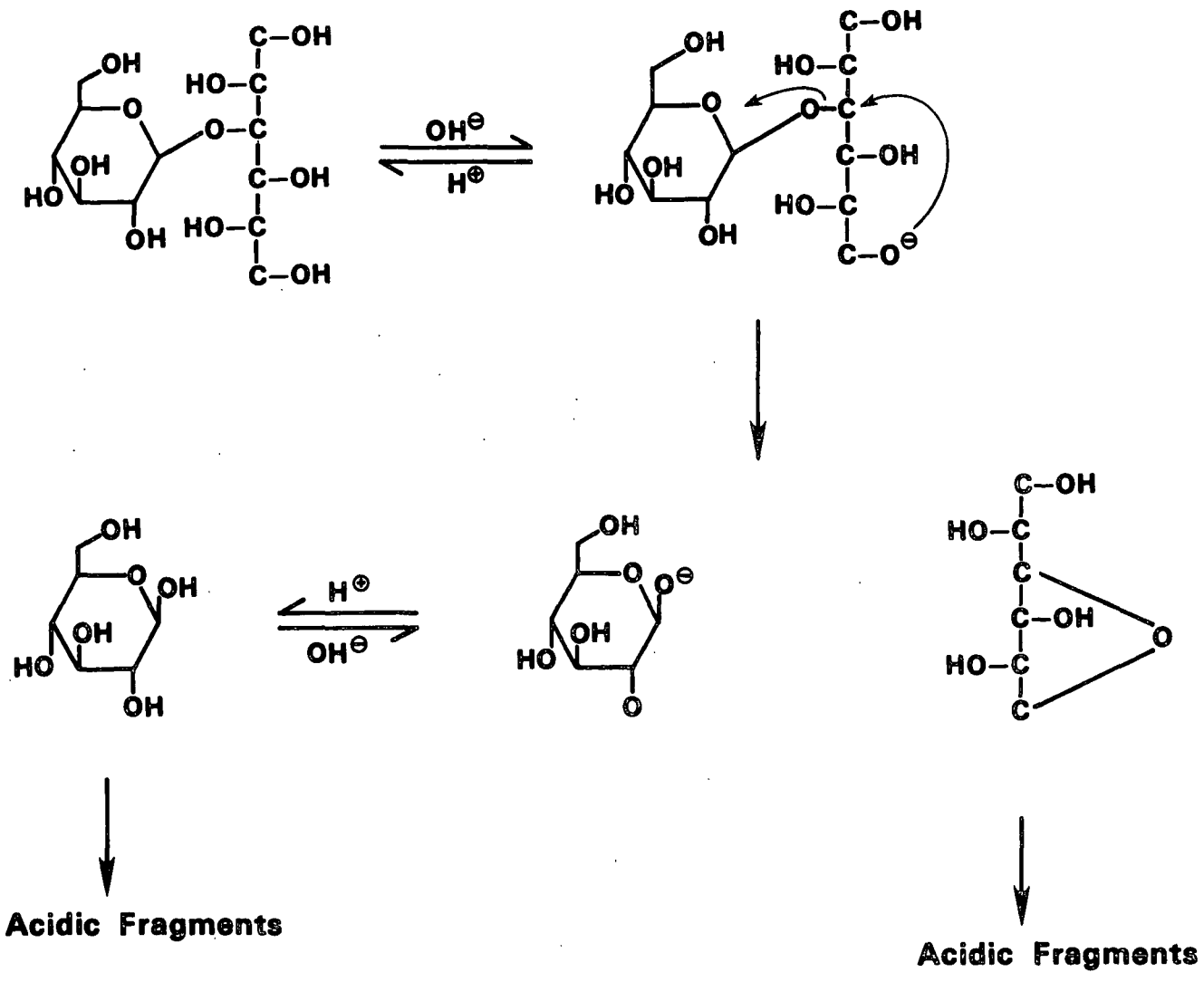

Figure 2. Degradation of cellobiitol at the oxygen-aglycon bond via an $S_N1cB(1)$ mechanism.[30]

Since that time, disaccharides in which the aglycon is a 1,5-anhydro-alditol have been studied. An extensive study of 1,5-anhydro-4-O-β-D-glucopyranosyl-D-glucitol (1,5-anhydrocellobiitol)[13,14] showed that 10% of the glycosidic chain

cleavage occurs at the oxygen-aglycon bond.* Cleavage of the oxygen-aglycon bond had the characteristics of an S_N1 mechanism. This conclusion was supported by a study of 1,5-anhydro-2,3,6-tri-O-methyl-cellobiitol.[31] Since methylating the hydroxyl groups in the aglycon did not affect the rate of oxygen-aglycon bond cleavage, it was concluded that the oxygen-aglycon bonds in 1,5-anhydro-cellobiitol and its methylated analog must react via an S_N1 mechanism.

The remaining 90% of the 1,5-anhydrocellobiitol degradation occurred at the glycosyl-oxygen bond.* The results from kinetic studies of glycosyl-oxygen bond cleavage were all consistent with a predominantly neighboring group-type mechanism. However, only 35% of the 1,5-anhydrocellobiitol which cleaved at the glycosyl-oxygen bond formed levoglucosan.[13,14] In contrast, phenyl β-D-glucopyranoside[15,18] and 1,5-anhydro-2,3,6-tri-O-methyl-cellobiitol,[31] which degrade via S_N1cB(2) pathways, yield 70-80% levoglucosan. The smaller amount of levoglucosan formed from 1,5-anhydro-cellobiitol led Brandon to conclude that

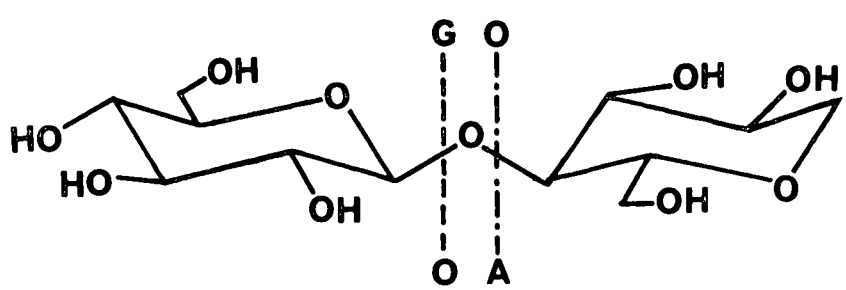

*The dotted line between G and O represents cleavage at the glycosyl-oxygen bond; the dashed line between O and A indicates cleavage of the oxygen-aglycon bond.

less than 50% of the glycosyl-oxygen bond cleavage was due to an $S_N1cB(2)$-type reaction.[13,14] Degradation of 1,5-anhydrocellobiitol in the presence of SH^- (kraft pulping conditions)[32,33] was not consistent with an S_N2 mechanism. The mechanism for the remaining portion of the glycosyl-oxygen bond cleavage was therefore tentatively identified as S_N1 in nature.

This review of studies of glycosidic bond cleavage in disaccharides shows that the $S_N1cB(2)$ mechanism is an important but by no means exclusive pathway for their degradation.

SCOPE AND OBJECTIVES OF THE THESIS

The preceding discussion of the mechanisms of alkaline glycosidic bond cleavage in various model compounds clearly shows that these reactions are not fully understood. Although the $S_N1cB(2)$ mechanism appears to be important, much evidence suggests that other mechanisms play significant roles. In particular, less than 55% of the glycosyl-oxygen bond cleavage in 1,5-anhydrocellobiitol, the model compound most like cellulose, appears to occur via an $S_N1cB(2)$ mechanism. Since the $S_N1cB(2)$ mechanism requires that a glucosyl unit convert to its least stable conformation, the $S_N1cB(2)$ mechanism may not occur at all in the cellulose polymer where the necessary conformational change would be extremely hindered.[14] Other mechanisms may therefore be the most important ones in cellulose, and warrant further investigation.

The best way to look at these other mechanisms is to eliminate the $S_N1cB(2)$ route. There are two possible ways to do this: OH-2 can be etherified to prevent ionization or the relationship between OH-2 and the glycosidic bond can be changed from trans-1,2 to cis-1,2. Derivatizing OH-2 so that it cannot ionize

can cause stereochemical and electronic changes in a molecule and thus may alter the competing mechanisms.[13,14,31]

The relationship between OH-2 and the glycosidic bond can be changed from trans to cis either by switching from a β to α glycosidic linkage or by inverting the OH-2 group. The α-linked analog of 1,5-anhydrocellobiitol, 1,5-anhydro-4-O-α-glucopyranosyl-D-glucitol (1,5-anhydromaltitol), has a cis-1,2 configuration. However, switching the type of bond changes the steric factors and anomeric effects of the bond being broken.[13,14] A cis-1,2 configuration is also present in the C-2 epimer of 1,5-anhydrocellobiitol, 1,5-anhydro-4-O-β-mannopyranosyl-D-mannitol (1,5-anhydromannobiitol). Because this compound still has the β-1,4 bond found in cellobiitol, mechanisms other than $S_N1cB(2)$ should be less affected by the change. Therefore 1,5-anhydromannobiitol should be a good model compound for investigating the alternate mechanisms of glycosyl-oxygen bond cleavage in cellulose model compounds.

In conclusion, the objective of this thesis was to study the mechanisms of glycosidic bond cleavage in 1,5-anhydromannobiitol under high temperature alkaline conditions. This information should provide additional insight into the mechanisms which may degrade cellulose and other wood polysaccharides.

POTENTIAL MECHANISMS FOR THE ALKALINE DEGRADATION OF 1,5-ANHYDRO-4-O-β-MANNOPYRANOSYL-D-MANNITOL

Glycosidic linkages can be broken in two places; between the glycon and oxygen (glycosyl-oxygen bond), or between the oxygen and aglycon group (oxygen-aglycon bond), as shown in Fig. 3. The potential mechanisms for cleaving each of these bonds in 1,5-anhydromannobiitol are discussed in the following sections.

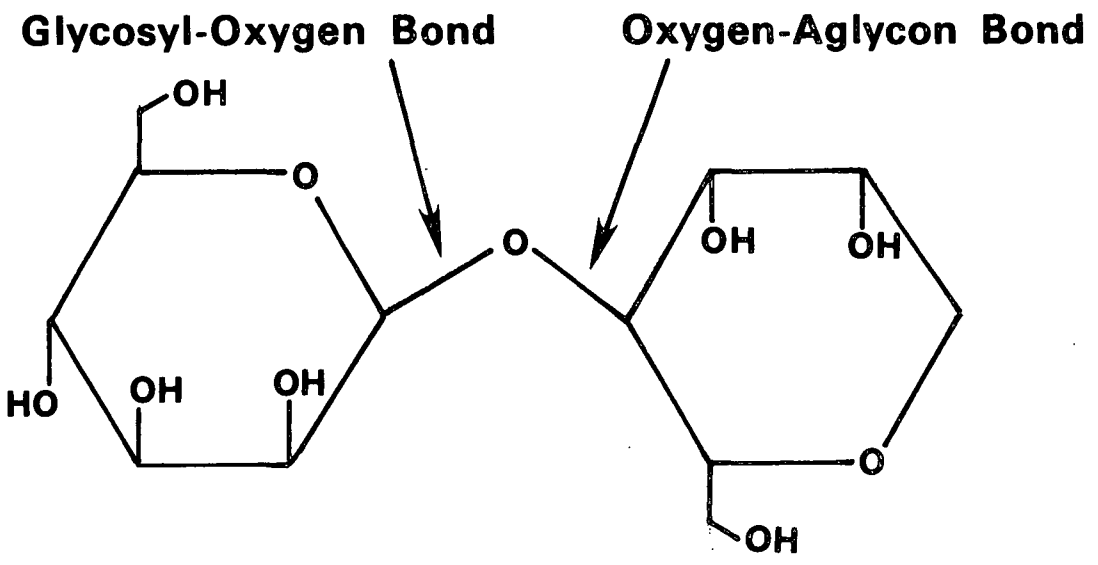

Figure 3. Potential points of bond cleavage in the glycosidic linkage of 1,5-anhydromannobiitol.

Glycosyl-Oxygen Bond

Unimolecular Nucleophilic Substitution (S_N1)

In a unimolecular nucleophilic substitution (S_N1) mechanism, bond cleavage occurs heterolytically, producing carbocation and anion intermediates. The carbocation is quickly attacked by a nucleophile. The glycosyl-oxygen bond in 1,5-anhydromannobiitol is shown undergoing S_N1-type cleavage in Fig. 4. In an S_N1-type reaction, the reaction rate is strongly affected by the stability of both the carbonium ion formed in the substrate and the anion created in the leaving group. Hence altering either the substrate or leaving group may affect the reaction rate. Since the nucleophile does not participate in the rate-determining step, the rate is independent of the strength of the nucleophile. Compounds which react by an S_N1 mechanism follow first-order kinetics as shown in Eq. (1).

$$\text{rate} = k[\text{reactant}] \qquad (1)$$

where k = rate constant.

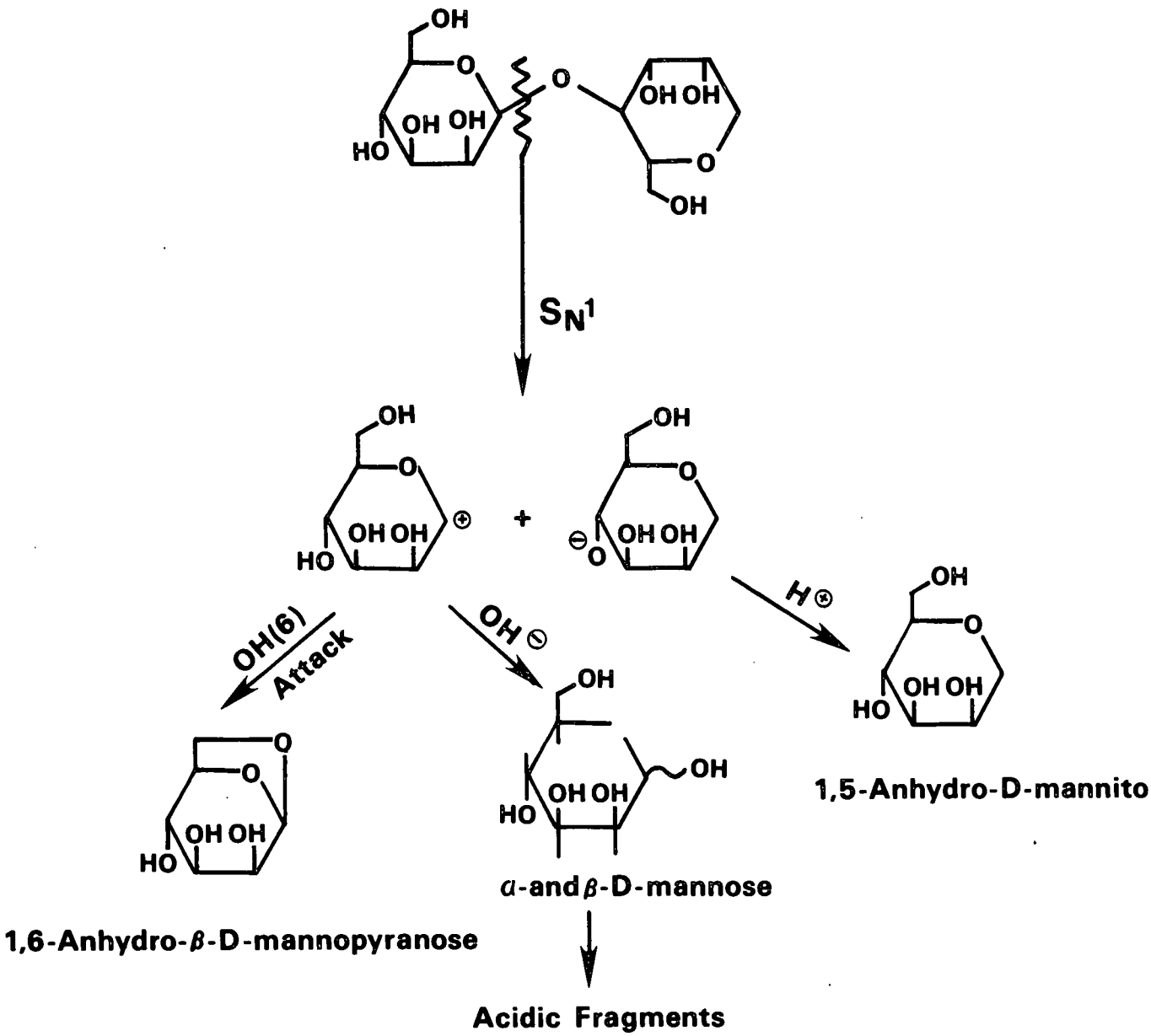

Figure 4. Cleavage of the glycosyl-oxygen bond in 1,5-anhydromannobiitol via an S_N1 mechanism.

For a neutral substrate undergoing unimolecular substitution, increasing the ionic strength of the medium by the addition of a noncommon ion salt increases the reaction rate. This is due to the fact that the intermediates are more charged than the reactants, and hence stabilized to a greater degree by the increase in ionic strength. Because the rate-determining step in an S_N1-type reaction requires enough energy to break a bond, and no energy is being generated by the simultaneous formation of another bond, these reactions have relatively high enthalpies of activation. A single reactant molecule forms two ions in the transition state, hence the entropies of activation are relatively positive.[34,35]

The cleavage of the glycosyl-oxygen bond in 1,5-anhydromannobiitol via an S_N1 mechanism should produce 1,5-anhydro-D-mannitol. A mixture of α- and β-D-mannose should also be formed, but these compounds will degrade too quickly to be detected.[36] Another possible product is 1,6-anhydro-β-D-mannopyranose. Compounds analogous to 1,6-anhydro-β-mannopyranose are unstable under high temperature alkaline conditions, but if the rate constant for formation is larger than the rate constant for degradation, these compounds will still be detected in the reaction mixture.

Bimolecular Nucleophilic Substitution (S_N2)

The bimolecular nucleophilic substitution (S_N2) mechanism involves simultaneous attack by the nucleophile and departure of the leaving group. Figure 5 shows the glycosyl-oxygen bond in 1,5-anhydromannobiitol cleaving by this mechanism. Because the nucleophile participates in the rate-determining step, its nucleophilicity has a strong effect on the reaction rate. The leaving ability of the leaving group also affects the rate, so S_N2-type reactions have second-order rate expressions. In the present alkaline degradation studies, however,

the nucleophile (OH^-) is present in such excess that the rate expression reduces to a pseudo-first-order form, as given in Eq. (2).

$$\text{rate} = k' [\text{reactant}] \qquad (2)$$

where $k' = k\, f[OH^-]$ = pseudo-first-order rate constant

k = true rate constant

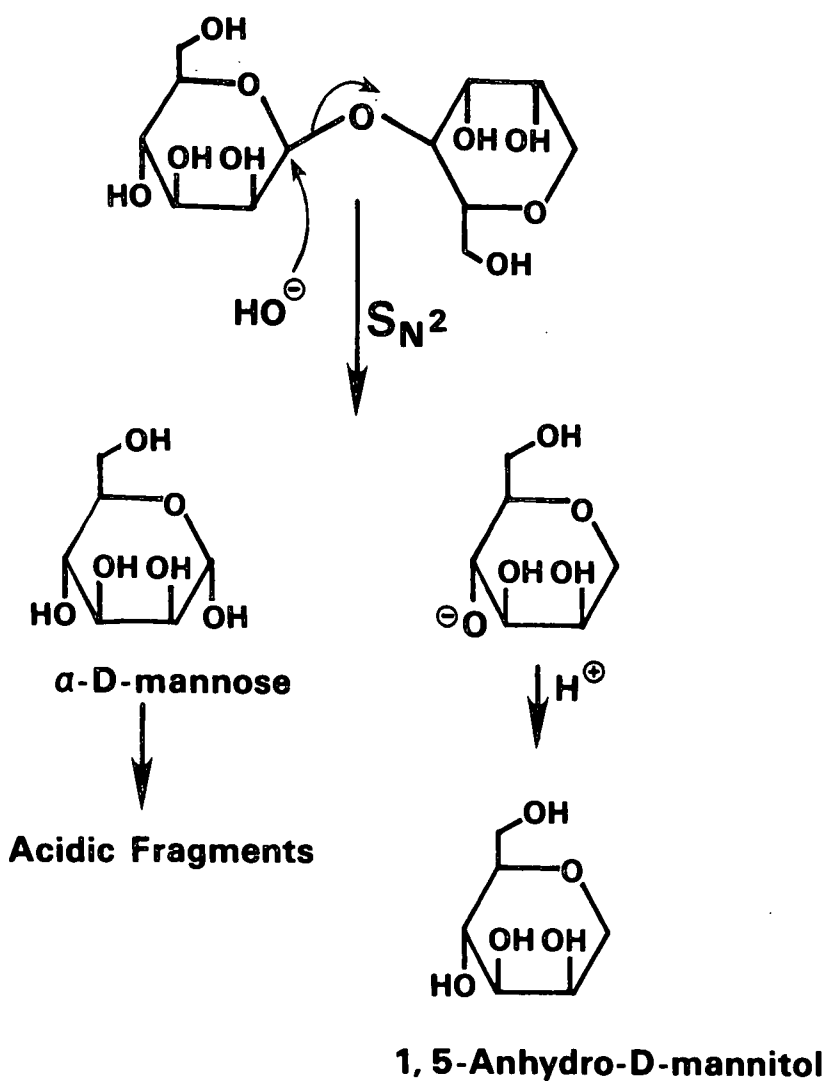

Figure 5. Cleavage of the glycosyl-oxygen bond in 1,5-anhydromannobiitol via an S_N2 mechanism.

The transition state of this postulated S_N2 mechanism has a more delocalized charge than the reactants. Therefore, increasing the ionic strength of the medium stabilizes the reactants more than the transition state, which decreases the reaction rate. Hence S_N2-type reactions generally exhibit negative salt effects.[34,35]

In an S_N2 mechanistic scheme, the rate determining step involves the simultaneous cleavage and formation of bonds. Some of the energy required for breaking the old bond is recovered by the formation of the new bond. Therefore S_N2-type reactions have relatively low enthalpies of activation. The transition state requires that two molecules form one, decreasing the translational degrees of freedom in the system and giving rise to relatively negative entropies of activation.[34,35]

Cleavage of the glycosyl-oxygen bond in 1,5-anhydromannobiitol via an S_N2 pathway should produce α-D-mannose and 1,5-anhydro-D-mannitol. Only the 1,5-anhydro-D-mannitol would be observed because mannose degrades very rapidly under the reaction conditions.[36]

Ring Opening with Neighboring Group Assistance [S_N1cB(2)-ro]

Lindberg et al.[37] reported that the alkaline degradation of methyl α-L-arabinofuranoside yielded about 2.6% methyl α-L-arabinopyranoside. This observation led them to propose a mechanism in which OH-2 ionizes, attacks C-1, and displaces the ring oxygen. They suggested that ring opening by the nucleophilic attack of a neighboring group [S_N1cB(2)-ro mechanism] could be responsible for the alkaline degradation of other cis-1,2 glycosides. Figure 6 shows 1,5-anhydromannobiitol reacting according to this mechanism. Once the 1,2-epoxide forms, it can be opened by base to give a hemiacetal. The hemiacetal would

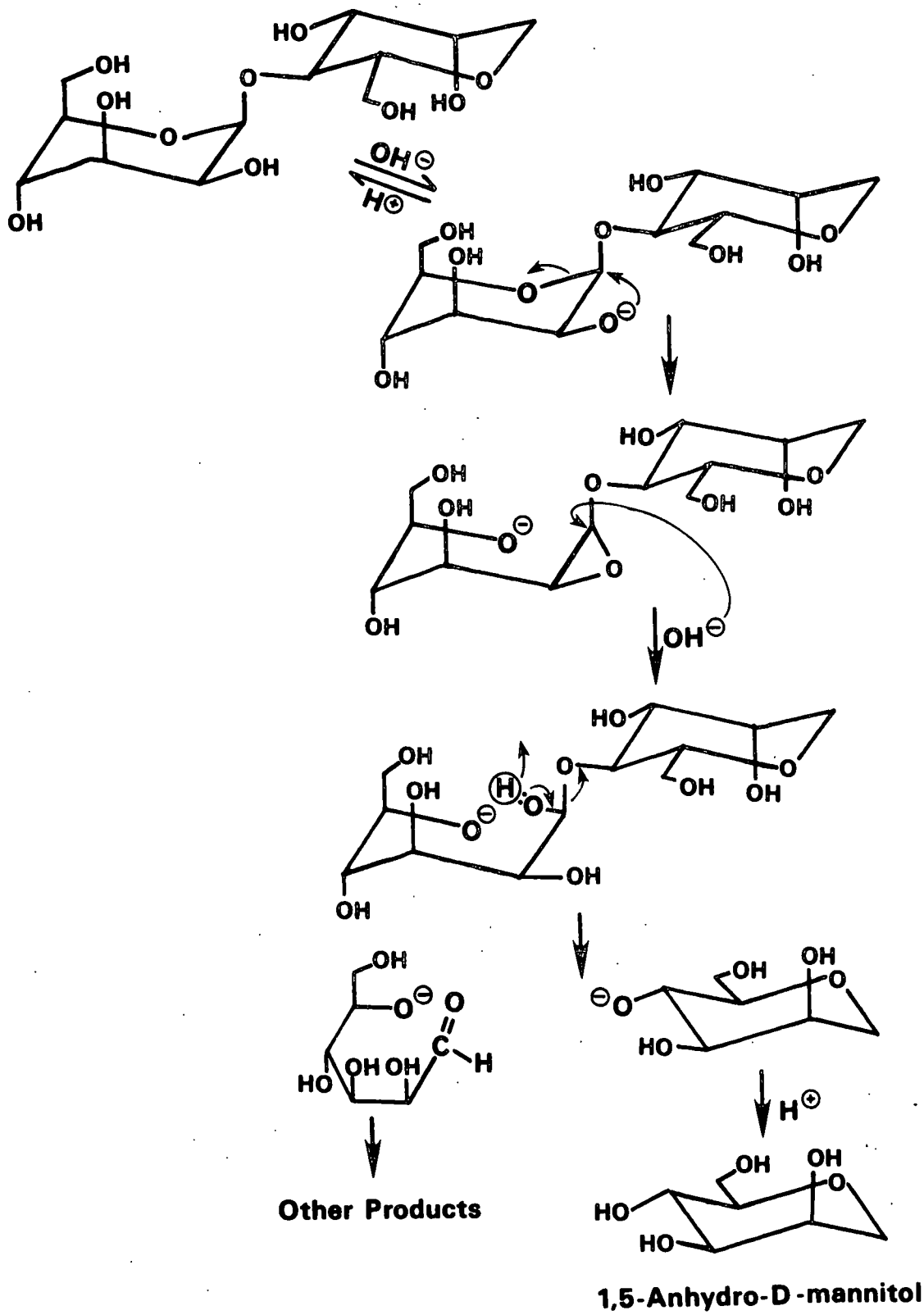

Figure 6. Cleavage of the glycosyl-oxygen bond in 1,5-anhydromannobiitol via the $S_N1cB(2)$-ro mechanism.

probably rapidly rearrange to an aldose, cleaving the glycosidic bond. An $S_N1cB(2')$-ro mechanism should have characteristics similar to other neighboring group mechanisms, including a negative salt effect, a relatively low enthalpy of activation, and an intermediate entropy of activation.[34,35]

Unimolecular Nucleophilic Substitution with Neighboring Group Assistance from OH-4 [$S_N1cB(4')$]

Capon[9] proposed that phenyl β-D-mannopyranoside might react via an $S_N1cB(4)$ route. This mechanism can also be proposed for 1,5-anhydromannobiitol, as illustrated in Fig. 7. According to this mechanism, OH-4' ionizes and displaces the aglycon via a nucleophilic attack at C-1. This requires that the glycon assume a boat conformation, which is considerably strained, particularly when the aglycon group is large. DeBruyne[16] reports that blocking the OH-2 group in p-nitrophenyl β-D-xylopyranoside caused the compound to react 1000X more slowly and switch from an $S_N1cB(2)$ to an S_N2Ar mechanism rather than follow the $S_N1cB(4)$ route. Thus the $S_N1cB(4)$ mechanism appears to be a very high energy pathway and is considered an unlikely mechanism.

Oxygen-Aglycon Bond

Unimolecular Nucleophilic Substitution (S_N1)

Unimolecular nucleophilic substitution (S_N1) is a possible mode of cleavage for the oxygen-aglycon bond in 1,5-anhydromannobiitol (Fig. 8). Reaction via this mechanism could produce 1,5-anhydro-D-mannitol, 1,5-anhydro-D-iditol, 1,5-anhydro-D-talitol, and fragments, as shown. The other characteristics of the reaction should be the same as those described for the S_N1 hydrolysis of the glycosyl-oxygen bond.

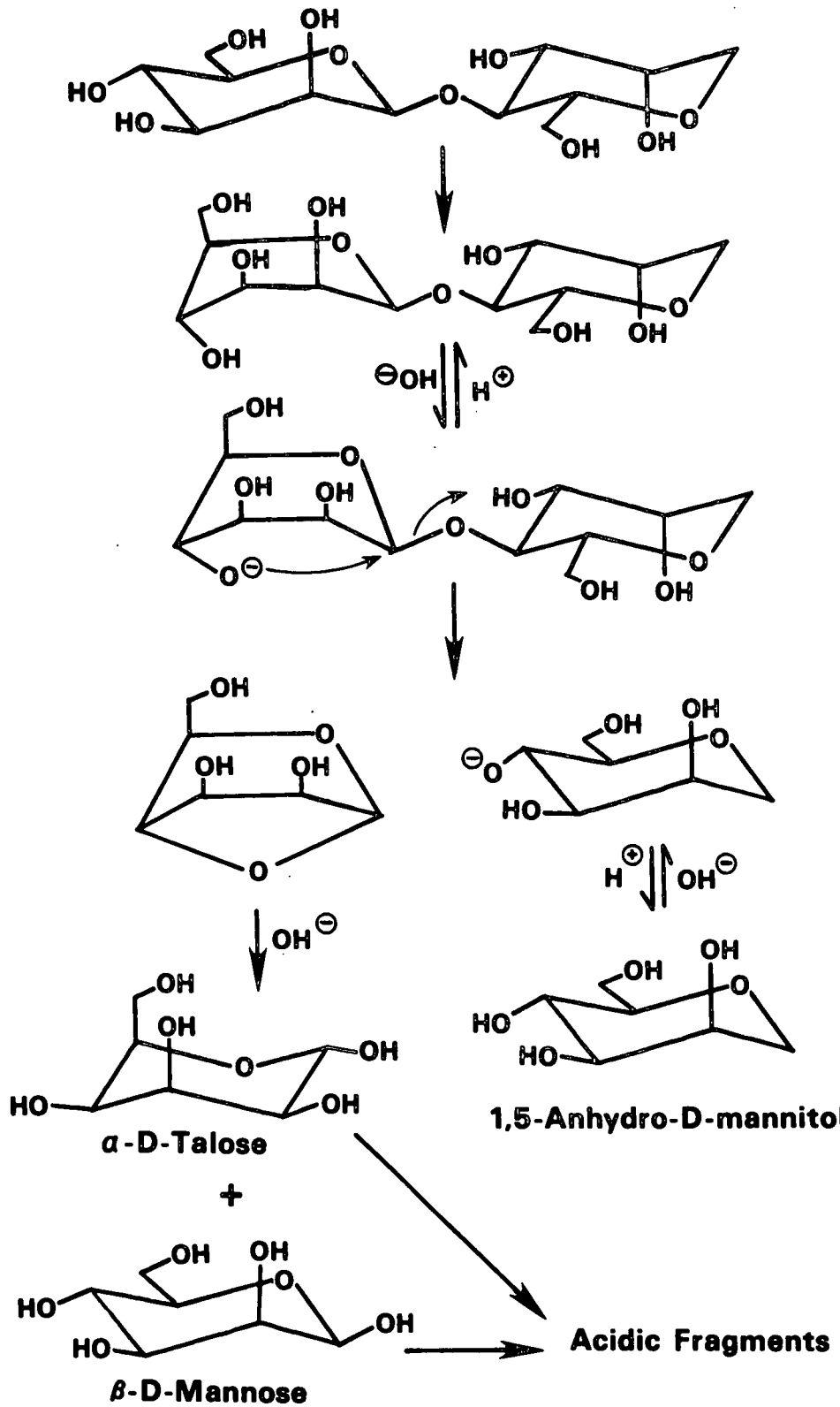

Figure 7. Potential cleavage of the glycosyl-oxygen bond in 1,5-anhydro-mannobiitol via an $S_N1cB(4)$ mechanism.

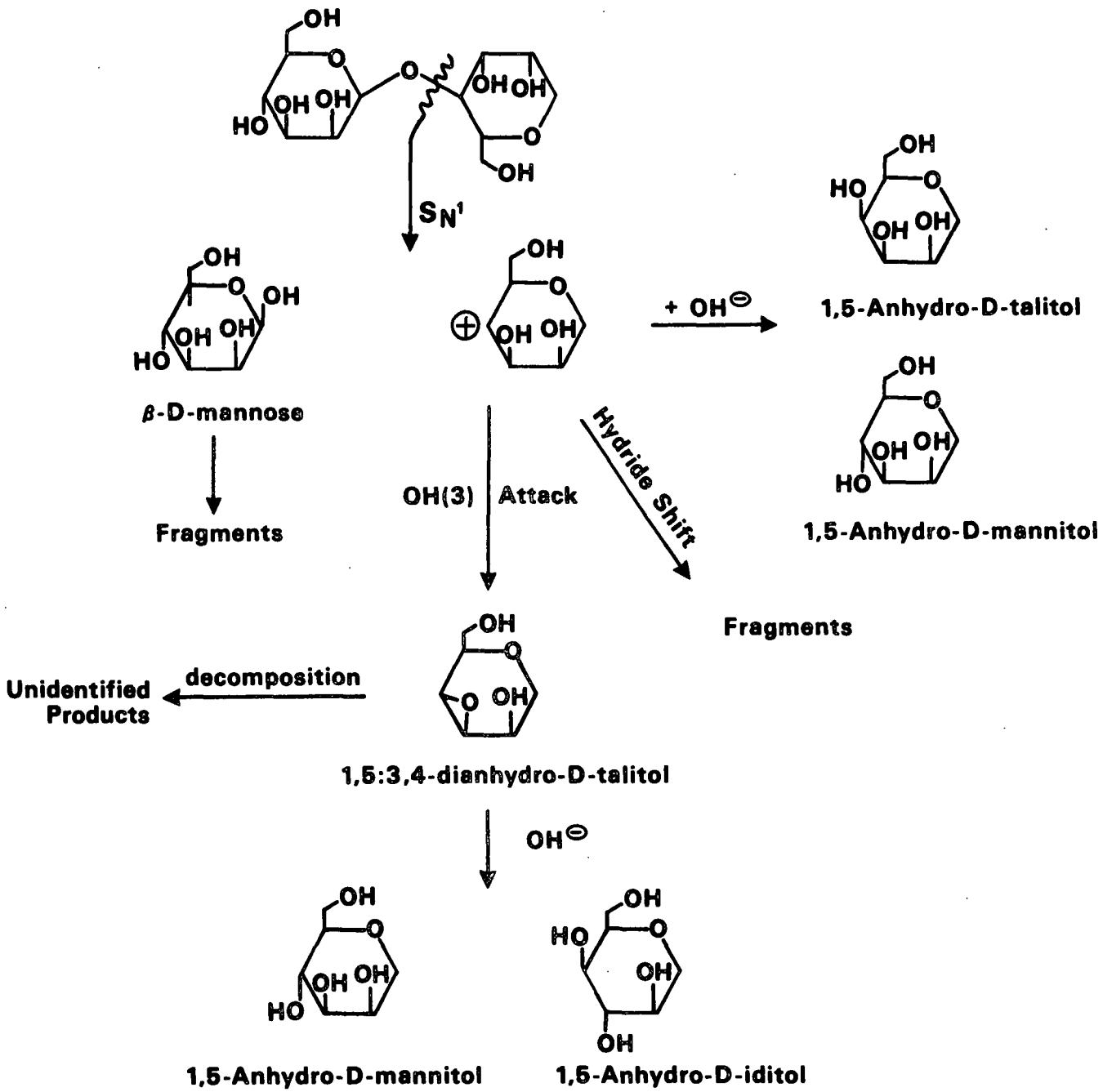

Figure 8. Cleavage of the oxygen-aglycon bond in 1,5-anhydromannobiitol via an S_N1 mechanism.

Bimolecular Nucleophilic Substitution (S_N2)

A bimolecular nucleophilic substitution (S_N2) mechanism is another way in which the oxygen-aglycon bond could be cleaved. This is illustrated in Fig. 9. The major stable product from S_N2-type cleavage should be 1,5-anhydro-D-talitol. The reaction should have the standard characteristics of an S_N2 mechanism as described previously for glycosyl-oxygen bond cleavage.

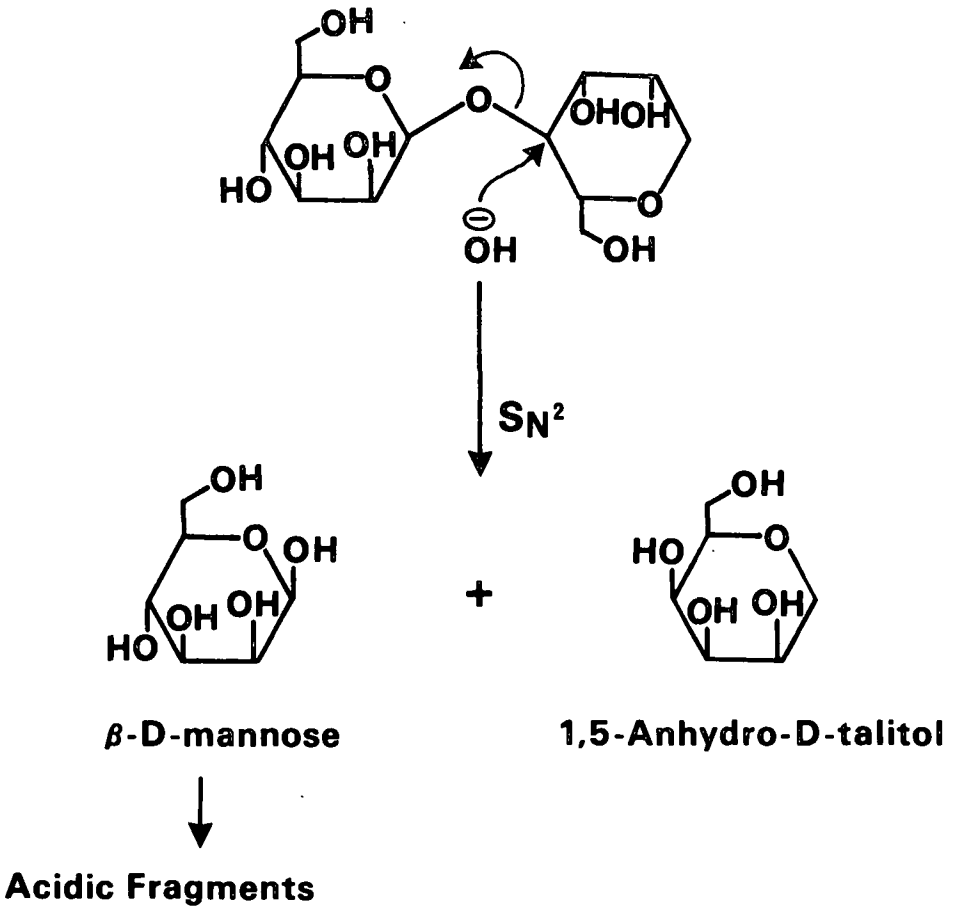

Figure 9. Cleavage of the oxygen-aglycon bond in 1,5-anhydromannobiitol via an S_N2 mechanism.

Unimolecular Nucleophilic Substitution with Neighboring Group Assistance from OH-3 [$S_N1cB(3)$]

Another possible mechanism for oxygen-aglycon bond cleavage is neighboring group attack by the conjugate base of OH-3 [$S_N1cB(3)$]. The $S_N1cB(3)$ reaction would result in formation of a 3,4-epoxide intermediate which could be opened by base to give 1,5-anhydro-D-iditol and 1,5-anhydro-D-mannitol, as shown in Fig. 10. This reaction should exhibit the traits common to $S_N1cB(i)$ mechanisms, namely negative salt effects, relatively low enthalpies of activation and intermediate entropies of activation. The rate constants should also have a strong, positive dependence on the hydroxide ion concentration.

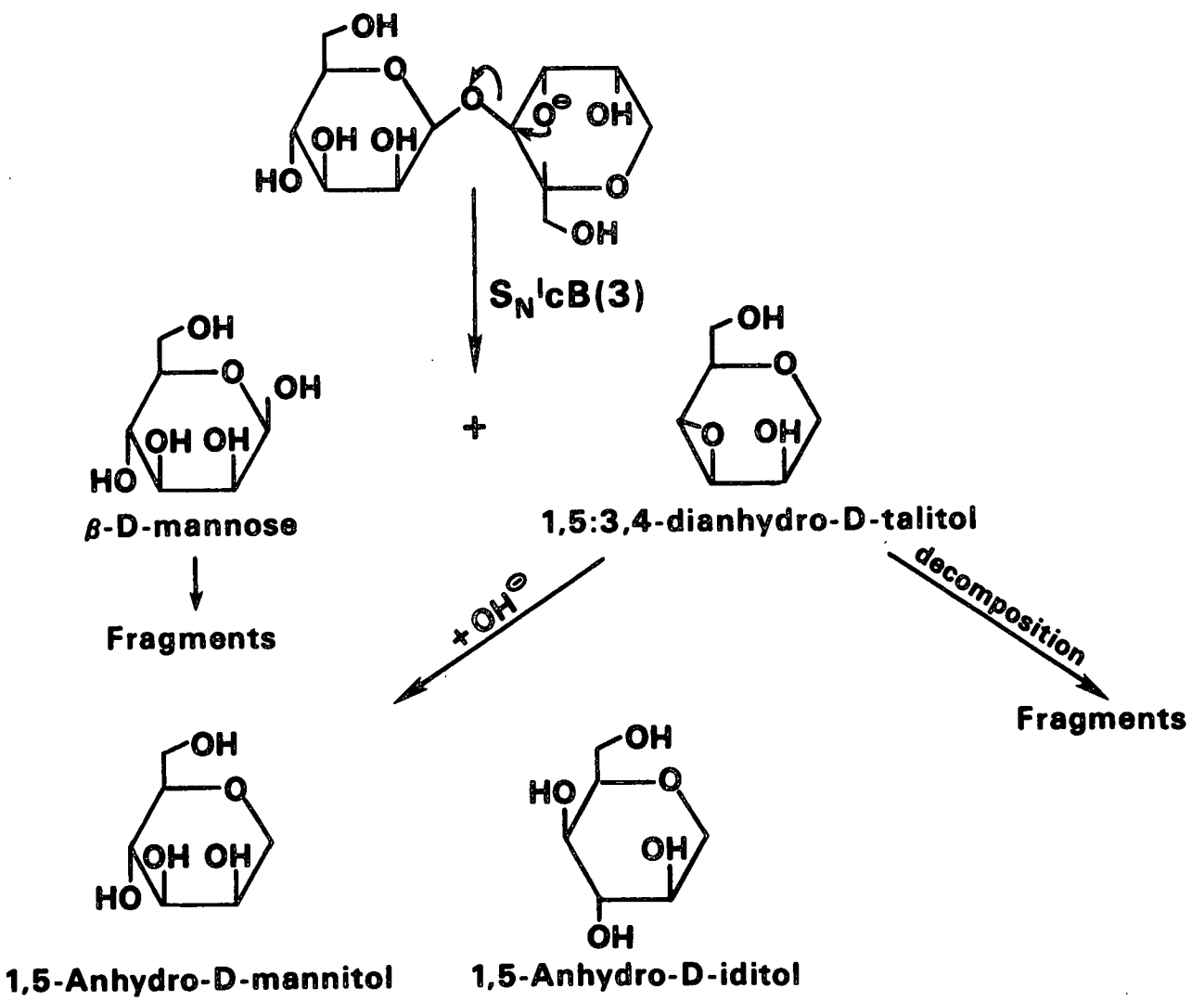

Figure 10. Cleavage of the oxygen-aglycon bond in 1,5-anhydromannobiitol via an SN1cB(3) mechanism.

Unimolecular Nucleophilic Substitution with Neighboring Group Assistance from OH(6) [$S_N1cB(6)$]

Another possible neighboring group mechanism could involve displacement of the oxygen-aglycon bond by the conjugate base of OH-6. This would result in formation of a four-membered ring intermediate. These have been calculated to be very strained[38] and are seldom if ever found. Reaction via this mechanism would probably yield 1,5-anhydro-D-talitol and 1,5-anhydro-D-mannitol, as shown in Fig. 11. The kinetic behavior of the $S_N1cB(6)$ mechanism would be the same as that of the $S_N1cB(3)$ mechanism.

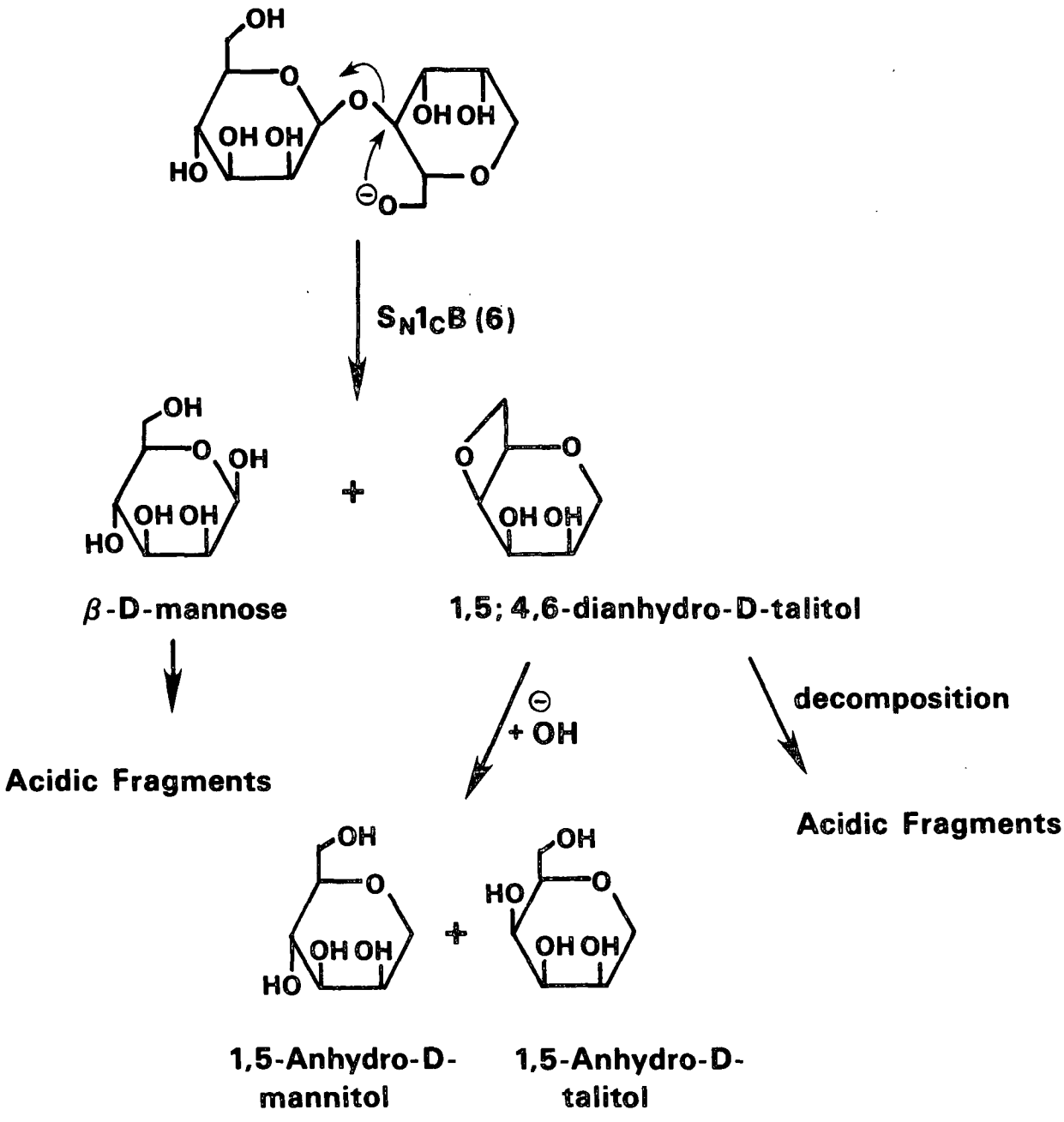

Figure 11. Potential cleavage of the oxygen-aglycon bond in 1,5-anhydro-mannobiitol via an $S_N1_{CB}(6)$ mechanism.

RESULTS AND DISCUSSION

SYNTHESIS AND CHARACTERIZATION OF 1,5-ANHYDRO-4-O-β-D-MANNOPYRANOSYL-D-MANNITOL

The model compound used in this study, 1,5-anhydro-4-O-β-D-mannopyranosyl-D-mannitol (1,5-anhydromannobiitol), is a novel compound not previously reported in the literature. It was synthesized from mannobiose, which was isolated from ivory nuts using the procedure developed by Thiem, Sievers, and Karl,[39] except for a modified acetolysis step.[40] Ground, extracted, and bleached ivory nuts were digested in sodium hydroxide to give mannan A which contained 98.8% mannose. Acetolysis of the mannan A yielded a mixture of acetylated mannosaccharides. Deacetylation and fractionation on Sephadex G-15 produced mannobiose. This compound had a gas chromatographic retention time and NMR spectra identical to those of known mannobiose.[41-42]

Mannobiose was converted to 1,5-anhydromannobiitol as shown in Fig. 12. Acetylation gave mannobiose octaacetate, which was converted to the hepta-O-acetyl-mannopyranosyl bromide, then reduced with Raney nickel to yield 1,5-anhydromannobiitol heptaacetate. Deacetylation, fractionation, and crystallization yielded pure 1,5-anhydromannobiitol.

The crystalline 1,5-anhydromannobiitol was characterized in several ways. Elemental analysis showed that the carbon, hydrogen, and oxygen contents were almost identical to the expected values. Fehling's test demonstrated that the product was a nonreducing sugar. HPLC analysis showed that acid hydrolysis gave equimolar amounts of 1,5-anhydro-D-mannitol and D-mannose. The ^{1}H- and ^{13}C-NMR spectra were consistent with 1,5-anhydromannobiitol. Gas chromatography showed that this product and 1,5-anhydrocellobiitol had almost identical retention

times, indicating that the two compounds are similar in size and structure. These results demonstrated that the desired product, 1,5-anhydromannobiitol, had been synthesized.

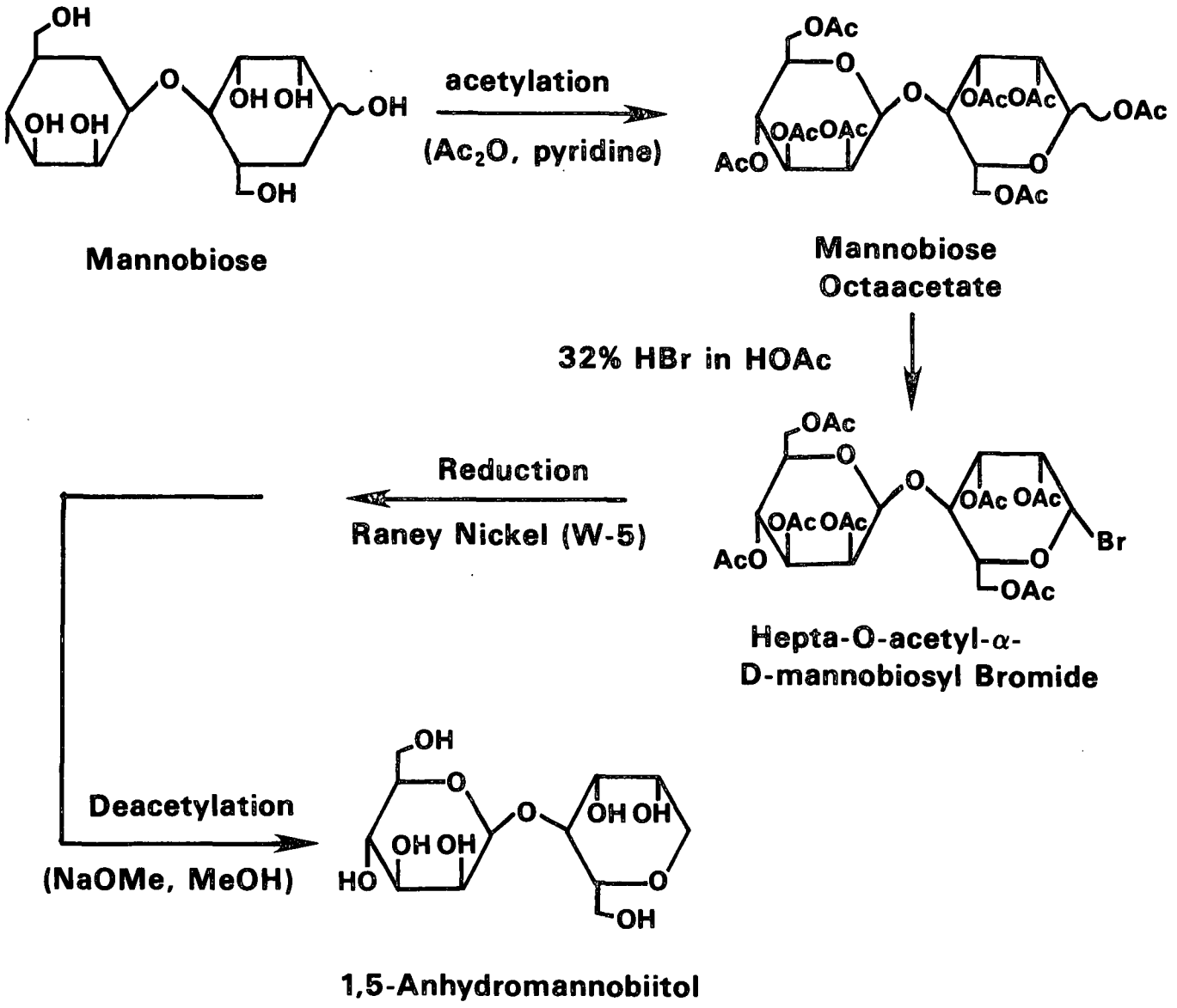

Figure 12. Synthesis of 1,5-anhydromannobiitol from mannobiose.

KINETIC ANALYSES

The concentrations of the reactant and products were measured as a function of time throughout each degradation. The following sections describe how apparent rate constants were calculated from these measurements.

Disappearance of Reactant

The general kinetic expression used for the disappearance of reactant during alkaline degradation was:

$$\frac{dR'}{dt} = - k\, f[R']\, f[OH^-] \qquad (3)$$

where t = time, seconds
k = specific rate constant
f[R'] = unknown function of reactant activity
$f[OH^-]$ = unknown function of hydroxide ion concentration

Because the ionic strength is constant throughout a run, it may be assumed that the activity coefficient of R' is constant. Reactant concentration may therefore be used as an estimate of activity. Previous work with similar compounds[13,14,24,25,32,33] demonstrated that the reaction is first order with respect to the reactant. Thus

$$f[R'] = R \qquad (4)$$

where R = reactant concentration, mole/liter.

The activity of the hydroxide ion will be constant if its activity coefficient and concentration are constant. The activity coefficients depend on temperature, pressure, and ionic strength, which were all constant during a run. The ratio between sodium hydroxide and reactant concentrations was very large (50-250), and thus the hydroxide concentration remained essentially constant throughout a given degradation. For these reasons, Eq. (3) simplifies to:

$$\frac{dR}{dt} = -k_r \cdot R \qquad (5)$$

where R = reactant concentration, moles/L
k_r = pseudo-first-order rate constant for the disappearance of reactant, sec^{-1}.

Integration of (5) and rearrangement yields:

$$\ln R = -k_r t + \ln R_o \tag{6}$$

where R_o = initial reactant concentration, moles/L.

Values of k_r were determined by fitting the concentration-time data to Eq. (6) using least-squares linear regression (Program 1, Appendix I). A representative plot of ln R versus time is shown in Fig. 13. The validity of the use of pseudo-first-order kinetics was checked by verifying that a plot of ln R versus time was linear over two half-lives.

Formation of Stable Products

A reactant can simultaneously undergo two or more independent reactions to give one or more products. This case is known as parallel reactions and has been described mathematically by Frost and Pearson.[43] The general rate expression for the formation of a product from a parallel reaction is:

$$\frac{dP_i'}{dt} = k_i' \, f[R] \, f[OH^-] \tag{7}$$

where P_i' = activity of product i, moles/L
k_i' = specific rate constant

The pseudo-first-order assumptions, discussed previously, reduce this to:

$$\frac{dP_i}{dt} = k_i \, R \tag{8}$$

where P_i = concentration of product i, moles/L
k_i = pseudo-first-order rate constant for the appearance of product i, sec^{-1}

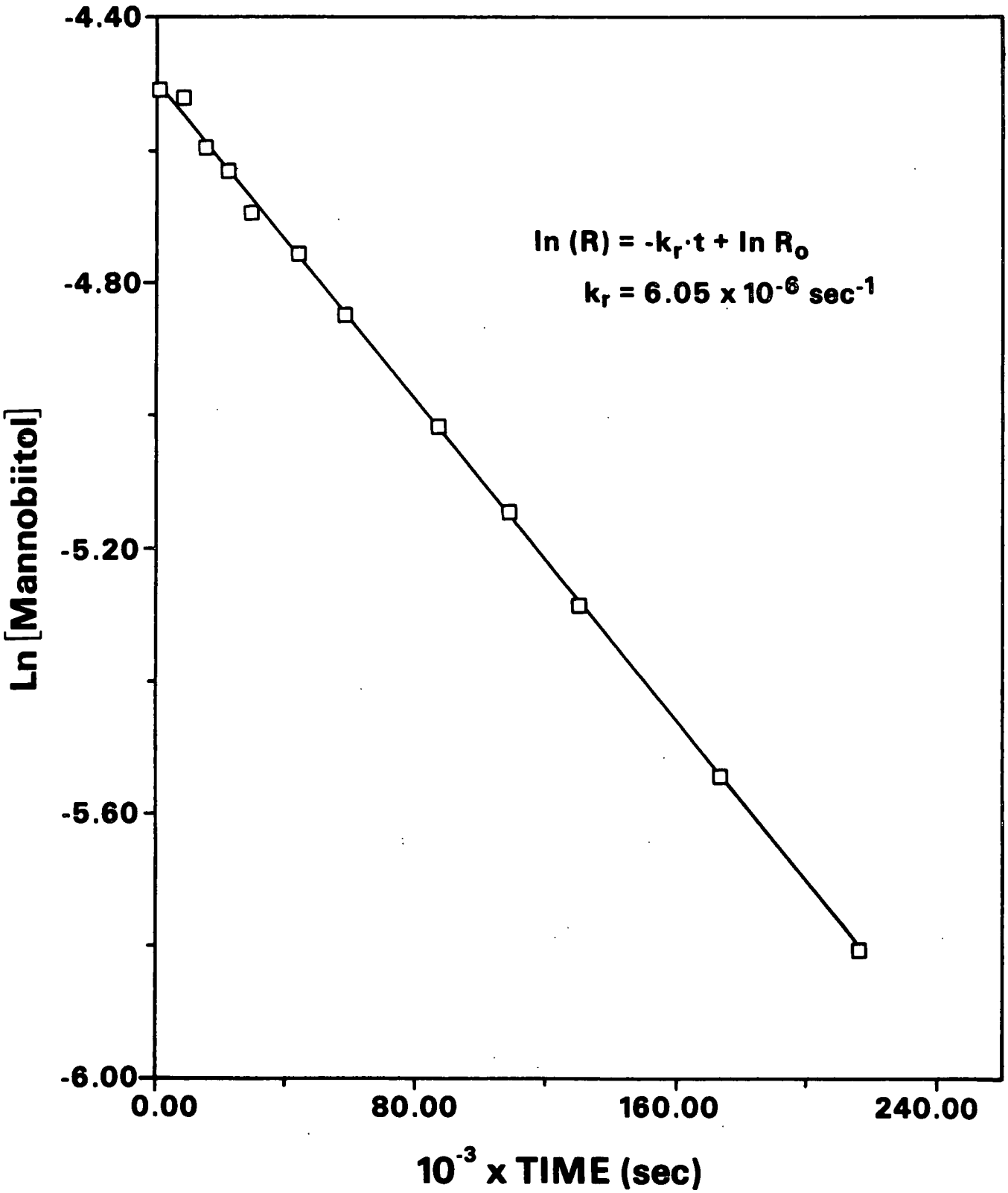

Figure 13. Disappearance of 1,5-anhydromannobiitol in 2.5M NaOH at 170°C.

The exponential form of Eq. (6) is:

$$R = R_o \exp(-k_r t) \tag{9}$$

Substituting this expression for R into Eq. (8) yields:

$$\frac{dP_i}{dt} = k_i R_o \exp(-k_r t) \tag{10}$$

Integrating Eq. (10) and evaluating the integration constant leads to the parallel pseudo-first-order rate expression:

$$(P_i - P_{io}) = k_i (R_o/k_r)[1-\exp(-k_r t)] \tag{11}$$

where P_{io} = initial product concentration, moles/L

Values for k_i were determined by fitting each data set to Eq. (11) using least-squares linear regression (Program 2, Appendix I). Figure 14 shows a representative data set plotted according to Eq. (11).

Alternate forms of the equations describing parallel, pseudo-first-order reactions are useful for presenting the data in a consolidated form. The rate equation for the disappearance of reactant can be written as:

$$\ln X_{r,t} = -k_r t \tag{12}$$

where $X_{r,t}$ = mole fraction of reactant at time t

$k_r = \Sigma k_i$ = pseudo-first-order rate constant for reactant disappearance, sec^{-1}

k_i = pseudo-first-order specific rate constant for the formation of product i, sec^{-1}

Equation (13) describes the appearance of product:

$$\ln(X_{i,oo} - X_{i,t}) = -k_r t + \ln X_{i,oo} \tag{13}$$

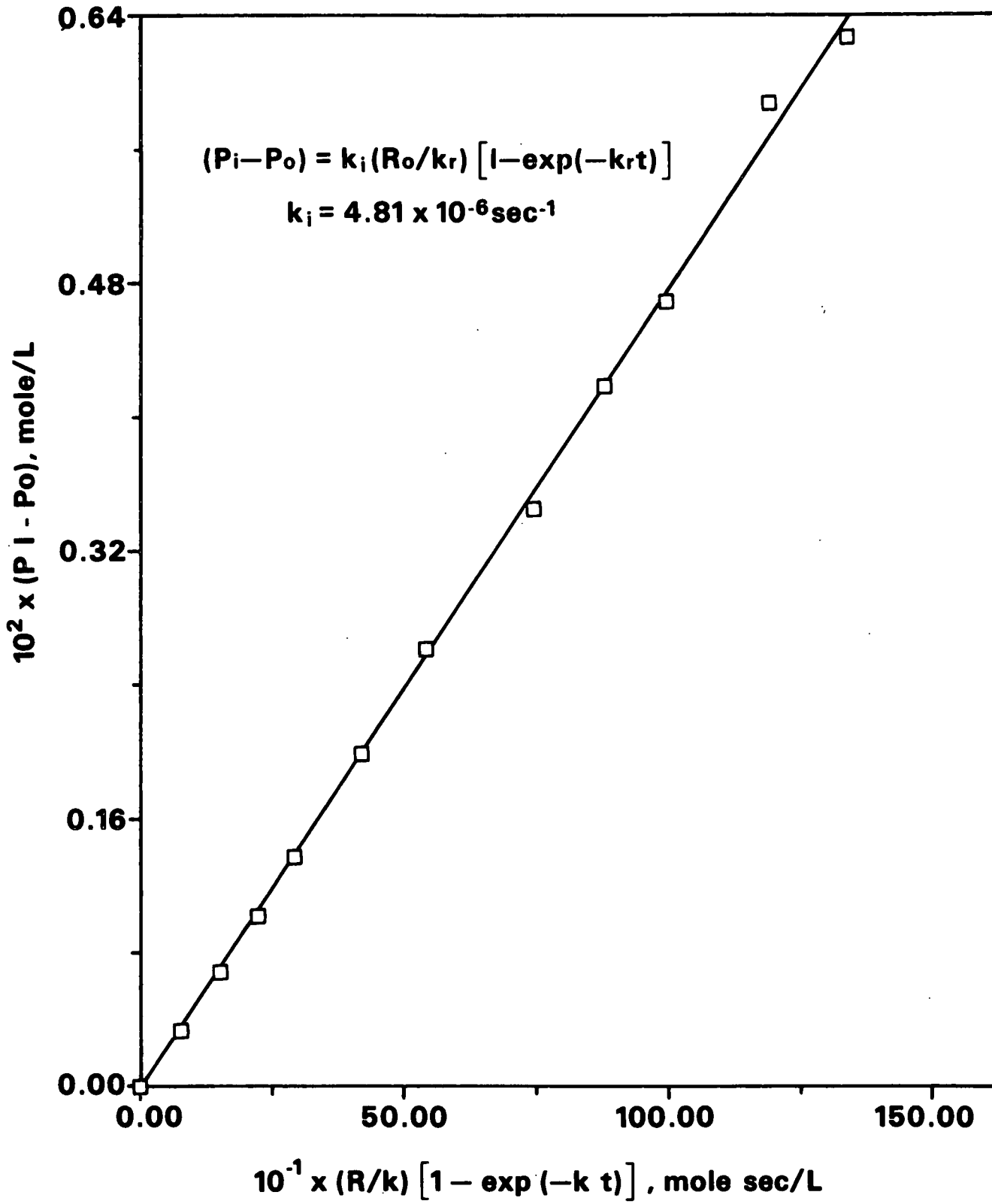

Figure 14. Appearance of 1,5-anhydro-D-mannitol during the degradation of 1,5-anhydromannobiitol in 2.5M NaOH at 170°C.

where $X_{i,t}$ = mole fraction of product i at time t

$X_{i,oo} = X_{i,t}$ at completion (the relative proportion of product i formed)

In these equations:

$$X_{i,t} = C_{i,t}/C_{r,o} \tag{14}$$

and

$$X_{i,oo} = C_i/C_{r,o}-C_{r,t}) \tag{15}$$

where $C_{i,t}$ = concentration of product i at time t, mole/L

$C_{r,o}$ = concentration of reactant at t = 0, mole/L

$C_{r,t}$ = concentration of reactant at time t, mole/L

By plotting either ln X_{rt} or $\ln(X_{i,oo}-X_{it})$ as a function of time, reactant disappearance and product appearance can be plotted on one graph (Program 3, Appendix I). In Fig. 15, one data set is shown plotted in this manner.

Formation of Unstable Products

Some products formed may be unstable under the reaction conditions. In this case, the observed concentration of product will be less than what has actually formed and plotting the observed concentration against time using Eq. (11) will not give the correct rate of formation. A mathematical method for determining the pseudo-first-order rate constant for the formation of an unstable product was described by Brandon.[13] The reaction scheme can be pictured as:

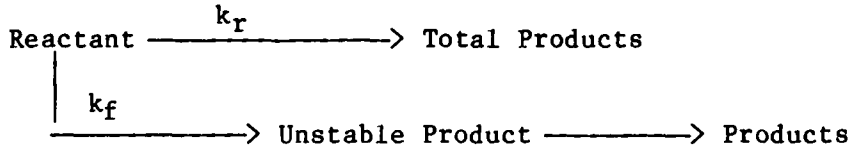

The change in the unstable product concentration with respect to time can be expressed as:

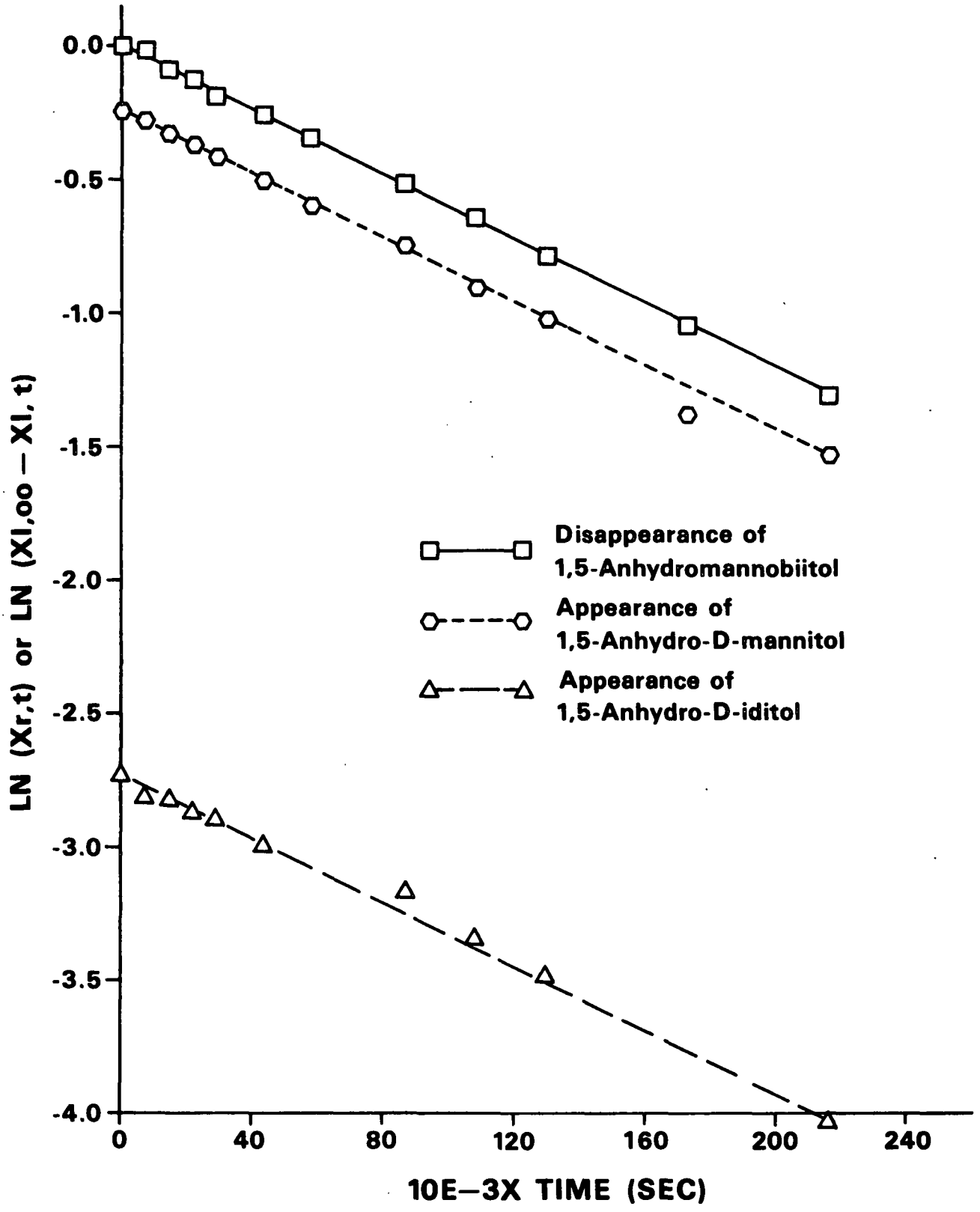

Figure 15. Parallel pseudo-first-order kinetic analysis of 1,5-anhydro-mannobiitol in 2.5M NaOH at 170°C.

$$\frac{dL}{dt} = k_f\ R - k_d\ L \qquad (16)$$

where L = concentration of unstable product, moles/L
R = concentration of reactant, moles/L
k_f = pseudo-first-order rate constant for unstable product formation, sec^{-1}
k_d = pseudo-first-order rate constant for unstable product degradation, sec^{-1}

Substituting Eq. (9) into Eq. (12) gives:

$$\frac{dL}{dt} = k_f\ R_o\ \exp(-k_r t) - k_d\ L \qquad (17)$$

Integration and rearrangement yields:

$$L - L_o\exp(-k_d t) = k_f\ [R_o/(k_d-k_r)]\ [\exp(-k_r t)-\exp(-k_d t)] \qquad (18)$$

The pseudo-first-order rate constant for the formation of an unstable product can be calculated from Eq. (18) if the pseudo-first-order rate constant for the degradation of the unstable product is also known.

APPARENT THERMODYNAMIC FUNCTIONS OF ACTIVATION

The Universal Rate Law [Eq. (19)] can be derived from the transition state theory of chemical kinetics.[43,44]

$$\ln(k_r/T) = [\ln(k/h) + \Delta S^{\ddagger}/R] - \Delta H^{\ddagger}/RT \qquad (19)$$

where k = Boltzmann's constant, 1.380×10^{-6} erg K^{-1}
T = absolute temperature, °K
h = Planck's constant, 6.625×10^{-27} erg sec
$\Delta S^{\ddagger}$ = apparent entropy of activation, cal/mole °K
R = gas constant, 1.987 cal/mole °K
$\Delta H^{\ddagger}$ = apparent enthalpy of activation, cal/mole

Fitting the rate constants obtained at various temperatures to Eq. (19) using least-squares linear regression (Program 4, Appendix I) allowed calculation of $\Delta H^{\ddagger}$ and $\Delta S^{\ddagger}$ from the slope and intercept, respectively. A representative plot is shown in Fig. 16.

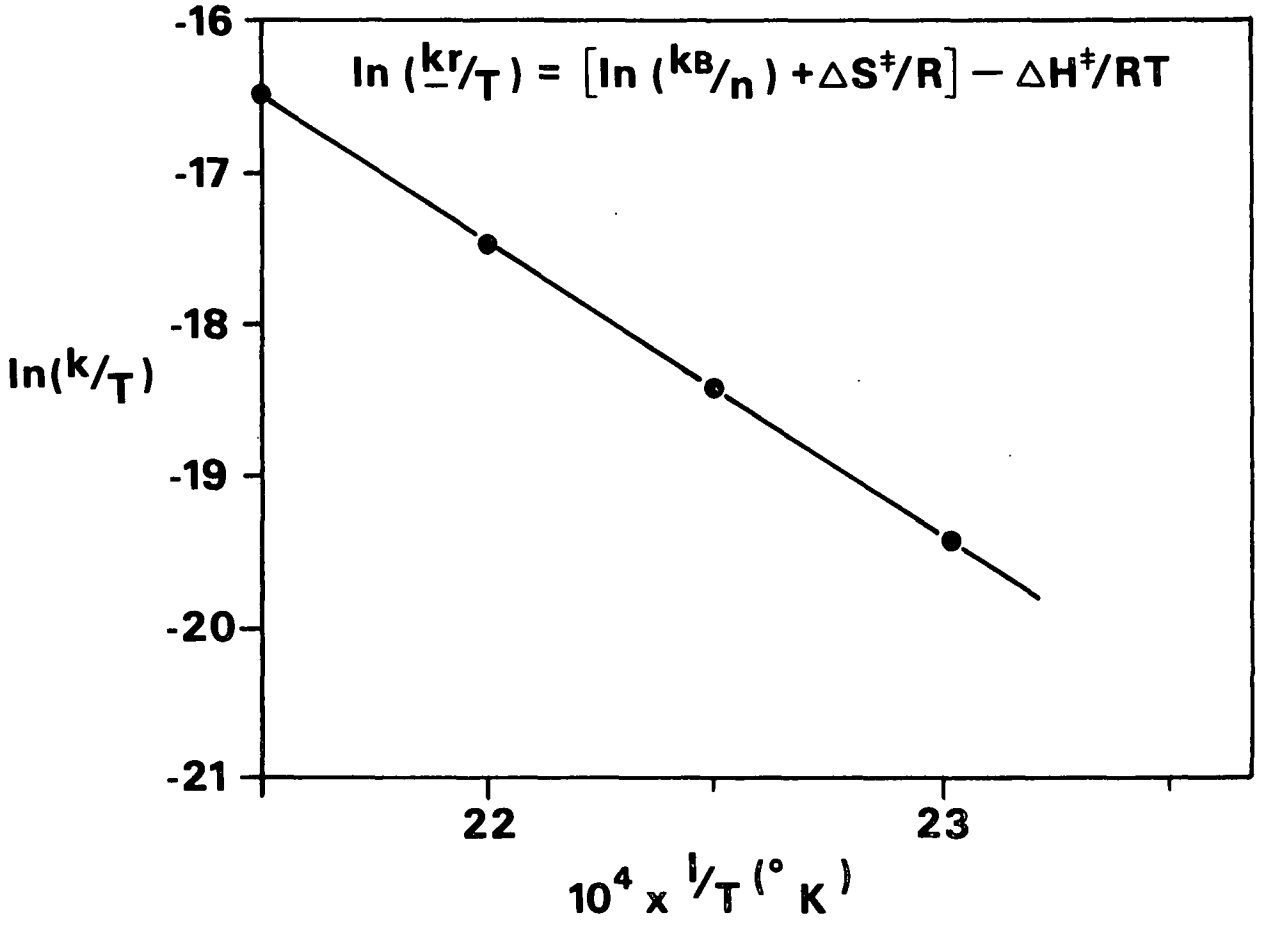

Figure 16. Rate constants for the degradation of 1,5-anhydromannobiitol plotted as a function of temperature according to the Universal Rate Law.

In order to compare rate constants obtained from reactions run at slightly different temperatures, all rate constants were adjusted to a common temperature. This was done using the following form of the Arrhenius equation:

$$k_{T2} = \exp[\ln k_{T1} - (E_a/R)\ (1/T2 - 1/T1)] \qquad (20)$$

where k_{T2} = pseudo-first-order rate constant at the common temperature, sec^{-1}

K_{T1} = pseudo-first-order rate constant at the reaction temperature, sec^{-1}

E_a = apparent activation energy, cal/mole

T1 = absolute reaction temperature, °K

T2 = absolute common temperature, °K

A computer program which adjusts the rate constants according to Eq. (20) is available (Program 6, Appendix I). Temperatures were adjusted less than 2°C.

ALKALINE DEGRADATION OF 1,5-ANHYDRO-4-O-β-D-MANNOPYRANOSYL-D-MANNITOL

Analysis of Products

Alkaline degradation of 1,5-anhydromannobiitol produced two stable products, 1,5-anhydro-D-mannitol (70-85%) and 1,5-anhydro-D-iditol (0-8%). These compounds were identified by comparing their gas chromatographic retention times and gas chromatography/mass spectra to those of known compounds. A separate reaction showed that 1,5-anhydro-D-mannitol was stable under typical reaction conditions for over 28 half-lives of 1,5-anhydromannobiitol. Other 1,5-anhydro-D-alditols have been shown to be stable under similar conditions.[13,14] Since 1,5-anhydro-D-iditol is also an anhydroalditol, it is almost certainly stable under the reaction conditions as well. A 0-30% difference between the moles of 1,5-anhydromannobiitol degraded and moles of products formed from the aglycon was observed. This mole deficit is probably due to fragmentation of the aglycon into products undetectable with the gas chromatography procedures used, and will be referred to as the unidentified fragments.

Because large amounts (ca. 60%) of 1,6-anhydro-β-D-mannopyranose (levomannosan) reportedly formed from the alkaline degradation of phenyl β-D-mannopyranoside,[45] this product was searched for in the 1,5-anhydromannobiitol

system. None was found. Compounds analogous to levomannosan degrade under high temperature alkaline conditions. If the rate constant for degradation of levomannosan is larger than its rate constant for formation, no levomannosan would accumulate in the system. Thus none would be detected even if it were forming.

The fraction of levomannosan formed during the degradation of 1,5-anhydromannobiitol can be defined by Eq. (21).

$$F = k_f/k_r \tag{21}$$

where F = the fraction of 1,5-anhydromannobiitol which degrades to levomannosan

k_f = rate constant for levomannosan formation

k_r = rate constant for 1,5-anhydromannobiitol degradation

Substituting Eq. (21) into (18) and assuming that the initial concentration of levomannosan (L_o) equals zero gives:

$$L = F^{*}k_r[R_o/(k_d-k_r)]\ [\exp(-k_r t)-\exp(-k_d t)] \tag{22}$$

Equation (22) can be used to calculate the concentration of levomannosan at any time if the rate constants for both 1,5-anhydromannobiitol and levomannosan degradation are known.

The rate constant for levomannosan degradation was therefore measured by degrading levomannosan under one set of reaction conditions (160°C, 2.5M NaOH). The measured rate constant was 5.6×10^{-6} sec^{-1}. Once the rate constant for the degradation of levomannosan had been determined, the fraction of levomannosan which could form without being detected in the gas chromatographic analysis could be calculated using Eq. (22). Figure 17 shows the concentration of levomannosan plotted as a function of time for different fractions of formation.

The minimum concentration of levomannosan detectable by gas chromatography was approximately 0.00002M. Therefore, if more than 1% of the 1,5-anhydromannobiitol had degraded to give levomannosan, levomannosan should have been found in the GC chromatograms.

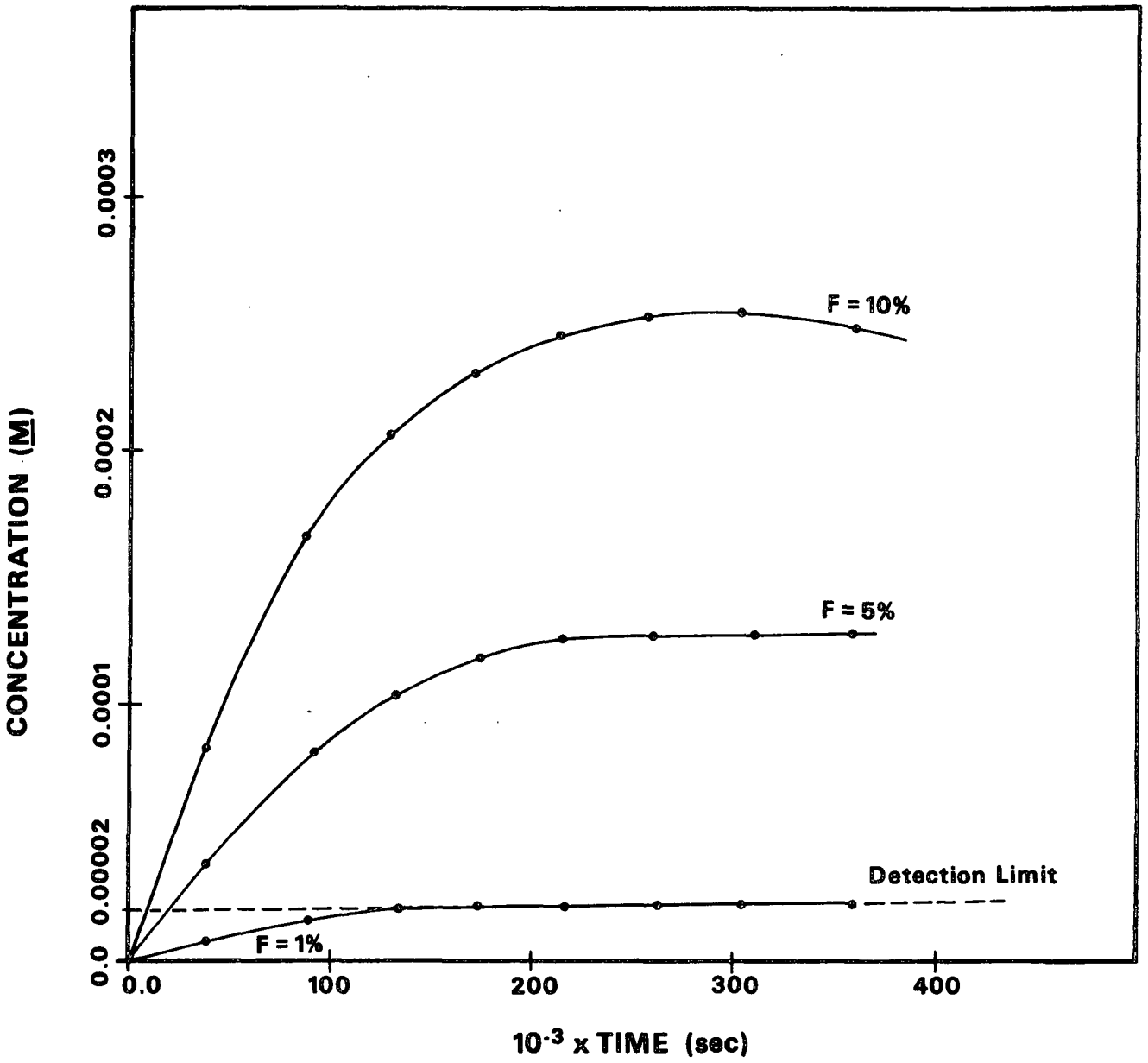

Figure 17. Predicted concentrations of 1,6-anhydro-β-D-mannopyranose as a function of time at various fractions of formation from the degradation of 1,5-anhydromannobiitol in 2.5M NaOH at 160°C.

Points of Bond Cleavage

The glycosidic linkage in 1,5-anhydromannobiitol can cleave in two places; at either the glycosyl-oxygen or oxygen-aglycon bond. To correctly analyze the kinetic results, it is important to know what fraction of the cleavage occurs at each bond. The major stable product, 1,5-anhydro-D-mannitol, always forms when the glycosyl-oxygen bond cleaves. This same product sometimes forms from oxygen-aglycon bond cleavage as well. To calculate the fractions of glycosyl-oxygen and oxygen-aglycon cleavage, the 1,5-anhydro-D-mannitol produced from each cleavage must be identified. This was done by degrading the 1,5-anhydro-mannobiitol in liquors enriched with ^{18}O. 1,5-Anhydro-D-mannitol formed by glycosyl-oxygen bond cleavage does not add any oxygen from the liquor; thus it will not become enriched in ^{18}O. 1,5-Anhydro-D-mannitol formed by oxygen-aglycon bond cleavage, however, must pick up an oxygen atom from the liquor and therefore will become enriched with ^{18}O. A mass spectrometer was used to measure the amount of enriched and unenriched 1,5-anhydro-D-mannitol produced from the degradation of 1,5-anhydromannobiitol. From these measurements, it is possible to calculate the fractions of oxygen-aglycon and glycosyl-oxygen bond cleavage. A method for doing this is outlined in Appendix V.

The percent of the total 1,5-anhydro-D-mannitol which formed from oxygen-aglycon bond cleavage is shown in Table 2. The ^{18}O incorporation studies also showed that 100% of the 1,5-anhydro-D-iditol results from cleavage of the oxygen-aglycon bond.

Rates of Bond Cleavage

Formation of 1,5-anhydro-D-mannitol from 1,5-anhydromannobiitol is analogous to the formation of 1,5-anhydro-D-glucitol from 1,5-anhydrocellobiitol. In the 1,5-anhydrocellobiitol system, it was assumed that all of the 1,5-anhydro-D-

glucitol resulted from glycosyl-oxygen bond cleavage.[13,14] Therefore, the rate constant for formation of 1,5-anhydro-D-glucitol was used as the rate constant for glycosyl-oxygen cleavage. Degradation of 1,5-anhydrocellobiitol in ^{18}O-enriched liquor showed that less than 1% of the glucitol formed has been produced by oxygen-aglycon bond cleavage,[46] hence this was a good assumption. During the degradation of 1,5-anhydromannobiitol, however, significant amounts of 1,5-anhydro-D-mannitol formed from oxygen-aglycon bond cleavage as well as glycosyl-oxygen bond cleavage. Therefore, the overall rate of 1,5-anhydro-D-mannitol formation (k_{MNT}) cannot be equated with the rate of glycosyl-oxygen bond cleavage (k_{GO}).

Table 2. Percentage of 1,5-anhydro-D-mannitol resulting from the cleavage of the oxygen-aglycon bond in 1,5-anhydromannobiitol.

Temperature, °C	[NaOH]	[NaOTs]	% MNT-OA[a]
161.8	2.51	0.0	3.89
170.5	2.50	0.0	5.05
180.7	2.50	0.0	5.37
190.6	2.51	0.0	5.51
170.5	2.50	0.0	5.05
170.5	1.50	1.0	4.14
170.5	1.00	1.5	3.95
170.5	0.50	2.0	3.54
170.5	0.50	0.0	3.81
171.1	1.51	1.0 (NaSH)	0.07

[a]Percentage of the total 1,5-anhydro-D-mannitol formed from cleavage of the oxygen-aglycon bond in 1,5-anhydromannobiitol.

The rate constants for oxygen-aglycon and glycosyl-oxygen bond cleavage can be calculated, however, once both the overall rate constant for mannitol formation and the percentage of 1,5-anhydro-D-mannitol resulting from cleavage of the oxygen-aglycon bond are known. The mannitol formed by oxygen-aglycon bond

cleavage and that formed by glycosyl-oxygen bond cleavage must equal the total mannitol formed, so:

$$k_{MNTGO} = k_{MNT} - k_{MNTOA} \tag{23}$$

where k_{MNTGO} = the rate constant for formation of 1,5-anhydro-D-mannitol via glycosyl-oxygen bond cleavage.

k_{MNTOA} = the rate constant for formation of 1,5-anhydro-D-mannitol via the oxygen-aglycon bond cleavage.

k_{MNT} = overall rate constant for 1,5-anhydro-D-mannitol formation.

Cleavage of the glycosyl-oxygen bond always produces mannitol. Therefore the rate constant for the formation of mannitol via glycosyl-oxygen cleavage must equal the rate constant for glycosyl-oxygen bond cleavage:

$$k_{GO} = k_{MNTGO} \tag{24}$$

Cleavage must occur at either the glycosyl-oxygen or oxygen-aglycon bonds. Therefore the overall rate constant for degradation must equal the sum of the rate constants for each bond:

$$k_r = k_{GO} + k_{OA} \tag{25a}$$

or

$$k_{OA} = k_r - k_{GO} \tag{25b}$$

Thus the rate constants for the cleavage of both the glycosyl-oxygen and oxygen-aglycon bonds can be calculated.

Glycosyl-Oxygen Bond Cleavage

Products

Cleavage of the glycosyl-oxygen bond in 1,5-anhydromannobiitol always produces 1,5-anhydro-D-mannitol, regardless of the mechanism of cleavage. Therefore, production of this product indicates nothing about the mechanisms of cleavage.

Effect of Temperature

Table 3 shows how the rate constant for glycosyl-oxygen bond cleavage varies with temperature. As expected, the rate of glycosyl-oxygen cleavage increased markedly with temperature.

Table 3. Effect of temperature on the glycosyl-oxygen bond cleavage of 1,5-anhydromannobiitol in 2.5M NaOH.

Temperature, °C	10^6 k_{GO}, sec^{-1}
162.2	1.91 ± 0.11
171.1	4.57 ± 0.13
181.3	10.9 ± 0.34
191.9	28.1 ± 0.21

Apparent thermodynamic functions of activation were calculated from this data as described previously. Table 4 shows the enthalpy and entropy values obtained.

Table 4. Apparent thermodynamic functions of activation for cleavage of the glycosyl-oxygen bond in 1,5-anhydromannobiitol.

	$\Delta H^{\ddagger}$, kcal/mole	$\Delta S^{\ddagger}$, cal/mole °K
GO bond	35.3 ± 2	-4.3 ± 0.9
Overall	36.4 ± 2	-1.4 ± 0.3

Apparent thermodynamic functions are relative, and therefore must be compared to the values obtained from compounds degrading via previously identified mechanisms to be meaningful. Table 5 lists the enthalpy and entropy values for some reference compounds.

Table 5. A comparison of the apparent thermodynamic functions of various reactions.

Compound	Mechanism	$\Delta H^{\ddagger}$, kcal/mole	$\Delta S^{\ddagger}$, cal/mole °K	Reference
GO bond in mannobiitol[a]	?	35.3 ± 2	-4.3 ± 0.9	--[b]
Na methyl-α-D-glucopyranosiduronate	S_N1	40.0	+15.0	47
OA bond in 1,5-anhydrocellobiitol[c]	S_N1	41.7	+ 6.9	13, 14
Levoglucosan	$S_N1cB(2)$	32.8	- 3.8	25, 26
GO[d] bond in 1,5-anhydro-2,3,6-tri-O-methylcellobiitol	$S_N1cB(2)$	35.5	- 3.2	31
Methyl α-D-glucopyranoside	S_N2	32.4	-13.6	25, 26
GO bond in 1,5-anhydrocellobiitol[e]	Mixed S_N1 & $S_N1cB(2')$	37.1	+ 1.0	13, 14

[a]Glycosyl-oxygen bond in 1,5-anhydromannobiitol.
[b]This work.
[c]Oxygen-aglycon bond in 1,5-anhydrocellobiitol.
[d]Glycosyl-oxygen bond.
[e]Glycosyl-oxygen bond in 1,5-anhydrocellobiitol.

The enthalpy value for the glycosyl-oxygen bond in 1,5-anhydromannobiitol falls between that of the compounds thought to degrade via S_N1 mechanisms and those thought to cleave by S_N2 mechanisms. It is quite similar to the enthalpy value for the glycosyl-oxygen bond in 1,5-anhydro-2,3,6-tri-O-methyl-cellobiitol, which appears to degrade by an $S_N1cB(2)$ mechanism.

The entropy for the glycosyl-oxygen bond in 1,5-anhydromannobiitol is similar to the values found for levoglucosan and 1,5-anhydro-2,3,6-tri-O-methyl-cellobiitol, which are both thought to degrade via pure $S_N1cB(2)$ mechanisms.

The apparent thermodynamic functions of activation for the glycosyl-oxygen bond in 1,5-anhydromannobiitol therefore suggest that this bond is cleaved primarily by an $S_N1cB(i)$-type mechanism.

Effect of a Stronger Nucleophile

In an S_N2-type reaction, the nucleophile participates in the rate determining step. Therefore, the addition of a stronger nucleophile should accelerate an S_N2 reaction. In this work, the nonnucleophilic salt sodium tosylate was replaced with strongly nucleophilic sodium hydrosulfide. Earlier studies have shown that the hydrosulfide ion is a stronger nucleophile than hydroxide ion even at 170°C.[32,33] Table 6 shows the effect which addition of SH^- had on the cleavage of the glycosyl-oxygen bond.

Table 6. The effect of addition of a stronger nucleophile on the cleavage of the glycosyl-oxygen bond in 1,5-anhydromannobiitol at 170°C.

[NaOH]	[NaOTs]	[NaSH]	10^6k_{GO}, sec^{-1}
1.50	1.00	0.00	2.98 ± 0.06
1.50	0.00	1.00	3.07 ± 0.10

There is statistically no difference between the rate constants for glycosyl-oxygen cleavage when either sodium tosylate or sodium hydrosulfide is present. This indicates that an S_N2-type mechanism does not govern the glycosyl-oxygen bond cleavage. The reaction site is probably too hindered for the nucleophile to attack and cause S_N2-type cleavage. The possibility that hydroxide ion causes S_N2-type cleavage of the glycosyl-oxygen bond but that hydrosulfide ion is unable to do so because it is larger appears unlikely, since the size difference between these two ions is slight (1.5 vs. 1.85 Å, respectively).[48,49] However, solvation of the anions plays an unknown role.

Effect of Ionic Strength

The ionic strength of the reaction medium was varied by adding differing amounts of the nonnucleophilic salt, sodium tosylate, to liquors having the same hydroxide concentration. Table 7 illustrates the effect which this had on the rate constant for glycosyl-oxygen bond cleavage.

Table 7. The effect of varying the ionic strength at constant hydroxide concentration on the cleavage of the glycosyl-oxygen bond in 1,5-anhydromannobiitol at 170°C.

I (μ)	[NaOH]	[NaOTs]	$10^6 k_{GO}$, sec^{-1}
0.50	0.50	0.00	1.61 ± 0.05
2.50	0.50	2.00	1.79 ± 0.02

A fivefold increase in the ionic strength of the reaction medium caused an 11% increase in the rate of glycosyl-oxygen bond cleavage. The oxygen-aglycon bond in 1,5-anhydrocellobiitol, which is thought to cleave via an S_N1 mechanism, exhibited a 64% rate increase when the ionic strength was increased five times.[13,14] Levoglucosan, which degrades via an $S_N1cB(2)$ mechanism, had a negative 19% salt effect.[25,26] Therefore, the 11% rate increase observed for the glycosyl-oxygen bond cleavage in 1,5-anhydromannobiitol may indicate a mixed $S_N1cB(i)$ and S_N1 mechanism. Because S_N1 reactions have strong positive salt effects while $S_N1cB(i)$ mechanisms exhibit weak negative salt effects, it is possible that a very minor S_N1 component to the reaction could produce the small positive salt effect observed here.

Effect of Hydroxide Ion Concentration

A series of degradations at different hydroxide concentrations, in which the ionic strength was maintained at a constant level by adding appropriate amounts of sodium tosylate, were performed. Table 8 shows how these changes in

hydroxide concentration affected the rate constants for glycosyl-oxygen bond cleavage. Increasing the hydroxide ion concentration increases the rate of glycosyl-oxygen bond cleavage.

Table 8. Effect of varying hydroxide concentration at constant ionic strength on glycosyl-oxygen bond cleavage in 1,5-anhydromannobiitol at 170°C.

[NaOH]	[NaOTs]	$10^6 k_{GO}$, sec^{-1}
2.50	0.00	4.10 ± 0.13
1.50	1.00	2.98 ± 0.06
1.00	1.50	2.52 ± 0.10
0.50	2.00	1.79 ± 0.02

Lai showed that a compound which degrades via an $S_N1cB(2)$-type mechanism should show a linear reciprocal dependence on hydroxide concentration.[50] However, S_N1 and S_N2 mechanisms also exhibit linear reciprocal relationships when certain assumptions are made.[24-26] Figure 18 shows the reciprocal plot for the rate constants of glycosyl-oxygen cleavage vs. hydroxide concentration. The graph is linear.

The rate constants for the glycosyl-oxygen bond in 1,5-anhydrocellobiitol, which is thought to degrade via a mixed $S_N1cB(2)$ and S_N1 mechanism, are also linear when plotted in this manner, as shown in Fig. 18. This suggests that mixed mechanisms may also exhibit linear reciprocal behavior. Appendix VI gives the derivation of the hydroxide dependence equation for a mixed $S_N1cB(i)$ and S_N1 cleavage of the glycosyl-oxygen bond in 1,5-anhydromannobiitol. The assumed reaction scheme is shown at the top of page 48.

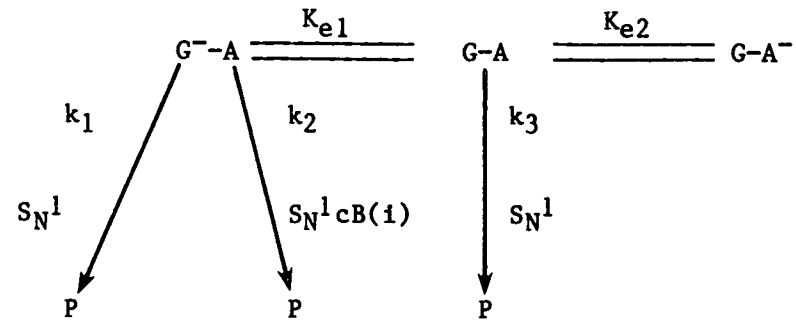

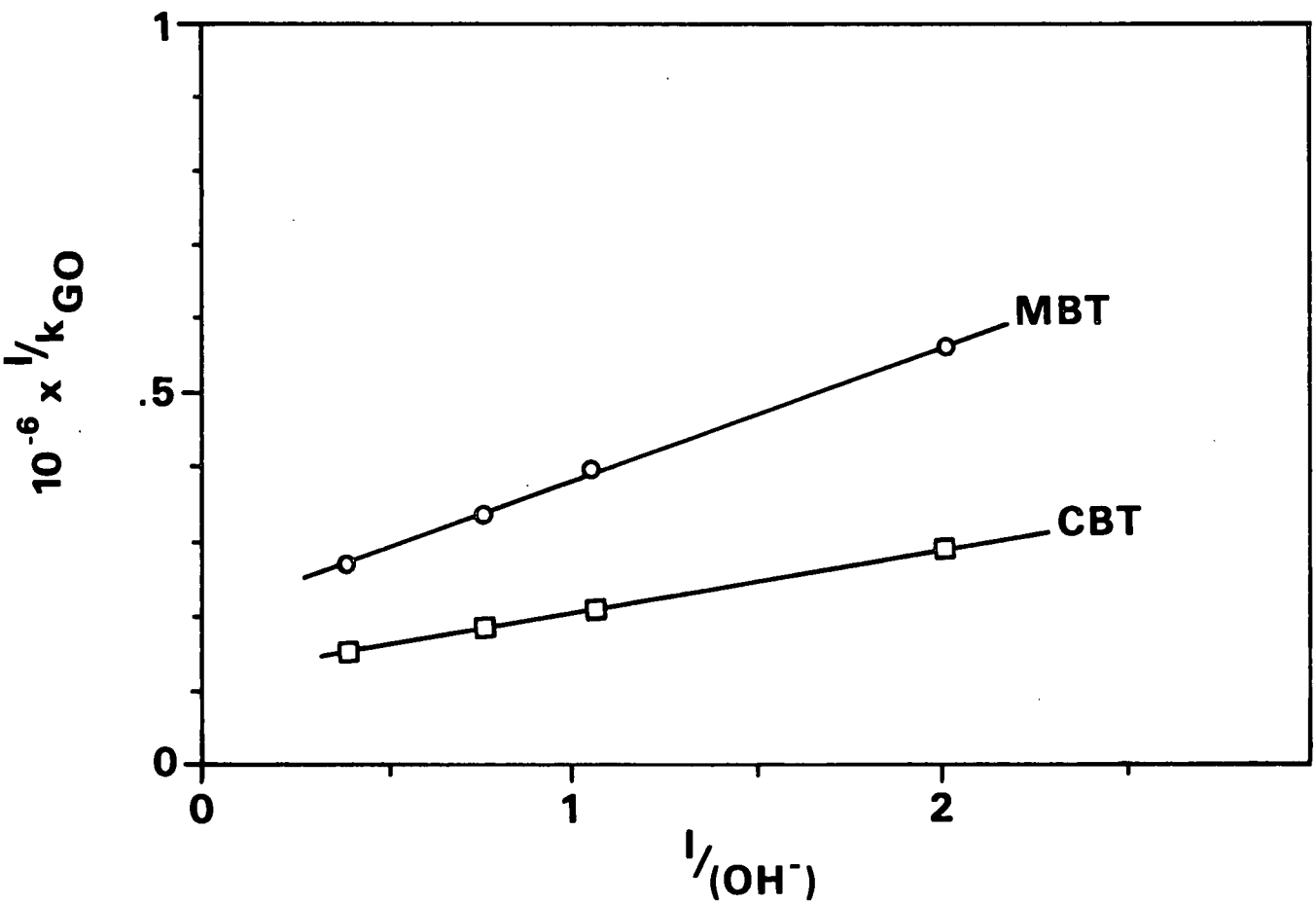

Figure 18. Relationship between reciprocal hydroxide concentration and rate constants for the cleavage of the glycosyl-oxygen bond in 1,5-anhydromannobiitol at 170°C.

The resulting equation is:

$$k_{GO} = \frac{\{k_1 K_e\ [OH^-] + k_2 K_{e1}\ [OH^-] + k_3\}}{\{1 + K_{e1}\ [OH^-] + K_{e2}\ [OH^-]\}} \qquad (26)$$

where k_{GO} = pseudo-first-order rate constant for cleavage of the glycosyl-oxygen bond.

k_1 = rate constant for cleavage of the glycosyl-oxygen bond in ionized MBT via an S_N1 mechanism.

k_2 = rate constant for cleavage of the glycosyl-oxygen bond in ionized MBT via an $S_N1cB(i)$ mechanism.

k_3 = rate constant for cleavage of the glycosyl-oxygen bond in neutral MBT via an S_N1 mechanism.

K_{e1} = equilibrium constant for ionization of the glycon.

K_{e2} = equilibrium constant for ionization of the aglycon.

$[OH^-]$ = hydroxide ion concentration.

If it is assumed that ionization of the glycon is important in stabilizing the carbocation formed during S_N1 cleavage, then k_3 should be much smaller than k_1 and k_2, and Eq. (26) reduces to:

$$k_{GO} \frac{\{(k_1 = k_2)\ K_{e1} * [OH^-]\}}{\{1 + (K_{e1} + K_{e2})\ [OH^-]\}} \qquad (27)$$

The inverse of Eq. (27) is:

$$\frac{1}{k_{GO}} = \frac{1}{K_{e1}\ (k_1 + k_2)} \cdot \frac{1}{[OH^-]} + \frac{(K_{e1} + K_{e2})}{(k_1 + k_2)} \qquad (28)$$

Equation (28) is linear with respect to hydroxide concentration. Therefore, the observed linear plot of $1/k_{GO}$ as a function of $1/[OH^-]$ could be consistent with either a mixed $S_N1/S_N1cB(i)$ mechanism or a pure $S_N1cB(i)$ mechanism. The fact that a linear relationship was found does not prove that either of these are the "correct" mechanism, since many different mechanisms may yield a linear reciprocal plot.

Effect of Methylating the Hydroxyl Groups

Neighboring group type mechanisms require that the hydroxyl group which acts as the conjugate base be able to ionize. Methylating a hydroxyl group prevents ionization and therefore stops neighboring group cleavage. To further test the importance of hydroxyl group ionization to glycosyl-oxygen bond cleavage in 1,5-anhydromannobiitol, the hydroxyl groups were fully methylated. The model compound was completely instead of selectively methylated for experimental reasons. Selective methylation is a multistep, low-yield process and only a small amount of 1,5-anhydromannobiitol was available for methylation.

Cleavage of the glycosyl-oxygen bond in methylated 1,5-anhydromannobiitol should yield 1,5-anhydro-2,3,6-tri-O-methyl-D-mannitol. This product was not found, suggesting that cleavage of the glycosyl-oxygen bond had stopped entirely. This result is indicative of a neighboring group mechanism. If ionization of the hydroxyl groups is important in stabilizing the cation formed during S_N1 cleavage of the glycosyl-oxygen bond, methylation could also slow or halt this type of reaction as well. However, the oxygen-aglycon bond in 1,5-anhydrocellobiitol is thought to degrade via an S_N1 mechanism and its rate of cleavage was unaffected when the aglycon was methylated.[31]

Summary

Six different mechanistic probes were used to elucidate the mechanism of glycosyl-oxygen bond cleavage in 1,5-anhydromannobiitol. The products found were consistent with all of the proposed mechanisms. The apparent thermodynamic functions of activation were typical for $S_N1cB(i)$ mechanisms. The lack of a rate increase upon the addition of a stronger nucleophile is not consistent with an S_N2 mechanism. The small positive salt effect was intermediate between that expected for either a pure S_N1 or $S_N1cB(i)$ mechanism. The reaction rate

constants had a strong positive dependence on hydroxide concentration, which indicates a major $S_N1cB(i)$ component to the mechanism. The plot of reciprocal rate vs. reciprocal hydroxide concentration was linear. This may be consistent with either a pure $S_N1cB(i)$ or mixed $S_N1cB(i)/S_N1$ mechanism, among others. Finally, the complete stoppage of the reaction when the hydroxyl groups were methylated is indicative of an $S_N1cB(i)$ mechanism. Thus it appears that the mechanism of cleavage for the glycosyl-oxygen bond in 1,5-anhydromannobiitol is primarily $S_N1cB(i)$ in nature. The small positive salt effect may indicate that the mechanism also has a minor S_N1 component.

The structure of 1,5-anhydromannobiitol prohibits backside neighboring group displacement of the aglycon by the 2, 3, and 6 hydroxyl groups. The hydroxyl at C-4 could conceivably displace the aglycon [an $S_N1cB(4)$ mechanism], but, as discussed previously, this is a very unlikely mechanism. The only other probable neighboring group mechanism is the $S_N1cB(2)$-ro one described earlier. This therefore is probably the major mechanism governing cleavage of the glycosyl-oxygen bond in 1,5-anhydromannobiitol.

Comparison to the Glycosyl-Oxygen Bond Cleavage in 1,5-Anhydro-4-O-β-Glucopyranosyl-D-Glucitol

If the glycosyl-oxygen bond in 1,5-anhydromannobiitol cleaves via the $S_N1cB(2')$-ro mechanism, it is interesting to consider whether this same mechanism can occur in 1,5-anhydrocellobiitol. Figure 19 shows that it is indeed possible. Whereas the traditional $S_N1cB(2)$ mechanism requires that 1,5-anhydrocellobiitol flip into its least stable chair conformation, the $S_N1cB(2)$-ro mechanism could take place when the molecule is in its most stable conformation. The $S_N1cB(2)$ro mechanism should therefore be even more energetically favored than the $S_N1cB(2)$ mechanism for 1,5-anhydrocellobiitol.

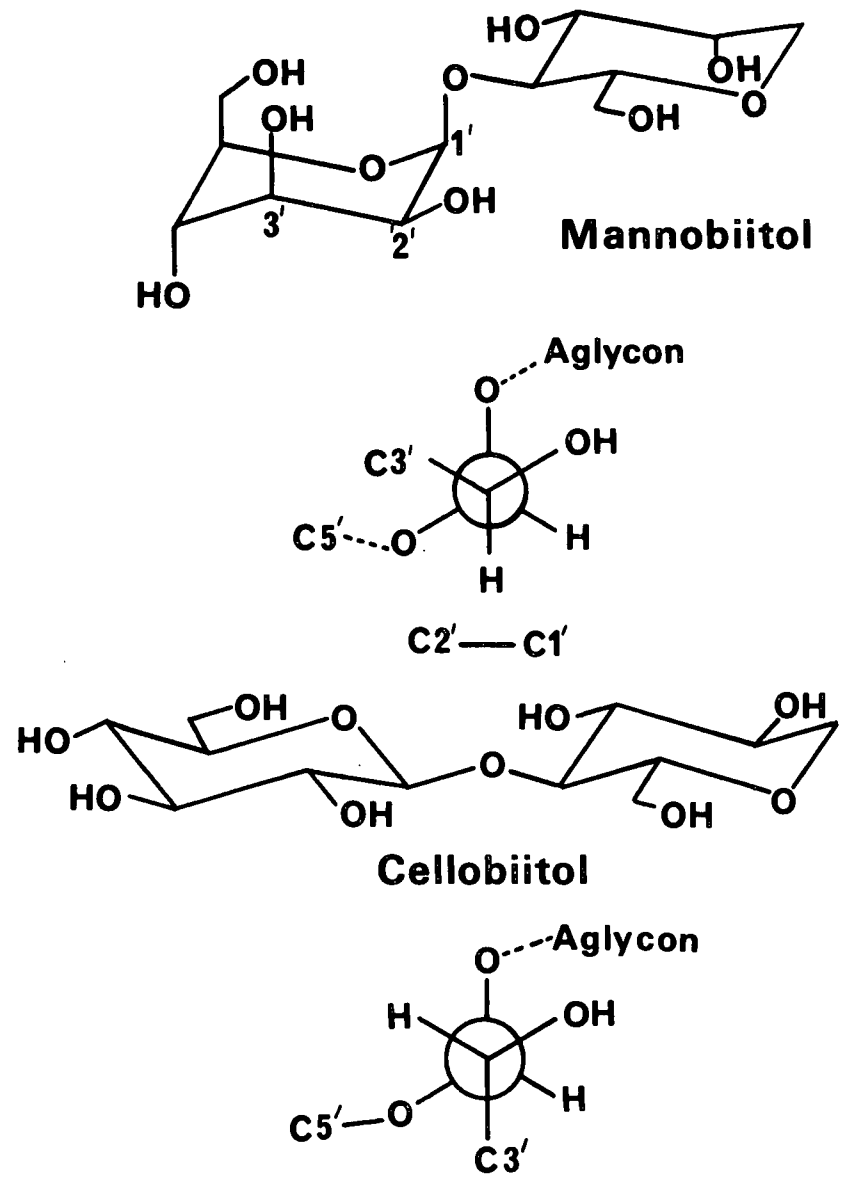

Figure 19. Possibility of the $S_N1cB(2)$-ro mechanism in 1,5-anhydrocellobiitol.

Some of the discrepancies observed in Brandon's study of 1,5-anhydrocellobiitol would be resolved if the $S_N1cB(2)$-ro mechanism operates for that compound. As discussed earlier, cleavage of the glycosyl-oxygen bond in 1,5-anhydrocellobiitol had the characteristics of a neighboring group mechanism, but the expected product of $S_N1cB(2)$ cleavage, levoglucosan, was formed only in low yield.[13,14] Since the $S_N1cB(2)$-ro mechanism would not produce levoglucosan but would otherwise behave like any neighboring group mechanism, it is quite

possible that some cleavage of the glycosyl-oxygen bond via the $S_N1cB(2)$-ro mechanism accounts for the lack of levoglucosan formation in 1,5-anhydrocellobiitol degradation.

OXYGEN-AGLYCON BOND CLEAVAGE

Products

Cleavage of the oxygen-aglycon bond in 1,5-anhydromannobiitol produced 1,5-anhydro-D-mannitol (0-22%), 1,5-anhydro-D-iditol (0-40%), and unidentified fragments (40-100%), as shown in Table 9. If S_N2 or $S_N1cB(6)$ mechanisms governed the reaction, 1,5-anhydro-D-talitol should have been produced, as discussed earlier. This compound was not found. In general, a 1:2 ratio of 1,5-anhydro-D-mannitol and 1,5-anhydro-D-iditol formed. The opening of a 3,4-anhydro-talopyranosyl intermediate under alkaline conditions gives mannose and idose derivatives in a 1:2 ratio.[51] A 1,5:3,4-dianhydro-D-talitol intermediate could form from either S_N1 or $S_N1cB(3)$ cleavage of the oxygen-aglycon bond, as shown in Fig. 8 and 10. Therefore, either of these two mechanisms is consistent with the observed products.

Effect of Temperature

Table 10 shows how the rate of oxygen-aglycon bond cleavage varied with temperature. The rates rise as temperature is increased.

The temperature-rate data were used to calculate apparent thermodynamic functions of activation. These values are listed in Table 11.

The 95% confidence intervals for $\Delta H^{\ddagger}$ and $\Delta S^{\ddagger}$ are large because the values of k_{OA} are small, and because so many mathematical manipulations of the data are necessary to compute these rate constants. Comparison of the $\Delta H^{\ddagger}$ and $\Delta S^{\ddagger}$ values

for the oxygen-aglycon bond in 1,5-anhydromannobiitol to those values for some compounds with previously identified degradation mechanisms (Table 5) shows that the enthalpy value is most similar to that for an S_N1 mechanism while the entropy is part way between typical S_N1 and $S_N1cB(i)$ mechanisms. Because of the large errors associated with the thermodynamic functions, however, they are not definitive.

Table 9. Rates of glycosyl-oxygen and oxygen-aglycon bond cleavage in 1,5-anhydromannobiitol.

Temp., °C	NaOH, M	NaOTs,[a] M	NaSH,[b] M	10^6k_{OA}, sec^{-1}	$X_{i,oo}$[c]		
					MNTOA[d]	X4[e]	UF[f]
162.2	2.5	--	--	0.51	0.15	0.29	0.56
171.1	2.5	--	--	1.48	0.16	0.27	0.57
181.3	2.5	--	--	4.30	0.14	0.21	0.64
191.9	2.5	--	--	10.12	0.16	0.30	0.54
170.0[g]	2.5	--	--	1.32	0.16	0.27	0.57
170.0[g]	1.5	1.0	--	1.03	0.12	0.21	0.67
170.0[g]	1.0	1.5	--	0.85	0.13	0.19	0.68
170.0[g]	0.5	2.0	--	0.51	0.13	0.22	0.65
170.0[g]	0.5	--	--	0.28	0.22	0.38	0.40
170.0[g]	1.5	--	1.0	1.21	0.00	0.00	1.00

[a]Sodium toluenesulfonate.
[b]Sodium hydrosulfide, added as Na_2S.
[c]Product fractions at infinity, k_i/k_{OA}.
[d]1,5-Anhydro-D-mannitol resulting from oxygen-aglycon bond cleavage.
[e]1,5-Anhydro-D-iditol.
[f]Unidentified fragments from the aglycon.
[g]Rate constants adjusted to 170.0°C.

Table 10. Effect of temperature on the rate of oxygen-aglycon bond cleavage for 1,5-anhydromannobiitol in 2.5M NaOH.

Temperature, °C	10^6k_{OA}, sec^{-1}
162.2	0.51 ± 0.22
171.1	1.48 ± 0.16
181.3	4.30 ± 0.55
191.9	10.1 ± 0.34

Table 11. Thermodynamic functions of activation for the oxygen-aglycon bond in 1,5-anhydromannobiitol.

	$\Delta H^{\ddagger}$, kcal/mole	$\Delta S^{\ddagger}$, cal/mole °K
k_{OA}	39.7 ± 8	+ 3.28 ± 2
overall	36.4 ± 2	- 1.37 ± 0.3

Effect of a Stronger Nucleophile

The effect of replacing the nonnucleophilic salt, sodium tosylate (NaOTs) with an equimolar amount of hydrosulfide ion (SH^-) is shown in Table 12. Although the addition of sodium hydrosulfide appeared to cause a 17% rate increase, the difference between the two rates is not statistically significant.

Table 12. The effect of addition of a stronger nucleophile on the cleavage of the oxygen-aglycon bond in 1,5-anhydromannobiitol at 170°C.

[NaOH]	[NaOTs]	[NaSH]	$10^6 k_{OA}$, sec^{-1}
2.50	1.00	0.00	1.03 ± 0.11
2.50	0.00	1.00	1.21 ± 0.18

When smaller amounts of SH^- (0.2-0.6M) were added to a methyl α-D-glucopyranoside reaction, which is known to proceed via an S_N2 pathway, rate increases of 60-992% were observed. Therefore, even if the 17% rate increase is real, it probably does not indicate any significant S_N2 pathway in this reaction. A small rate increase might be due to the fact that sodium hydrosulfide is a stronger base than sodium tosylate[52,53,54] and therefore would be better at ionizing the hydroxyl groups. It will be shown later that ionization of the hydroxyl groups promotes oxygen-aglycon bond cleavage.

The product distribution also shifts when SH^- is added to the system (refer to Table 9). Cleavage of the oxygen-aglycon bond no longer results in formation

of either 1,5-anhydro-D-mannitol or 1,5-anhydro-D-iditol. This suggests that SH^- interferes with the product-forming steps. In both the S_N1 and $S_N1cB(3)$ mechanisms, 1,5:3,4-dianhydro-D-talitol is the postulated intermediate (see Fig. 8 and 10). The SH^- nucleophile may compete very effectively with OH^- in opening this 3,4 epoxide ring. Attack by SH^- would yield thio-sugars and disulfides instead of anhydro-alditols.

Effect of Ionic Strength

The effect of changing the ionic strength of the medium while maintaining the hydroxide concentration is shown in Table 13. A fivefold increase in ionic strength caused an 82% increase in the rate of oxygen-aglycon bond cleavage. Because of the confidence intervals associated with these rates, the effect of the change in ionic strength could actually be anywhere between +25 and +144%. Since S_N1-type reactions typically have positive salt effects of +60-70%, this reaction appears to have significant S_N1 character.

Table 13. The effect of ionic strength on the rate of oxygen-aglycon bond cleavage in 1,5-anhydromannobiitol at 170°C.

I (μ)	[NaOH]	[NaOTs]	10^6k_{OA}, sec^{-1}
0.50	0.50	0.00	0.28 ± 0.07
2.50	0.50	2.00	0.51 ± 0.06

Effect of Hydroxide Ion Concentration

Table 14 shows that as the hydroxide concentration was increased while holding the ionic strength steady, the rate of oxygen-aglycon bond cleavage also increased sharply.

Table 14. Effect of varying the hydroxide concentration at constant ionic strength on the oxygen-aglycon bond cleavage in 1,5-anhydromannobiitol at 170°C.

[NaOH]	[NaOTs]	$10^6 k_{OA}$, sec^{-1}
0.50	2.00	0.51 ± 0.06
1.00	1.50	0.85 ± 0.12
1.50	1.00	1.03 ± 0.11
2.50	0.00	1.32 ± 0.16

Figure 20 is a plot of reciprocal rate vs. reciprocal hydroxide concentration. The rates for the cleavage of the oxygen-aglycon bond in 1,5-anhydromannobiitol are linear when plotted in this manner. For comparison, the rates of oxygen-aglycon cleavage in 1,5-anhydrocellobiitol are also plotted in Fig. 18. They follow a very different trend, decreasing somewhat in a non-linear manner as the hydroxide concentration increases.

The strong linear relationship observed for the oxygen-aglycon cleavage rates in 1,5-anhydromannobiitol is indicative of a neighboring group mechanism. As discussed for glycosyl-oxygen bond cleavage, either a pure $S_N1cB(i)$ or mixed $S_N1/S_N1cB(i)$ mechanism could give the observed linear relationship. The fact that oxygen-aglycon bond cleavage depends on the hydroxide concentration more strongly than the glycosyl-oxygen cleavage rates do may reflect the difficulty of ionizing the appropriate hydroxyl group rather than the extent to which an $S_N1cB(i)$ mechanism is occurring.[55]

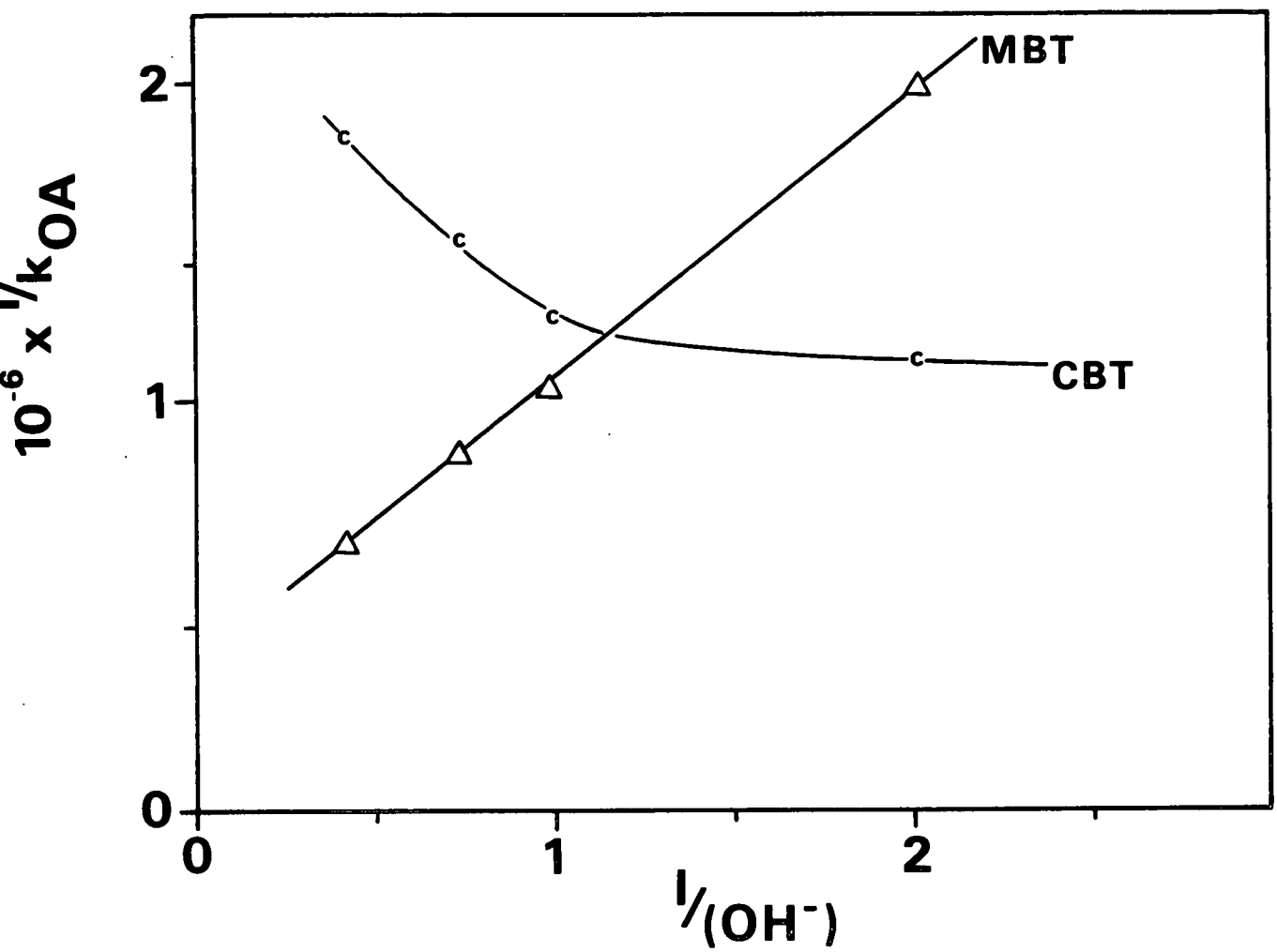

Figure 20. Relationship between reciprocal hydroxide concentration and rate constants for the cleavage of the oxygen-aglycon bond in 1,5-anhydromannobiitol at 170°C.

Effect of Methylating the Hydroxyl Groups

When 1,5-anhydromannobiitol was fully methylated, the rate of oxygen-aglycon bond cleavage was reduced by a factor of 17, as illustrated in Table 15. This suggests that cleavage of the oxygen-aglycon bond occurs partially via a neighboring group mechanism. The fact that the cleavage does not stop entirely indicates that some other mechanism, probably an S_N1 type, is also operative.

Table 15. The effect of fully methylating 1,5-anhydromannobiitol on the rate of oxygen-aglycon bond cleavage in 2.5M NaOH at 170°C.

Compound	$10^6 k_{OA}$, sec^{-1}
1,5-anhydromannobiitol	1.48
1,5-anhydro-2,3,6,2-,3-,4-,6-septa-O-methyl mannobiitol	0.086

Summary

The six probes used to investigate the mechanism of oxygen-aglycon bond cleavage yielded a variety of information. Lack of 1,5-anhydro-D-talitol formation ruled out the S_N2 and $S_N1cB(6)$ mechanisms. Based on the products found, either an S_N1 or $S_N1cB(3)$ mechanism is possible. The enthalpy of activation is characteristic of an S_N1 mechanism while the entropy indicates a mixed S_N1/$S_N1cB(i)$ mechanism. These thermodynamic functions are not conclusive, however, due to the large confidence intervals associated with them. The small rate increase observed when a stronger nucleophile than hydroxide, SH^-, was added is inconsistent with a major S_N2 component. A fivefold increase in ionic strength caused an 80% rise in the rate of oxygen-aglycon bond cleavage, indicating that the mechanism has significant S_N1 character. The rate of oxygen-aglycon bond cleavage showed a strong positive dependence on hydroxide concentration, which is typical of an $S_N1cB(i)$ mechanism. A plot of reciprocal rate vs. reciprocal hydroxide concentration was linear. Finally, the methylated analog of 1,5-anhydromannobiitol degraded 17 times more slowly than the free sugar. This indicates that a significant fraction of the oxygen-aglycon bond is cleaved via a neighboring group mechanism. Thus there is evidence that both S_N1 and $S_N1cB(i)$ mechanisms operate in the cleavage of the oxygen-aglycon bond.

As discussed earlier, theoretical considerations and the products found make the $S_N1cB(3)$ mechanism the most likely neighboring group mechanism for this

reaction. Therefore, the oxygen-aglycon bond in 1,5-anhydromannobiitol probably cleaves via a mixed $S_N1cB(3)/S_N1$ mechanism.

Comparison to the Oxygen-Aglycon Bond Cleavage in 1,5-Anhydro-4-O-β-Glucopyranosyl-D-Glucitol

The oxygen-aglycon bond in 1,5-anhydromannobiitol cleaved approximately twice as fast as the same bond in 1,5-anhydrocellobiitol. The cleavage of the oxygen-aglycon bond in 1,5-anhydrocellobiitol had all the characteristics of an S_N1-type mechanism, while the same bond in 1,5-anhydromannobiitol appears to cleave via a mixed $S_N1/S_N1cB(3)$ mechanism. This difference in mechanisms was unexpected, since the immediate environment around the oxygen-aglycon bond is quite similar in both compounds.

The $S_N1cB(3)$ mechanism requires that the OH(3) group and oxygen-aglycon bond at C-4 be trans-diaxial. To achieve this configuration, the aglycon must assume either the alternate chair ($^1C_4$) or a quasi-boat conformation. Figure 21 shows both 1,5-anhydrocellobiitol and 1,5-anhydromannobiitol in these two conformations. In the $^1C_4$ chair conformation, 1,5-anhydrocellobiitol has all its groups in axial positions. 1,5-Anhydromannobiitol, on the other hand, has the OH(2) group equatorial. Free-energy calculations show that,[56] because of this difference, 1,5-anhydromannobiitol is about twice as stable as 1,5-anhydrocellobiitol in the $^1C_4$ conformation at 25°C. In the quasi-boat conformation, 1,5-anhydrocellobiitol has axial OH(3) and OH(2) groups, whereas mannobiitol has only an axial OH(3); the OH(2) group is equatorial. Thus the mannobiitol should also be more stable than cellobiitol in the quasi-boat conformation. Greater stability of the conformation with the trans-diaxial-3,4 configuration should promote an $S_N1cB(3)$ reaction. This conformational difference is therefore a possible explanation as to why the $S_N1cB(3)$ mechanism occurs for mannobiitol but not cellobiitol.

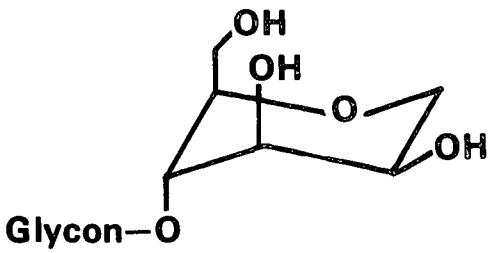

1,5-Anhydromannobiitol in the $^{1}C_{4}$ Conformation

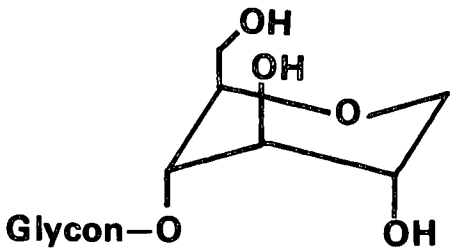

1,5-Anhydrocellobiitol in the $^{1}C_{4}$ Conformation

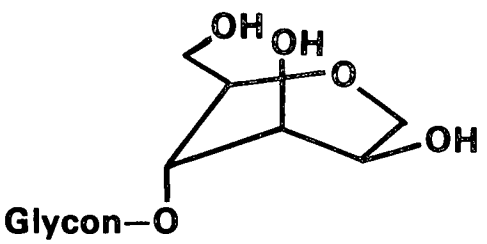

1,5-Anhydromannobiitol in the Quasi-boat Conformation

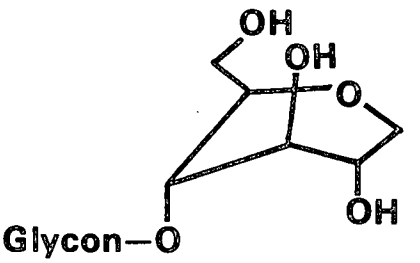

1,5-Anhydrocellobiitol in the Quasi-boat Conformation

Figure 21. Comparison of 1,5-anhydromannobiitol and 1,5-anhydrocellobiitol in conformations in which OH-3 and the glycosidic bond are trans-diaxial.

CONCLUSIONS

It is proposed that the glycosyl-oxygen bond in 1,5-anhydromannobiitol is cleaved primarily by an $S_N1cB(2')$-ro mechanism. An S_N1-type reaction may also be occurring to a small extent. The oxygen-aglycon bond appears to degrade by a mixed $S_N1cB(3)/S_N1$ mechanism.

This mechanism for oxygen-aglycon bond cleavage is quite different from that found for the oxygen-aglycon bond of 1,5-anhydrocellobiitol. Since 1,5-anhydromannobiitol and 1,5-anhydrocellobiitol differ only in the configuration of their OH(2) groups, it is clear that a small change in the conformation of a molecule can drastically affect its reaction mechanisms.

The $S_N1cB(2)$-ro mechanism proposed for the glycosyl-oxygen bond of 1,5-anhydromannobiitol is also a viable route for cleavage of the glycosyl-oxygen bond in 1,5-anhydrocellobiitol. In cellobiitol it can occur without a change in conformation. It is conceivable that the $S_N1cB(2)$-ro mechanism could also occur in the alkaline degradation of cellulose.

EXPERIMENTAL

GENERAL ANALYTICAL METHODS

Melting points were measured on a calibrated Thomas-Hoover capillary apparatus. Optical rotations were determined on a Perkin-Elmer 141-MC polarimeter. Thin layer chromatography (tlc) was done on silica gel D-5 (Camag) coated microscope slides using a sulfuric acid-methanol (1:4, v:v) spray followed by charring to detect components. Elemental analyses were performed by Huffman Laboratories (Wheat Ridge, Colorado).

The ^{1}H- and ^{13}C-NMR spectra were recorded on a Jeol FX-100 spectrometer. Samples were dissolved in deuterated solvents with tetramethylsilane added as an internal standard.

Gas chromatography was done on a Perkin-Elmer Sigma 2 chromatograph equipped with a flame-ionization detector and linked to a Perkin-Elmer Sigma 10 data station. Analyses were performed on a column (stainless steel, 6 ft x 0.125 inch) packed with OV-101 (3%) on Supelcoport (80-100 mesh), rigged for on-column injection. Nitrogen (30 mL/min) was used as the carrier gas. The following operating conditions were used: (A) Injector, 275°C; detector, 300°C; and column, 130°C for 1 min, 5°/min to 275°C, and held at 275°C. (B) Injector, 275°C; detector, 300°C; and column, 130°C for 1 min, 5°/min to 260°C, and held at 260°C. (C) Injector, 275°C; detector, 300°C; and column, 100°C for 1 min, 5°/min to 250°C, and held at 250°C for 1 min.

Fehling's tests were run by placing a few grains or drops of the material to be tested in a test tube, adding 2 drops of solution A (0.277M cupric sulfate pentahydrate) and 2 drops of solution B (2.5M NaOH and 1.23M potassium sodium

tartrate) or enough to give a dark blue solution. The mixture was then heated with steam for a few minutes. The formation of a red precipitate indicated the presence of a reducing sugar.[57]

The ferric hydroxamate test for esters was performed by placing several milligrams of sample in a test tube, and adding 1 drop of hydroxylamine in ethanol (0.5M) and 2 drops of methanolic KOH (2M). The mixture was heated to boiling, cooled under tap water, then mixed with several drops of dilute HCl (2N) and one drop of aqueous ferric chloride solution (10%). The formation of a dark red or magenta color indicated the presence of an ester or lactone.[57]

High Pressure Liquid Chromatography (HPLC) was performed with a Varian 8500 pump using degassed, distilled water at 0.6 mL/min. A Bio-Rad HPX-87 carbohydrate column (300 x 7.8 mm ID) was maintained at 82°C and protected with a Bio-Rad carbohydrate Micro-Guard column. A Valco six-way valve fitted with a 50 µL loop was used to inject samples. Distilled water was used as the trapped reference in a Waters R401 differential refractometer maintained at 30°C. Chromatograms were recorded on a Varian A-25 recorder equipped with a disk integrator.

Gas chromatography/mass spectrometry was performed on a Hewlett-Packard 5985 system. The ^{18}O-enriched liquors were analyzed using a Porapak-Q column, 100°C isothermal conditions, and electron impact mass spectrometry. Analysis of the ^{18}O-content of 1,5-anhydro-D-alditols utilized an OV-225 column and negative chemical ionization mass spectrometry. The operating conditions were: 1 min at 130°C, 4°/min to 200°C. Selective ion monitoring was used to collect data in both cases.

SOLVENTS, REAGENTS, AND CATALYSTS

Anhydrous Methanol

Magnesium turnings (20 g) were covered with reagent grade methanol (300 mL). Iodine (0.05 g) was added slowly until a vigorous reaction occurred. After this subsided, additional methanol (1.5 L) was added. The mixture was refluxed for 3 hours, then fractionally distilled.[58] The first 100 mL of distillate were discarded, and the next 1600 mL were collected and stored in tightly-sealed bottles.

Anhydrous Ethanol

Absolute ethanol was reacted with magnesium and iodine as described for methanol, but the mixture was heated to initiate the reaction. The dry ethanol was fractionally distilled and stored in dark, tightly-sealed bottles.[58]

Anhydrous Pyridine

Pyridine (1500 mL) was refluxed over KOH pellets (250 g) for 3 hours, and then fractionally distilled.[58]

Dimethylformamide

Dimethylformamide was dried by refluxing with benzene. The benzene was then distilled off and the dimethylformamide was purified of decomposition products by distilling under vacuum.[59]

Dimethyl Sulfoxide

Anhydrous dimethyl sulfoxide was prepared by stirring dimethyl sulfoxide (1500 mL) over powdered calcium hydroxide (30 g) for 2 hours, followed by fractional distillation at ca. 10 mm Hg and 80-90°C.[60]

Acetic Anhydride

Acetic anhydride (reagent grade, 1500 L) was fractionally distilled.[58] The first 200 mL were discarded and the next 1000 mL collected.

Methyl Iodide

Methyl iodide was purified by fractional distillation. It was stored over clean copper wire in a dark bottle.[60]

Sodium Methoxide (1N)

Sodium methoxide (1N) was prepared by dissolving sodium metal (5.8 g) in anhydrous methanol (250 mL). Pea-sized sodium chunks were weighed in mineral oil, washed once with toluene, and twice with methanol, then carefully dropped into the anhydrous methanol.

Triphenylmethyl Chloride

Triphenylmethyl chloride (98%, Aldrich) was crystallized from benzene/acetyl chloride, then recrystallized from benzene/petroleum ether.[61]

p-Toluenesulfonyl Chloride

Crude p-toluenesulfonyl chloride (100 g) was dissolved in a minimum amount of $CHCl_3$ (200 mL), diluted with low boiling petroleum ether (1250 mL), and decolorized with carbon. The mixture was placed in loosely covered beakers and warmed gently while stirring. When the volume had been reduced 95%, the solution was cooled and crystals formed. These were filtered, washed with petroleum ether, and dried in vacuo. The total yield was 84.62 g (84.6%): m.p. 65.7-70.0°C. Literature: m.p. 67.5-68.5°C.[62]

Silver Nitrate Solution (3%)

Silver nitrate (3 g) was dissolved in water (5 mL), then diluted with acetone (95 mL).

Hydrogen Bromide in Glacial Acetic Acid

Solutions of hydrogen bromide in acetic acid were made by bubbling hydrogen bromide gas through a known weight of glacial acetic acid in tared 1 L bottles. After the first 30 minutes the bottles were cooled in ice. The amount of hydrogen bromide absorbed was monitored gravimetrically, and addition of gas was stopped when the concentration reached 32-40%.[32,33] The bottles were sealed, wrapped with aluminum foil, and refrigerated.

Raney Nickel (Type W-5)

Raney nickel alloy (400 g) was added slowly to a stirred, cooled sodium hydroxide solution (6.4M, 2080 mL) such that the temperature remained between 45 and 55°C. The slurry was digested at 50°C for 30-60 minutes, decanted, and extracted continuously until the effluent water was neutral. It was then solvent-exchanged into tetrahydrofuran:ethanol (1:1, v:v) by decantation (3 x 200 mL) and centrifugation and decantation (3 x 200 mL).[63]

SYNTHESIS OF COMPOUNDS

Mannan A

Coarsely ground ivory nuts (Phytelephas macrocarpa), obtained from Pfanstiehl, were ground in a Wiley mill using a No. 5 screen. The final consistency was similar to that of beach sand. Ground ivory nuts (165 g) were extracted with chloroform:methanol (1:1, 2000 mL) for twelve hours in a Soxhlet extraction apparatus, then 100 g of the extracted nuts were added to a warm (30°C) solution of sodium chlorite (250 g) in water (2500 mL). After heating to 35°C, glacial acetic acid (250 mL) was added and the mixture was placed in a 30°C water bath for 24 hours. The bleached nuts were filtered, washed with water and methanol, and dried in vacuo at 40°C to yield 90 g (90%) of a white solid.

Bleached ivory nuts (75 g) were placed in an NaOH solution (6%, 2.82 L) and left at room temperature for 3 days, with occasional shaking. The mixture was filtered and the collected solids (Mannan B) were washed with water and methanol, then dried. The filtrate was neutralized with glacial acetic acid (300 mL) and Mannan A was precipitated by adding methanol (3 L). The precipitate was collected by filtration, washed with hydrochloric acid (1N, 100 mL), water (5 x 500 mL), and methanol (2 x 500 mL), and dried under vacuum at 40°C. This yielded 15-25 g Mannan A and 35-50 g Mannan B.[39]

Mannobiose

Mannan A (55 g) was mixed with acetic anhydride (330 mL) and cooled to 0°C. First glacial acetic acid (330 mL), then concentrated sulfuric acid (33 mL) were added dropwise. The mixture was stirred at room temperature and the amount of acetolysis monitored via tlc (chloroform:ethyl acetate, 10:1). After approximately 3 days, the mixture was filtered, poured into water (2 L), and stirred for 1 hour. This mixture was extracted with chloroform (1 x 200 mL, 4 x 50 mL) and the combined extracts were washed with aqueous sodium bicarbonate (saturated, 3 x 200 mL) and water (2 x 250 mL), dried over anhydrous potassium carbonate, and reduced *in vacuo* to a thick oil (130 g).[40]

Sodium methoxide (1M, 50 mL) was added to a solution of the mannosaccharide acetate mixture (130 g) dissolved in anhydrous methanol (250 mL). The mixture was shaken for an hour and stored overnight in the freezer. A small sample was dissolved in water, deionized, and reduced to an oil. A ferric hydroxamate test was run on this sample to check for the presence of acetate groups. If the ferric hydroxamate test was positive, additional sodium methoxide was added. Otherwise, the mixture was dissolved in water (200 mL), deionized with resin

(Dowex 5W-X8H, 5 g), decolorized with carbon (J. T. Baker), then reduced in vacuo to a thick syrup (62 g).

A 5 x 100 cm column was slurry-packed with 500 g of Sephadex G-15 swollen in 10 L of water for 12 hours. The deacetylated syrup was pipetted onto the column, the column eluted with water, and 10 mL fractions were collected. Sugars appeared in fractions 50-115. Analysis by tlc suggested the following identities for the fractions; 93-118, mannose (5.83 g); 83-92, mannobiose (3.44 g); 76-82, mannotriose (1.25 g); 66-74, mannotetrose (0.57 g); 60-65, mannopentose (0.14 g). Attempts to crystallize the crude mannobiose from isopropanol and n-butanol were unsuccessful. The ^{1}H-NMR spectrum (D_2O) was consistent with literature spectra.[41] A ^{13}C-NMR spectrum (D_2O) (Fig. 27, Appendix III) showed: 61.6 (C_6), 62.1 (C_6'), 67.7 (C_4'), 70.1 (α-C_3), 71.3 (α-C_2), 71.6 (β-$C_{2,2'}$), 72.0 (α-C_5), 72.8 (β-C_3), 73.9 (C_3'), 75.9 (β-C_5), 77.5 (β-$C_{4,5'}$), 77.9 (α-C_4), 94.9 (α-C_1, β-C_1), 101.3 (C_1'). The ^{13}C spectrum was also consistent with published spectra for mannobiose.[41,42]

Mannobiose Octaacetate

Crude mannobiose (19.8 g) was dissolved in hot pyridine, and the solution was cooled to 0°C in an ice bath. Acetic anhydride (300 mL) was added dropwise while cooling and stirring. The solution was stirred for twelve hours, quenched with water (300 mL), and extracted with chloroform (1 x 300 mL, 2 x 50 mL). The combined chloroform extracts were washed with hydrochloric acid (1.0N) until the spent aqueous layer was acidic (10 x 100 mL) and then with water until neutral (5 x 100 mL), dried over potassium carbonate, filtered, and reduced in vacuo to a thick syrup. The ^{13}C-NMR spectrum is shown in Fig. 28, Appendix III.

1,5-Anhydro-4-O-β-Mannopyranosyl-D-Mannitol

Mannobiose octaacetate syrup (27.4 g) in 1,2-dichloroethane (40 mL) was mixed with hydrogen bromide in glacial acetic acid (36%, 30 mL). The solution was stirred for two hours, then water (200 mL) was added. The mixture was extracted with chloroform (2 x 50 mL). The combined chloroform extracts were washed with water (4 x 100 mL), sodium bicarbonate solution (saturated, 5 mL), and water (2 x 100 mL); dried over potassium carbonate; and reduced *in vacuo*. The oil was thinned with THF and concentrated twice.

The crude mannobiosyl bromide peracetate was dissolved in tetrahydrofuran (ca. 25 mL) and mixed with Raney nickel (ca. 164 g) and triethylamine (40 mL). The mixture was refluxed for 5 hours. The reaction was monitored with tlc (chloroform:ethyl acetate, 1:1). The mixture was filtered and the Raney nickel solids were washed with tetrahydrofuran, acetone, and tetrahydrofuran. The combined organic filtrates were concentrated to an oil (14.5 g). This oil was purified by silica gel column chromatography (Kieselgel 70-230 mesh, $CHCl_3$:EtOAc, 4:1).

Purified 1,5-anhydromannobiitol octaacetate (2.0 g) was dissolved in anhydrous methanol (15 mL) and sodium methoxide (1N, 5 mL) was added. When tlc ($CHCl_3$:EtOAC, 10:1) showed that deacetylation was complete (ca. 30 minutes), the solution was deionized with resin (Dowex H^+, 5 g), filtered, and reduced *in vacuo* to an oil. Successive additions of anhydrous ethanol and concentration *in vacuo* yielded a white solid, which was crystallized (ethanol:water, 10:1); m.p. 231.0-231.5°C; $[\alpha]_D$-39.46 (*c* 1,506, H_2O); *Anal.* Calc. $C_{12}H_{22}O_{10}$: C, 44.17; H, 6.80; O, 49.03. Found: C, 44.09; H, 6.86; O, 49.05; ^{13}C-NMR ($CDCl_3$, δ): 61.9 (t,C_6); 62.2 (t,C_6'); 70.8 (t,C_1); 68.0, 69.6, 71.7, 73.3, 74.2, 77.7, 78.2, and 80.1 (all d, C_2,C_3,C_4,C_5,C_2',C_3',C_4',C_5'); 101.3 (D,C_1').

Fehling's test demonstrated that the product was a nonreducing sugar. The product (0.13 g) was hydrolyzed by refluxing in trifluoroacetic acid solution (2N, 30 mL) for 1 hour. The solution was reduced in vacuo to a syrup, 10 mL of water added, and the mixture evaporated in vacuo to dryness until the pH was neutral (12 times).[64] The residue was taken up in 5 mL water, passed through deionizing resin (MB-3, 5 mL), and evaporated to dryness (0.0448 g). Cyclohexyl-β-D-glucosyl (0.0362 g) was added as an HPLC internal standard, and the mixture was taken up in water (1 mL). Analysis via HPLC demonstrated that the hydrolyzate contained equimolar amounts of mannose and 1,5-anhydro-D-mannitol.

1,5-Anhydro-2,3,6-tri-O-methyl-4-O-β-(2,3,4,6-tetra-O-methyl-mannopyranosyl)-D-mannitol

Pure 1,5-anhydromannobiitol crystals (0.36 g) were dissolved in anhydrous dimethyl sulfoxide (8.5 mL), and powdered sodium hydroxide (1.1 g) was added. Distilled methyl iodide (1.5 mL) was added dropwise over a 10 minute period to the vigorously stirred mixture. After 30 minutes, the reaction was quenched with water (15 mL), and extracted with benzene (1 x 25 mL, 3 x 10 mL). The benzene extracts were washed with saturated sodium chloride solution (3 x 15 mL) and water (1 x 10 mL), dried over sodium sulfate, filtered, and reduced in vacuo to a thick syrup (0.23 g, 49% yield). The aqueous layers were reextracted with benzene (3 x 10 mL). The secondary extracts were treated in a manner similar to the first extracts and yielded additional syrup (0.6 g), which was combined with the first syrup. Gas chromatographic analysis (conditions C) indicated that the product was pure. The ^{13}C-NMR spectrum ($CDCl_3$, δ) (Fig. 32, Appendix III) had: 29.5 (unassigned), 61.2-56.8 (O-$\underline{C}H_3$ groups), 64.8 (C_1), 71.7 (C_6 or C_6'), 71.9 (C_6' or C_6), 74.1, 74.6, 75.0, 75.4 (C_4, C_4', C_2, C_2'), 76.1 ($CDCl_3$), 76.7 (C_5 or C_5'), 77.1 ($CDCl_3$), 77.7 ($CDCl_3$), 78.0 (C_5 or C_5'), 81.9 (C_3), 84.2 (C_3'), 100.9 (C_1').

1,5-Anhydro-2,3,4,6-Tetra-O-Acetyl-D-Mannitol

D-Mannose (15 g) was mixed with cooled pyridine (105 mL) and acetic anhydride (75 mL). After 12 hours, the solution was poured into chloroform (300 mL) and ice water (300 mL), and stirred vigorously. The water and chloroform layers were separated and the aqueous layer was extracted with chloroform (2 x 100 mL). The combined chloroform extracts were washed with hydrochloric acid (0.1N, 8 x 250 mL) and water (2 x 250 mL), dried over anhydrous potassium carbonate, filtered, and reduced *in vacuo* to a syrup.

The penta-O-acetyl-D-mannose syrup was reacted with a hydrogen bromide-glacial acetic acid solution (34%, 39 mL) for 3 hours at room temperature. Ethyl ether (300 mL) and ice water (300 mL) were added and the mixture was stirred vigorously for 20 minutes. The ether and aqueous layers were separated, and the aqueous fraction was washed with ether (2 x 150 mL). The combined ether fractions were washed with sodium bicarbonate solution (saturated, 4 x 450 mL) and water (3 x 500 mL), dried over potassium carbonate, filtered, and reduced *in vacuo* to a syrup.

The 2,3,4,6-tetra-O-acetyl-mannopyranosyl bromide syrup (35.92 g) was mixed with Raney nickel (ca. 100 g) in tetrahydrofuran:ethanol (1:1, 400 mL) at room temperature and the reaction was monitored via tlc. After 15 hours, the temperature was raised to 40°C. Two hours later, triethylamine (15 mL) was added. After an additional seven hours, the reaction mixture was filtered and the filtrate reduced *in vacuo* to a solid. This solid was crystallized from ethanol. The rhomboidal 1,5-anhydro-D-mannitol tetraacetate crystals were contaminated with a by-product which formed needlelike crystals. These were washed away with water. The total yield of 1,5-anhydro-D-mannitol tetraacetate was 12.32 g (44.28% based on D-mannose); m.p. 64.7-65.7°C, $[\alpha]_D$-38.46 (*c* 1.498, $CHCl_3$).

Literature: mp. 66-67°C, $[\alpha]_D$-42 ($CHCl_3$).[65] The ^{13}C-NMR is shown in Fig. 25, Appendix III.

1,5-Anhydro-D-Mannitol

Crystals of 1,5-anhydro-D-mannitol tetraacetate (7.38 g) were dissolved in anhydrous methanol (50 mL). Sodium methoxide (10 mL, 1M) was added and the mixture was shaken for ca. 30 minutes, until tlc ($CHCl_3$:EtOAc, 10:1) showed that deacetylation was complete. The solution was then deionized with Dowex H^+ resin (10 g), filtered, and reduced *in vacuo* to a thick syrup. Crystallization from ethanol yielded needlelike crystals (2.15 g, 60%): m.p. 155.8-156.7°C, $[\alpha]_D$-49.81 (H_2), *c* 1.495). Literature: m.p. 156-157°C, $[\alpha]_D$-50° (H_2O, *c* 1.1).[66] The ^{13}C-NMR spectrum ($CDCl_3$, δ) is shown in Fig. 26, Appendix III.

2,3,4,6-Tetra-O-Acetyl-α-D-Glucopyranosyl Bromide

Glucose pentaacetate (50 g) was mixed with hydrogen bromide/glacial acetic acid solution (33 mL, 34%) and allowed to sit for 2 hours. The solution was then mixed with chloroform (200 mL), poured into ice water (0.75 L) and stirred vigorously for 15 minutes. The chloroform and aqueous layers were separated and the aqueous layer was washed with chloroform (1 x 50 mL). The combined chloroform extracts were washed with sodium bicarbonate solution (saturated, 2 x 200 mL), dried over potassium carbonate, filtered, and reduced *in vacuo* to a syrup. The syrup was crystallized from diethyl ether (10 mL), yielding 2,3,4,6-O-tetraacetate glucosyl bromide (40.07 g, 76.08%): m.p. 88-89.5°C, $[\alpha]$ = +196.0. Literature: m.p. 88-89°C, $[\alpha]_D$+197.8 ($CHCl_3$);[67] m.p. 89-90°C, $[\alpha]_D$+197.3°C (*c* 1.5, $CHCl_3$).[32,33]

2-Acetoxyethyl 2,3,4,6-Tetra-O-Acetyl-1-Thio-β-D-Glucopyranoside

2,3,4,6-Tetraacetate-α-D-glucosyl bromide (20 g) was dissolved in chloroform (50 mL) and added dropwise to a solution of methanol (100 mL), KOH (5.5 g), and mercaptoethanol (10 mL). After 4 hours, sodium methoxide (1N, 5 mL) was added. Tlc analysis ($CHCl_3$:EtOAc, 10:1) showed that complete deacetylation had occurred. The mixture was then filtered. The filtrate was neutralized with acetic acid (1N, 50 mL) and concentrated in vacuo to a thick syrup. The residue was extracted with hot pyridine (2 x 50 mL, 1 x 125 mL) and the pyridine was decanted and filtered. The pyridine solution was cooled in ice and mixed with acetic anhydride (60 mL). After 18 hours, tlc analysis showed that the compound was completely acetylated. The reaction mixture was then poured into water (250 mL), stirred vigorously, and extracted with chloroform (2 x 75 mL). The combined chloroform extracts were washed with acetic acid (1M, 4 x 250 mL); then reduced in vacuo to a thick syrup. The yield was 5.54 g (25.29%). The product, crystallized from ethanol, had: m.p. 106.7-108.3°C, $[\alpha]_D$-30.6 (c 1.501, $CHCl_3$). Literature: m.p. 106-106.5°C, $[\alpha]_D$-32.0 (c 1.5, $CHCl_3$);[32] m.p. 108.0-108.5°C, $[\alpha]_D$-31.5 ($CHCl_3$).[68] The ^{13}C-NMR spectrum ($CFCl_3$, δ) is shown in Fig. 23, Appendix III.

2-Hydroxyethyl 1-Thio-β-D-Glucopyranoside

Sodium methoxide (1M, 5 mL) was added to a solution of 2-acetoxyethyl tetra-O-acetyl-1-thio-β-D-glucopyranoside (5.0 g) in anhydrous methanol (50 mL). The reaction was monitored by tlc ($CHCl_3$:EtOAc, 1:1). When deacetylation was complete, the solution was deionized with resin (Dowex 5W-X8H, 5 g), filtered, and reduced in vacuo to a thick syrup. The product, crystallized from ethanol, had: m.p. 115.9-117.9°C and $[\alpha]_D$-53.4 (c 1.5, H_2O). Literature: m.p. 115.5-116.5°C and $[\alpha]_D$-54.9 (c 1.5, H_2O);[32,33] m.p. 114-116°C and $[\alpha]_D$-61.8 (H_2O).[68] The ^{13}C-NMR spectrum ($CDCl_3$, δ) is shown in Fig. 24, Appendix III.

2-Methoxyethyl 2,3,4,6-Tetra-O-Methyl-1-Thio-β-D-Glucopyranoside

2-Hydroxyethyl 1-thio-β-D-glucopyranoside (1.59 g) was dissolved in anhydrous dimethyl sulfoxide (31.2 mL) and powdered sodium hydroxide (3.79 g) was added. Distilled methyl iodide (6 mL) was added dropwise over a 40-minute period to the stirred mixture. The mixture was stirred for another 20 minutes, then the reaction was quenched with water (60 mL). After 5 minutes, the resulting yellow solution was extracted with benzene (1 x 50 mL, 3 x 25 mL). The colorless benzene extracts were washed with saturated sodium chloride solution (3 x 50 mL) and water (1 x 25 mL). The aqueous washes were back-extracted with benzene (2 x 45 mL). These second benzene extracts were washed with saturated sodium chloride solution (2 x 30 mL) and water (1 x 15 mL), then added to the earlier extracts. The combined benzene extracts were dried over sodium sulfate, filtered, and reduced in vacuo to a thin syrup (3.12 g). The product was purified by distillation at 0.5 mm Hg and 140°C. Gas chromatographic analysis showed that the middle fraction was pure. The ^{13}C-NMR spectrum ($CDCl_3$, δ) (Fig. 33, Appendix III) had: 30.1 (C_b), 58.5, 59.1, 60.3, 60.5, 60.7 (CH_3), 71.4, 72.3 (C_6 and C_a), 75.7, 77.0, 78.3 ($CDCl_3$), 78.7 (C_4), 79.4 (C_2), 83.4 (C_5), 85.0 (C_3), 88.3 (C_1).

KINETIC STUDIES

Reactor System

Kinetic studies were run in the reactor system described previously (Fig. 22).[13,14,24,25,26,32,33] This system consisted of a stainless steel reactor (140 mL capacity) fitted with a magnetic stir bar, thermocouple (Omega Iron-Constantan Type J) and sample line (Type 304 stainless super high pressure tubing, 1/8-inch o.d. x 0.049-inch wall x 18 inches long). Two gyrolok fittings connected the thermocouple and sample line to the removable reactor lid. A high

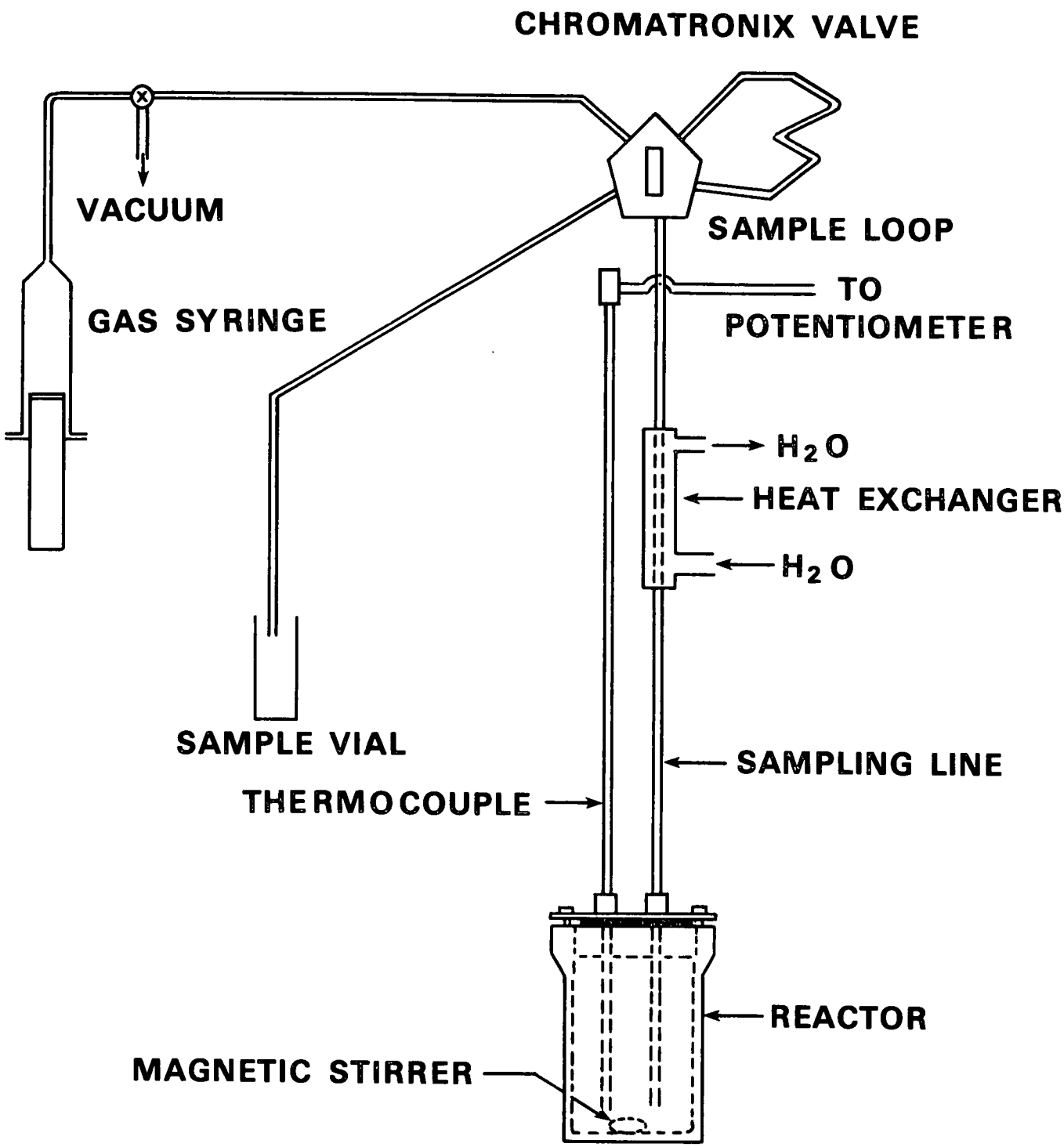

Figure 22. Schematic diagram of the kinetic reactor system.

pressure seal between the lid and reactor was obtained by compressing a Teflon ring around the lid with heat-treated retaining bolts. The sample line was connected to a Cheminert slider injection valve fitted with a 1 mL sample loop and gas syringe.

The oil bath, which held ca. 4.5 gallons of HTF-100 UCON high temperature oil, was fitted with a motor-driven magnetic stirrer and movable rack to raise and lower the reactor. Two continuous heaters (250 and 500 V) and a variable heater (500 V) controlled by a fixed-point thermostat and electronic relay maintained the bath temperature at ± 0.1°C of the desired temperature. The reactor temperature was measured by connecting the thermocouple to a precision potentiometer (Leeds and Northrup 8691-2) through an electronic cold junction compensator (Omega CJ-J).

Stock Sodium Hydroxide

The stock NaOH solution was prepared by slowly adding sodium hydroxide pellets (500 g) to cooled, stirred, triply-distilled water (500 mL). The resulting cloudy solution was filtered and stored in a paraffin-lined glass bottle. The concentration was measured by diluting an aliquot of stock solution to approximately 2N and titrating against a known amount of potassium acid phthalate using a phenolphthalein indicator.

Stock Sodium Sulfide

Crystals of sodium sulfide nonahydrate were placed in a Buchner funnel and washed with water until the crystals and filtrate were colorless. Under nitrogen, the purified sodium sulfide crystals (400 g) were dissolved in oxygen-free water (600 g) by stirring for three hours. The solution was stored in a paraffin-lined bottle. This bottle was opened only under nitrogen. The

concentration was measured by diluting 10 mL (ca. 11.2 g) of stock sodium sulfide solution to 100 mL. Aliquots of this solution (10 mL) were titrated with 0.1M $HgCl_2$ solution in the presence of sodium thiosulfate (5 g) and sodium hydroxide (1M, 100 mL).[32,33,69] The titration was followed potentiometrically using an Orion Ag/AgS electrode in conjunction with a double junction reference electrode.

Oxygen-Free Water

Oxygen-free water was made by boiling 1400 mL of triply-distilled water until the volume was reduced to 1200 mL, then purging it with nitrogen while cooling in ice. The container was sealed tightly and the water was used within 24 hours.

Standard Sodium Hydroxide

For each run, a standard sodium hydroxide solution having twice the sodium hydroxide concentration desired in the final liquor was prepared. Under nitrogen, the appropriate amount of stock sodium hydroxide solution, calculated according to Eq. (29), was weighed into a tared volumetric flask and diluted with oxygen-free water.

$$X = M_S V_S \delta / M_{STK} \qquad (29)$$

where X = weight of stock solution

M_S = desired molarity of standard solution

V_S = desired volume of standard solution, room temperature

δ = density of stock solution

M_{STK} = molarity of stock solution

The density of the standard sodium hydroxide solution was determined and the concentration was measured by titrating a known amount of potassium acid phthalate.

Reaction Liquor

The reaction liquors were prepared from standard solutions and crystalline salts under nitrogen. The thermal expansion of the solution must be accounted for when the amount of standard sodium hydroxide solution needed to give the desired liquor concentration is calculated. This is done using the volume expansivity factor, F_V, which is defined according to Eq. (30):

$$F_V = V_T/V_{RT} \tag{30}$$

where V_T = volume of water at reaction temperature, mL

V_{RT} = volume of water at room temperature, mL

Volume expansivity factors are listed in Table 16.

Table 16. Volume expansivity factors.

Reaction Temperature	Volume Expansivity Factor
160°C	1.101
170°C	1.113
180°C	1.126
190°C	1.140

Equating V_S with V_{RT} and substituting Eq. (30) into (29) gives (31):

$$X_S = M_R F_V V_{RT} \delta / M_S \tag{31}$$

where X_S = weight of standard solution

M_R = desired molarity of reaction liquor

δ = density of standard solution

M_S = molarity of standard solution

The analogous equation for solids is:

$$Y = M_C V_{RT} F_V W_{MW} \tag{32}$$

where Y = weight of sodium tosylate needed, g

M_C = desired molarity of solids in liquor, moles/L

W_{MW} = molecular weight of solid

F_V = volume expansivity factor

V_{RT} = volume of liquor at room temperature, mL

In liquors which contained only sodium hydroxide, the necessary volume of standard NaOH was diluted to the appropriate volume with oxygen-free water. The density of the reaction liquor was measured and the concentration determined via titration of potassium acid phthalate.

Some liquors contained sodium tosylate in addition to sodium hydroxide. In these cases, the sodium tosylate needed to give the desired concentration was calculated from Eq. (32). The necessary amount of sodium tosylate was weighed into a tared 100 mL volumetric flask. Under nitrogen, the appropriate amount of standard sodium hydroxide solution, calculated according to Eq. (31), was added, and the mixture was diluted to the mark with oxygen-free water. After measuring the density of the mixture, the flask was tightly stoppered, removed from the glove bag, and heated over steam until all the sodium tosylate dissolved. Because sodium tosylate interferes with the potassium acid phthalate titration, the sodium hydroxide concentration in the liquor could not be measured.

Liquors which contained sodium hydroxide and sodium sulfide were prepared by weighing appropriate amounts of standard sodium hydroxide solution and stock sodium sulfide solution, both determined using Eq. (31), into a tared volumetric

flask under nitrogen. The liquor was diluted with oxygen-free water and weighed to determine the density.

The concentration of sodium sulfide in the reaction liquor was measured by titrating 2-mL aliquots of liquor with 0.1000M $HgCl_2$ in the presence of sodium sulfite (5 g), sodium hydroxide (4M, 25 mL), and water (75 mL).[32,33,69] Active alkali was determined by titrating liquor aliquots (ca. 10 mL, determined gravimetrically) and formaldehyde (5 mL) with 1.0M hydrochloric acid to the phenolphthalein endpoint.[32,33,70] The sodium hydroxide concentration was found by subtracting the sodium sulfide concentration from the active alkali.

Loading the Reactor

The amount of carbohydrate needed for each degradation was calculated according to Eq. (32). If the carbohydrate was a solid, the appropriate amount was weighed into a weighing bottle, then added to the reaction under nitrogen. Reaction liquor (100 mL) was then added to the reactor. If the carbohydrate was an oil, it was dried under vacuum in a flask. A portion of the weighed liquor (100 mL) was added to the flask, swirled until the carbohydrate dissolved, and poured into the reactor. The flask was rinsed with additional portions of the reaction liquor. The reactor was sealed, connected to the temperature measurement and sampling lines, and placed in a hot oil bath.

When a liquor contained sodium tosylate, one reactor port was sealed with a cap instead of the sample line. The reactor was partially immersed in the bath, and when the temperature reached 65-70°C, the cap was replaced with the sample line. The reactor was then fully immersed in the bath, and the heat-up continued as usual.

Sampling

Sampling was started when the reactor reached temperature. The sample line was purged twice, then the timer was started and the first sample taken. Duplicate samples were withdrawn into tared, 4-mL vials at logarithmically-spaced intervals throughout the reaction. The sample line was purged once prior to withdrawing each set of samples. Internal standard solution (ca. 0.005M, 1 mL) was added to one of the samples in each set. Both the sample size and amount of internal standard solution added were determined gravimetrically.

Sample Analysis

Samples containing only sodium hydroxide and carbohydrates were passed through a fresh column of ion-exchange resin (MB-3, 10 mL), eluted with water (10 mL), and reduced *in vacuo* to dryness. Samples which contained 1.0M sodium tosylate were passed through a 10 mL column of the MB-3 resin, eluted with water (10 mL), passed through the same resin column a second time and again eluted with water (10 mL). They were reduced *in vacuo* to dryness. Samples which contained 1.5 or 2.0M sodium tosylate were passed through 10 mL of MB-3 resin, eluted with 5 mL water, passed through the same column again, eluted with 10 mL water, then passed through 5 mL of fresh MB-3 resin and eluted with 10 mL of water. These samples were also reduced to dryness *in vacuo*.

Samples were acetylated by adding pyridine (0.66 mL) and acetic anhydride (0.33 mL) and agitating overnight. The reaction was quenched with water (10 mL) and extracted with chloroform (2 x 5 mL). The combined chloroform extracts were washed with HCl (1N, 10 mL) and water (2 x 10 mL), reduced to dryness, taken up in chloroform (ca. 2 mL), transferred to a 4-mL vial, and reduced to dryness. The residue was taken up in chloroform (15 drops) and injected on the gas chromatograph using conditions B. The peak areas for each compound were converted

to concentrations using a calculator program (Program 5, Appendix I) based on Eq. (33):

$$M_X = \frac{A_X}{A_{IS}} \cdot M_{IS} \cdot \frac{W_{IS}}{W_X} \cdot \frac{\delta_X}{\delta_{IS}} \cdot F_X \qquad (33)$$

where M_X = concentration of unknown (M) at room temperature

M_{IS} = concentration of internal standard solution (M)

A_X = area of unknown peak

A_{IS} = area of internal standard peak

W_X = weight of unknown (sample) solution

W_{IS} = weight of internal standard solution added

δ_X = density of unknown (sample) solution

δ_{IS} = density of internal standard solution

F_X = response factor

Response factor samples were prepared by pipetting appropriate amounts of internal standard and carbohydrate solutions into 4-mL vials. The solutions were treated and derivatized in the same manner as the reaction samples. Response factors were calculated according to Eq. (34):

$$F_X = (A_{IS}/A_X)\ (M_X/M_{IS}) \qquad (34)$$

Samples of fully-methylated sugars were neutralized with aqueous hydrochloric acid (0.5 mL, 5M), then extracted with chloroform (3 x 3 mL), reduced *in vacuo* just to dryness, transferred to a 4-mL vial using ca. 2 mL of chloroform, and reduced to dryness again. The residue was then taken up in chloroform (15 drops) and injected on the GC using conditions C. Concentrations were calculated according to Eq. (33). Response factor samples were treated in the same manner, and response factors were calculated using Eq. (34).

OXYGEN-18 INCORPORATION STUDIES

Reactor System

The ^{18}O incorporation studies were carried out in 4-mL capacity stainless steel pressure vessels. These were placed in a rotating, motor-driven plate and immersed in an oil bath. The oil bath was filled with ca. 3.5 gallons of HTF-100 UCON high temperature oil (Blue M). The temperature was maintained with 2 continuous heaters (250, 500 V) and a variable heater (500 V) controlled by a fixed point thermostat and electronic relay, and monitored by a thermocouple inserted in the oil and connected to a digital thermometer (Omega Model 199) and strip chart recorder.

Oxygen-18 Water (50%)

In a nitrogen-filled glovebag, 95% O^{18}-water and oxygen-free water were mixed in a 1.07:0.82 (w:w) ratio. One drop of this mixture was set aside for mass spectral analysis.

Oxygen-18 Enriched Liquors (20%)

Liquors were prepared in 5-mL volumetric flasks. Appropriate amounts of sodium tosylate were weighed into these flasks. Under nitrogen, the proper weights of stock sodium hydroxide solution and 50% O^{18}-water were added, then each solution was diluted to 5 mL with oxygen-free water.

Loading the Reactors

In a nitrogen-filled glovebag, 1,5-anhydromannobiitol was weighed into bombs which had been heated at 120°C for two hours and cooled under vacuum. Liquors which contained sodium tosylate were heated on the steam cone until all the tosylate dissolved. Under nitrogen, 4-mL of liquor was pipetted into each

bomb. Bombs were covered with the inner cap, wrapped with Teflon tape, and sealed with the outer cap. A few drops of each liquor were set aside for mass spectral analysis.

The bombs were placed in the rack, the rack was put into the bath, and the timer was started when the bath temperature stabilized.

Sampling

To remove a bomb, the rotating plate was stopped in an upright position, the bomb grasped with pliers, and pulled out of the rack, being careful to not loosen the cap. It was immediately plunged into a metal beaker containing ice water to cool it rapidly.

Sample Analysis

The contents of each bomb were weighed into three 4-mL vials. Samples which contained no sodium tosylate were passed through an MB-3 resin column (10 mL), and eluted with water (20 mL). Samples which did contain sodium tosylate were passed through an MB-3 resin column (10 mL), eluted with water (10 mL), then passed through the same column a second time and eluted with more water (20 mL). All samples were reduced to dryness under vacuum in 25-mL Erlenmeyer flasks. Small quantities of water were used to transfer them to 6-mL hypovials, in which they were again reduced to dryness. They were then dried under vacuum at 35°C in the presence of phosphorus pentoxide.

Under nitrogen, anhydrous pyridine (freshly distilled, 0.5 mL) and N-methyl-bis(trifluoroacetamide) reagent (1 mL, Pierce) were added to each sample, the samples were tightly sealed with a Teflon disk and crimp-cap, and heated at 55°C for one hour. They were then injected on the gas chromatograph-mass spectrometer the same day.

ACKNOWLEDGMENTS

The author gratefully acknowledges the contributions of her thesis advisory committee: Dr. L. R. Schroeder, Dr. D. R. Dimmel, and Dr. N. S. Thompson. Special thanks are due to Dr. Schroeder for his guidance and support throughout the course of this work.

The author also wishes to thank Dr. J. Van Boom and Dr. J. Auge for their generous gifts of 1,6-anhydro-β-D-mannopyrannosyl and 1,5-anhydro-D-iditol. The author is also grateful to Mr. L. Borchardt for performing the gas chromatograph-mass spectral work, to Dr. M. Melius for his aid with the HPLC work, and to Dr. D. Blythe for his many helpful suggestions.

Finally, the author wishes to thank her family, particularly her husband, Jim, for support and encouragement throughout the course of this thesis.

LITERATURE CITED

1. Matthews, C. H., Svensk Papperstid. 77:629(1974).

2. Schroeder, L. R.; Wabers, B. A., Project Report 3475-1, The Institute of Paper Chemistry, Appleton, WI, 1982.

3. Ahlm, C. E.; Leopold, B. E., Tappi 46:102(1963).

4. Rydholm, S. A., Pulping Processes, Interscience, New York, 1965.

5. Machell, G.; Richards, G. N.; Sephton, H. H., Chem. Ind. 1957:467-9.

6. Haas, D. W.; Hrutfiord, B. F.; Sarkanen, K. V., J. Appl. Polymer Sci. 11:587-99(1967).

7. Melius, M., Doctoral Dissertation, The Institute of Paper Chemistry, Appleton, WI, June, 1985.

8. Meller, A., Tappi 48:231(1965).

9. Capon, B., Chem. Rev. 69:407(1969).

10. Whistler, R. L.; BeMiller, J. N., Adv. Carbohyd. Chem. 13:289(1958).

11. Corbett, W. M.; Richards, G. N., Svensk Papperstid. 60:791-4(1957).

12. Franzon, O.; Samuelson, O., Svensk Papperstid. 60:872-7(1957).

13. Brandon, R. E., Doctoral Dissertation, The Institute of Paper Chemistry, Appleton, WI, Jan., 1973.

14. Brandon, R. E.; Schroeder, L. R.; Johnson, D. C., Cellulose Technology Research, ACS Symp. Ser. 10:125-46(1975).

15. Montgomery, E. M.; Richtmeyer, N. K.; Hudson, C. S., J. Am. Chem. Soc. 65:3(1943).

16. DeBruyne, C. K.; Van Wijnendaele, F.; Carchon, H., Carbohyd. Res. 33:75 (1974).

17. Gasman, R. C.; Johnson, D. C., J. Org. Chem. 31:1830(1966).

18. McCloskey, C. M.; Coleman, G. H., J. Org. Chem. 15:184(1985).

19. Kyosaka, S.; Murata, S.; Tanaka, M., Chem. Pharm. Bull. 31(11):3902-5 (1983).

20. Ballou, C. E., Adv. Carbohyd. Chem. 9:59(1954).

21. Lai, Y. Z.; Ontto, D., Carbohyd. Res. 67:500(1978).

22. Lindberg, B.; Dryselius, E.; Theander, O., Acta Chem. Scand. 12:340(1958).

23. Lindberg, B.; Janson, J., Acta Chem. Scand. 13:138(1959).

24. Nault, J. J., Doctoral Dissertation, The Institute of Paper Chemistry, Appleton, WI, June, 1979.

25. Gilbert, F. A., Doctoral Dissertation, The Institute of Paper Chemistry, Appleton, WI, June, 1975.

26. Gilbert, F. A.; Schroeder, L. R.; Nault, J. J., 176th ACS National Meeting, Miami Beach, Florida, CARB 59, Sept., 1978.

27. Gleave, J. L.; Hughes, E. D.; Ingold, C. K., J. Chem. Soc. 236:8(1935).

28. Simkovic, I.; Bringerova, A. E.; Konigstein, J.; Mihalos, V.; Janecek, F., Chem. Zvesti 38(2):223-9(1984).

29. Best, E. V.; Green, J. W., Tappi 52(7):1321(1969).

30. Lindberg, B.; Dryselius, E.; Theander, O., Acta Chem. Scand. 11:663(1957).

31. Wylie, T. R., Doctoral Dissertation, The Institute of Paper Chemistry, Appleton, WI, Jan., 1979.

32. Blythe, D. A., Doctoral Dissertation, The Institute of Paper Chemistry, Appleton, WI, Jan., 1984.

33. Blythe, D. A.; Schroeder, L. R., J. Wood Chem. Tech. 5(3):313-34(1985).

34. March, J., Advanced Organic Chemistry, McGraw-Hill, 1977.

35. Lowry, T. H.; Richardson, K. S., Mechanism and Theory in Organic Chemistry, Harper and Row, 1976.

36. MacLeod, J. M.; Schroeder, L. R., J. Wood Chem. Tech. 2(2):187-205(1982).

37. Lindberg, B.; Janson, J., Acta Chem. Scand, B36(4):277(1982).

38. Elliel, E. L., Stereochemistry of Carbon Compounds, McGraw-Hill, 1962. p. 198.

39. Thiem, J.; Sievers, A.; Karl, H., J. Chromat. 130:305(1977).

40. Aspinall, G. O.; Rashbrook, R. B.; Kessler, G., J. Chem. Soc. 215, 1958.

41. Gast, J., Doctoral Dissertation, The Institute of Paper Chemistry, Appleton, WI, June, 1983.

42. Gorin, P. A. J., Can. J. Chem. 51:2375-83(1973).

43. Frost, A. A.; Pearson, R. G., Kinetics and Mechanism, J. Wiley and Sons, 1959.

44. Glasstone, S.; Laidler, I. J.; Eyring, H., The Theory of Rate Processes, McGraw-Hill, 1941.

45. Montgomery, E. M.; Richtmeyer, N. K.; Hudson, C. S., J. Am. Chem. Soc. 64: 1483(1942).

46. Henderson, M. E.; Leege, J. C.; Schroeder, L. R., unpublished results.

47. Robins, J. H., Doctoral Dissertation, The Institute of Paper Chemistry, Appleton, WI, June, 1968.

48. Masterson, W. L.; Bolocofsky, D.; Lee, T. P., J. Phys. Chem. 75:2809-15 (1971).

49. Johnson, O., Inorganic Chem. 12:780-5(1973).

50. Lai, Y. Z., Carbohyd. Res. 24:57-65(1972).

51. Percival, E.; Charlambous, G., J. Chem. Soc. 1954:2443.

52. Ochiai, K.; Seto, K., J. Nuclear Sci. Tech. 8(6):330(1971).

53. Weast, R., Handbook of Chemistry and Physics, 51st Ed., The Chemical Rubber Company, Cleveland, Ohio, 1973.

54. Skoog, D. A.; West, D. M., Analytical Chemistry, Holt, Rinehart, and Winston, 1974. p. 582.

55. Whistler, R. L.; BeMiller, J. N., Adv. Carbohyd. Chem. 13:295(1958).

56. Stoddart, J. F., Stereochemistry of Carbohydrates, Wiley-Interscience, New York, 1971.

57. Green, J., Laboratory Manual, Carbohydrate Course A-122, The Institute of Paper Chemistry, Appleton, WI, Oct., 1960.

58. Perrin, D. D.; Armarego, W. L. F., Perrin, D. R., Purification of Laboratory Chemicals, 2nd ed., Pergamon Press, New York, 1980.

59. Thomas, A. B.; Rochow, E. G., J. Am. Chem. Soc. 79:1843(1957).

60. Riddick, J. A.; Bunger, W. B., Techniques of Chemistry. Vol. II: Organic Solvents, Wiley Interscience, 1970.

61. Zinner, H.; Brandner, H.; Rembarz, G., Chem. Ber. 89:800(1956).

62. Pelletier, S. W., Chem. Ind. 1953:1034.

63. Augustine, R. L., Catalytic Hydrogenation, Marcel Dekker, New York, 1965. p. 27.

64. Fengel, D.; Wegner, G.; Heizman, A.; Przyklenk, M., Holzforschung 31(3): 65-71(1977).

65. Montgomery, R.; Wiggins, L., J. Chem. Soc. 1948:2204.

66. Fletcher, H. G., In Whistler's Methods in Carbohydrate Chemistry, Vol. II, 1963. p. 196.

67. Bates, F. J., Polarimetry, Saccharimetry, and the Sugars, Washington, DC, U.S. Govt. Printing Office, 1942.

68. Saunders, M. D.; Timell, T. E., Carbohyd. Res. 6:121-4(1968).

69. NCASI Atmospheric Quality Improvement Tech. Bull. 68:A2-6(Oct., 1973).

70. TAPPI Standard Method T 625 ts-64.

71. Que, L.; Gray, G. R., Biochem. 13(1):146(1974).

72. Perlin, A. S.; Ritchie, R. G. S.; Cyr, N., Can. J. Chem. 54:2301-9(1976).

APPENDIX I

COMPUTER AND CALCULATOR PROGRAMS

Program 1: MH/DISAPPEAR

```
$RESET FREE
C              LINEAR REGRESSION PROGRAM
C      FOR THE ANALYSIS OF PSEUDO-FIRST ORDER REACTIONS
C                 WRITTEN BY D. BLYTHE
C               MODIFIED BY M. HENDERSON
C
C      THIS PROGRAM IS DESIGNED TO GENERATE PSEUDO-FIRST ORDER RATE
C      CONSTANTS AND THEIR 95% CONFIDENCE LIMITS DIRECTLY FROM RAW
C      CONCENTRATION MEASUREMENTS.
C
C      THE OUTPUT CONSISTS OF A TABLE SHOWING EACH SAMPLE TIME
C      (IN SECONDS), THE MEAN CONCENTRATION (AT TEMPERATURE),
C      THE CALCULATED (REGRESSION) CONCENTRATIONS, AND THE
C      DIFFERENCE BETWEEN THE TWO CONCENTRATIONS. THE OUTPUT ALSO
C      INCLUDES THE SLOPE (AND ITS 95% CONFIDENCE INTERVAL), THE
C      INTERCEPT, AND THE CORRELATION COEFFICIENT FOR THE LEAST-SQUARES
C      REGRESSION LINE.
C      IF THE OUTPUT IS TO BE DIRECTED TO THE PRINTER,
C      THEN REMOVE THE COMMENT CHARACTER FROM:
FILE   6(KIND=PRINTER,MYUSE=OUT,MAXRECSIZE=22)
C      AND COMPILE WITH FORTRAN.
C
C           A FILE CONTAINING THE SAMPLE TIME (IN SECONDS) AND
C      THE LN OF THE AVERAGE MBT CONCENTRATION AT EACH TIME IS
C      ALSO GENERATED.  THIS FILE CAN BE USED WITH "ST*/PLOT"
C      TO PLOT THE DATA. IT IS DEFINED BY:
FILE   1(KIND=DISK,TITLE="PLOT13/MBT",PROTECTION=SAVE,
     +AREAS=1,AREASIZE=200)
C
C           THE INPUT DATA FILE IS DEFINED BY:
FILE   5(KIND=DISK, FILETYPE=7, TITLE="DATA13/MBT.")
C      A FILE WITH THE GIVEN TITLE MUST BE CREATED BEFORE RUNNING
C      THIS PROGRAM AND MUST CONTAIN A LEAD RECORD GIVING THE
C      REACTION NUMBER, THE REACTION TEMPERATURE, THE NAOH
C      MOLARITY, AND THE VOLUME EXPANSIVITY
C      FACTOR, THEN UP TO TWENTY DATA RECORDS (TIME IN MINUTES,
C      NUMBER OF CONCENTRATION MEASUREMENTS,
C      FOLLOWED BY UP TO SIX INDIVIDUAL CONCENTRATION MEASUREMENTS)
C      AND AN END RECORD OF 0,0,0.
C
       INTEGER NO,X,Y,I,N,NUM
       REAL TMIN,CONC(6),TSEC(20),AVG,CHI(20),POINT(20),TEMP,TFACT
       REAL SUMX,SUMX2,SUMY,SUMY2,SUMXY,M,B,DENOM,CC,MOL,XPT(20)
       REAL SSY,SSX,SSXY,THETA,ERROR,T(20),CALC(20),DIFF(20)
       READ(5,/)NUM,TEMP,MOL,TFACT
       WRITE(6,9000)NUM
 9000  FORMAT(1H/,' THIS IS REACTION NUMBER ',I5,/)
       WRITE(6,9001)TEMP
 9001  FORMAT(1H/,' THE TEMPERATURE OF THE REACTION WAS ',F8.2,/)
       WRITE(6,8000)MOL
 8000  FORMAT(1H/,' THE MOLARITY OF THE REACTION (AT TEMP) WAS ',
     +F5.2,/)
       Y=1
       X=1
C      THIS LOOP FINDS THE MEAN OBSERVED CONCENTRATIONS
C      NO IS THE NUMBER OF RAW CONCENTRATION MEASUREMENTS
     1 READ (5,/) TMIN,NO,(CONC(I),I=1,NO)
 9002  FORMAT(F10.1,I4,6F10.9)
C      THIS TESTS FOR THE LAST DATA CARD
```

```
4300          IF(NO)9,9,2
4400        2 TSEC(X)=TMIN*60.
4500          X=X+1
4600          AVG=0.
4700          DO 3 I=1,NO
4900        3 AVG=CONC(I)+AVG
  00    C     CHI IS THE MEAN OBSERVED CONCENTRATION
5000          CHI(Y)=(AVG/NO)/TFACT
5100          POINT(Y)=ALOG(CHI(Y))
5200          Y=Y+1
5300          GO TO 1
5400    C     N IS THE NUMBER OF SAMPLING TIMES (DATA CARDS)
5500        9 N=Y-1
5600          WRITE(6,9003)N
5700     9003 FORMAT(1H/,' THE NUMBER OF DATA POINTS IS ',I5,/)
5800    C     THIS SECTION FINDS THE REGRESSION PARAMETERS
5900          SUMX=0.
6000          SUMX2=0.
6100          SUMY=0.
6200          SUMY2=0.
6300          SUMXY=0.
6400          DO 10 I=1,N
6500          SUMX=TSEC(I)+SUMX
6600          SUMX2=TSEC(I)*TSEC(I)+SUMX2
6700          SUMY=POINT(I)+SUMY
6800          SUMY2=POINT(I)*POINT(I)+SUMY2
6900       10 SUMXY=TSEC(I)*POINT(I)+SUMXY
7000    C     CC IS THE CORRELATION COEFFICIENT
7100          DENOM=((SUMX2-(SUMX*SUMX)/N)*(SUMY2-(SUMY*SUMY)/N))**.5
7200          CC=(SUMXY-(SUMX*SUMY)/N)/DENOM
7300    C     B IS THE INTERCEPT
  00          B=(SUMX2*SUMY-SUMX*SUMXY)/(N*SUMX2-SUMX*SUMX)
.300    C     M IS THE SLOPE
7600          M=(N*SUMXY-SUMX*SUMY)/(N*SUMX2-SUMX*SUMX)
7700    C     THIS SECTION FINDS THE CONFIDENCE INTERVAL OF THE SLOPE
7800          SSY=SUMY2-(SUMY*SUMY/N)
7900          SSX=SUMX2-(SUMX*SUMX/N)
8000          SSXY=SUMXY-(SUMX*SUMY/N)
8100          THETA=((SSY-M*SSXY)/N)**.5
8200    C     THIS IS A TABLE OF STUDENT'S T VALUES OT THE 0.95 LEVEL
8300          T(1)=12.706
8400          T(2)=4.303
8500          T(3)=3.182
8600          T(4)=2.776
8700          T(5)=2.571
8800          T(6)=2.447
8900          T(7)=2.365
9000          T(8)=2.306
9100          T(9)=2.262
9200          T(10)=2.228
9300          T(11)=2.201
9400          T(12)=2.179
9500          T(13)=2.160
9600          T(14)=2.145
9700          T(15)=2.131
9800          T(16)=2.120
 900          T(17)=2.110
 ,00          T(18)=2.101
10100          T(19)=2.093
10200          T(20)=2.086
10300          ERROR=T(N-2)*THETA*((N/((N-2)*SSX))**.5)
10400    C     THIS CALCULATES THE REGRESSION CONTENTRATIONS
```

```
10500           DO 30 I=1,N
10600           CALC(I)=EXP(M*TSEC(I)+B)
10700        30 DIFF(I)=CHI(I)-CALC(I)
10800      C    THIS SECTION WRITES THE OUTPUT DATA
10900           WRITE(6,9004)
11000      9004 FORMAT('   SECONDS    CONCENTRATION    CALC. CONC.    DIFFERENCE')
11100           WRITE(6,9005)(TSEC(I),CHI(I),CALC(I),DIFF(I),I=1,N)
11200      9005 FORMAT(F10.1,3F15.6)
11300           WRITE(6,9006)M
11400      9006 FORMAT(1H /,' THE SLOPE OF THE REGRESSION LINE IS',E12.4,/)
11500           WRITE(6,9007)ERROR
11600      9007 FORMAT('  THE CONFIDENCE INTERVAL ON THE SLOPE IS ',E12.4,/)
11700           WRITE(6,9008)B
11800      9008 FORMAT('  THE INTERCEPT OF THE LINE IS ',E12.4,/)
11900           WRITE(6,9009)CC
12000      9009 FORMAT(' THE CORRELATION COEFFICIENT IS ',F6.4,/)
12010      C THIS WRITES TO FILE USED FOR PLOTTING
12020           DO 40 I=1,N
12030        40 XPT(I)=TSEC(I)/1000
12040           WRITE(1,9010)(XPT(I),POINT(I),I=1,N)
12050      9010 FORMAT(2F10.4)
12100           STOP
12200           END
```

Program 2: MH/APPEAR

```
100     $RESET FREE
300     C
400     C                LINEAR REGRESSION PROGRAM
500     C        FOR ANALYSIS OF THE FORMATION OF REACTION PRODUCTS
600     C
700     C                  WRITTEN BY D. BLYTHE
750     C                MODIFIED BY M. HENDERSON
800     C
900     C      THIS PROGRAM IS DESIGNED TO GENERATE PSEUDO-FIRST ORDER
1000    C      RATE CONSTANTS AND THEIR 95% CONFIDENCE LIMITS DIRECTLY
1100    C      FROM RAW CONCENTRATION MEASUREMENTS.
1600    C
1700    C      THE OUTPUT CONSISTS OF A TABLE SHOWING EACH SAMPLE
1800    C      TIME (IN SECONDS), THE MEAN CONCENTRATION (AT TEMPERATURE),
1900    C      THE CALCULATED (REGRESSION) CONCENTRATION, AND THE
2000    C      DIFFERENCE BETWEEN THE TWO CONCENTRATIONS.
2100    C      THE OUTPUT ALSO INCLUDES THE SLOPE (AND IT'S 95%
2200    C      CONFIDENCE INTERVAL), THE INTERCEPT, AND THE CORRELATION
2300    C      COEFFICIENT FOR THE LEAST-SQUARES REGRESSION LINE.
2310    C      IF THE OUTPUT IS TO BE DIRECTED TO THE PRINTER,
2320    C      THEN REMOVE THE COMMENT CHARACTER FROM:
2330    FILE    6(KIND=PRINTER,MYUSE=OUT,MAXRECSIZE=22)
2340    C      AND COMPILE WITH FORTRAN.
2342    C           A FILE CONTAINING THE X AND Y PARAMETERS WHICH MUST
2344    C      BE PLOTTED TO OBTAIN KI IS ALSO GENERATED. THIS FILE CAN
2346    C      BE USED WITH "ST*/PLOT". IT IS DEFINED BY:
2348    FILE   1(KIND=DISK,TITLE="PLOT15/X4",PROTECTION=SAVE,AREAS=1,
2350           *AREASIZE=200)
2400    C
2500    C           THE INPUT DATA FILE IS DEFINED BY:
2550    FILE   5(KIND=DISK,FILETYPE=7,TITLE="DATA15/X4")
2600    C      A FILE WITH THE GIVEN TITLE MUST BE CREATED BEFORE
2700    C      RUNNING THIS PROGRAM.  IT MUST CONTAIN A RECORD GIVING
2750    C      THE REACTION NUMBER,
2800    C      THE TEMPERATURE AND VOLUME EXPANSIVITY OF THE REACTION,
2900    C      THE INITIAL CONCENTRATION OF REACTANT(AT TEMPERATURE),
2950    C      THE REACTANTS RATE OF DISAPPEARANCE (IN MOLES/LITER),
2960    C      AND THE FINAL CONCENTRATION OF REACTANT(AT TEMPERATURE);
3000    C      THEN UP TO 20 DATA CARDS (SAMPLE TIME IN MINUTES, NUMBER OF
3050    C      CONCENTRATION MEASUREMENTS AT THAT TIME, AND UP TO SIX
3060    C      INDIVIDUAL CONCENTRATION MEASUREMENTS);
3100    C      AND AN END RECORD OF 0,0,0.
3300    C      NOTE - THE FIRST DATA CARD MUST BE THE TIME ZERO
3400    C      CARD, EVEN IF THE CONCENTRATION OF THE PRODUCT IS ZERO.
3500    C
4000    C
4100            INTEGER NO,X,Y,I,N,NUM
4200            REAL TMIN,CONC(6),TSEC(20),AVG,CHIT20),POINT(20),TEMP,TFACT
4300            REAL SUMX,SUMX2,SUMY,SUMY2,SUMXY,M,B,DENOM,CC,R,KR,XVAL(20)
4400            REAL SSY,SSX,SSXY,THETA,ERROR,T(20),CALC(20),DIFF(20)
4450            REAL XPT(20),YPT(20),CRF
4500            READ(5,/)NUM,TEMP,TFACT,R,KR,CRF
4600    9000    FORMAT(6F10.9)
4700            WRITE(6,9001)TEMP
4800    9001    FORMAT(1H /,'   THE TEMPERATURE OF THE REACTION WAS ',F8.2,/)
4900            WRITE(6,9002)R
5000    9002    FORMAT('   THE INITIAL REACTANT CONCENTRATION WAS ',F8.4,/)
5100            WRITE(6,9003)KR
5200    9003    FORMAT('   THE RATE OF DISAPPEARANCE OF REACTANT WAS ',E12.4,/)
```

```
      Y=1
      X=1
C     THIS LOOP FINDS THE MEAN OBSERVED CONCENTRATIONS
C     NO IS THE NUMBER OF RAW CONCENTRATION MEASUREMENTS
 1    READ (5,/) TMIN,NO,(CONC(I),I=1,NO)
9004  FORMAT(F10.1,I4,6F10.9)
C     THIS TESTS FOR THE LAST DATA CARD
      IF(NO)9,9,2
2     TSEC(X)=TMIN*60.
      XVAL(X)=(R/KR)*(1.-EXP(-KR*TSEC(X)))
      X=X+1
      AVG=0.
      DO 3 I=1,NO
3     AVG=CONC(I)+AVG
C     CHI IS THE MEAN OBSERVED CONCENTRATION
      CHI(Y)=(AVG/NO)/TFACT
      POINT(Y)=CHI(Y)-CHI(1)
      Y=Y+1
      GO TO 1
C     N IS THE NUMBER OF SAMPLING TIMES (DATA CARDS)
9     N=Y-1
      WRITE(6,9005)N
9005  FORMAT(1H /,'   THE NUMBER OF DATA POINTS IS ',I5,/)
C     THIS SECTION FINDS THE REGRESSION PARAMETERS
      SUMX=0.
      SUMX2=0.
      SUMY=0.
      SUMY2=0.
      SUMXY=0.
      DO 10 I=1,N
      SUMX=XVAL(I)+SUMX
      SUMX2=XVAL(I)*XVAL(I)+SUMX2
      SUMY=POINT(I)+SUMY
      SUMY2=POINT(I)*POINT(I)+SUMY2
10    SUMXY=XVAL(I)*POINT(I)+SUMXY
C     CC IS THE CORRELATION COEFFICIENT
      DENOM=((SUMX2-(SUMX*SUMX)/N)*(SUMY2-(SUMY*SUMY)/N))**.5
      CC=(SUMXY-(SUMX*SUMY)/N)/DENOM
C     B IS THE INTERCEPT
      B=(SUMX2*SUMY-SUMX*SUMXY)/(N*SUMX2-SUMX*SUMX)
C     M IS THE SLOPE
      M=(N*SUMXY-SUMX*SUMY)/(N*SUMX2-SUMX*SUMX)
C     THIS SECTION FINDS THE CONFIDENCE INTERVAL ON THE SLOPE
      SSY=SUMY2-(SUMY*SUMY/N)
      SSX=SUMX2-(SUMX*SUMX/N)
      SSXY=SUMXY-(SUMX*SUMY/N)
      THETA=((SSY-M*SSXY)/N)**.5
C     THIS IS A TABLE OF STUDENT'S T VALUES AT THE 0.95 LEVEL
      T(1)=12.706
      T(2)=4.303
      T(3)=3.182
      T(4)=2.776
      T(5)=2.571
      T(6)=2.447
      T(7)=2.365
      T(8)=2.306
      T(9)=2.262
      T(10)=2.228
      T(11)=2.201
      T(12)=2.179
      T(13)=2.160
      T(14)=2.145
```

```
11500           T(15)=2.131
11600           T(16)=2.120
11700           T(17)=2.110
11800           T(18)=2.101
11900           T(19)=2.093
  000           T(20)=2.086
 2100           ERROR=T(N-2)*THETA*((N/((N-2)*SSX))**.5)
12200     C     THIS CALCULATES THE REGRESSION CONTENTRATIONS
12300           DO 30 I=1,N
12400           CALC(I)=M*XVAL(I)+B+CHI(1)
12500     30    DIFF(I)=CHI(I)-CALC(I)
12600     C     THIS SECTION WRITES THE OUTPUT DATA
12700           WRITE(6,9006)
12800     9006  FORMAT('   SECONDS    CONCENTRATION    CALC. CONC.    DIFFERENCE'
12900           WRITE(6,9007)(TSEC(I),CHI(I),CALC(I),DIFF(I),I=1,N)
13000     9007  FORMAT(F10.1,3F15.6)
13100           WRITE(6,9008)M
13200     9008  FORMAT(1H /,'   THE SLOPE OF THE REGRESSION LINE IS',E12.4,/)
13300           WRITE(6,9009)ERROR
13400     9009  FORMAT('   THE CONFIDENCE INTERVAL ON THE SLOPE IS',E12.4,/)
13500           WRITE(6,9010)B
13600     9010  FORMAT('   THE INTERCEPT OF THE LINE IS',E12.4,/)
13700           WRITE(6,9011)CC
13800      9011 FORMAT('   THE CORRELATION COEFFICIENT IS  ',F6.4,/)
13802           DO 7 I=1,N
13804           XPT(I)=XVAL(I)/10
13806      7    YPT(I)=POINT(I)*100
13808           WRITE(1,9012)(XPT(I),YPT(I),I=1,N)
13810      9012 FORMAT(F10.4,F10.4)
13900           STOP
14000           END
```

Program 3: PARALLEL

```
  100     $RESET FREE
  200     C      CALCULATION OF PRODUCT DISAPPEARANCE USING
  300     C           PARALLEL, FIRST-ORDER KINETICS
  400     C
  500     C                WRITTEN BY M. HENDERSON
  600     C
  700     C      This program uses parallel, first-order kinetics to calculate
  800     C      rates of product formation and reactant disappearance from
  900     C      raw product concentrations, and generates a file for use in
 1000     C      plotting the appearance of product according to parallel,
 1100     C      first-order kinetics.
 1200     C
 1300     C      Data is read in from the file Data(no)/ant,
 1400     C      defined by:
 1500     FILE   5(KIND=DISK,FILETYPE=7,TITLE="DATA$3/X4")
 1600     C      This file must be created before running the program,
 1700     C      and contains a lead record giving the reaction number,
 1800     C      temperature,volume expansivity factor, initial reactant
 1900     C      concentration (at temperature), the reactants rate of
 2000     C      disappearance (in moles/liter),and the final reactant
 2100     C      concentration (at temperature).
 2200     C      This record is followed by up to 20 records each containing
 2300     C      the time (in minutes), the number of individual concentration
 2400     C      measurements at that time, and up to six concentration
 2500     C      of product measurements.  The file must terminate with an
 2600     C      end record of 0,0,0.
 2700     C
 2800     C      The output consists of a table listing the mean
 2900     C      concentrations of product (at temperature), the calculated
 3000     C      concentrations, and the differences as a function of time.
 3100     C      The regression parameters of the product disappearance
 3200     C      described by parallel, first-order kinetics are also printed.
 3300     C      If this output is to be directed to the printer, remove the
 3400     C      comment character from:
 3500     FILE   6(KIND=PRINTER,MYUSE=OUT,MAXRECSIZE=22)
 3600     C      A file containing the x and y values of the regression line
 3700     C      is generated on disk.  It can be used for plotting and is
 3800     C      defined by:
 3900     FILE   1(KIND=DISK,TITLE="PARALLEL/X4",PROTECTION=SAVE,
 4000          +AREAS=1,AREASIZE=200)
 4100           INTEGER NUM,X,Y,NO,I,J,N
 4200           REAL TEMP,TFACT,CRO,KR,CRF,TMIN,CONCI(20),TSEC(20),TOT
 4300           REAL MEANI(20),MIOO,MIT(20),YPOINT(20),SUMX,SUMX2,SUMY,SUMY2
 4400           REAL SUMXY,CC,DENOM,B,M,SSY,SSX,SSXY,THETA,T(20),CALC(20)
 4500           REAL DIFF(20),ERROR,XPT(20),KI
 4600     C     READ IN PRODUCT CONCENTRATIONS AND CALCULATE MEAN CONCS
 4700           READ(5,/)NUM,TEMP,TFACT,CRO,KR,CRF
 4702           WRITE(6,9001)NUM
 4704    9001   FORMAT(1H/, 'THIS IS REACTION NUMBER',I5,/)
 4706           WRITE(6,9002)TEMP
 4708    9002   FORMAT(1H/, 'THE REACTION TEMPERATURE WAS ',F6.2,/)
 4710           WRITE(6,9003)CRO
 4712    9003   FORMAT(1H/, 'THE INITIAL REACTANT CONCENTRATION WAS',F8.5,/)
 4714           WRITE(6,9004)CRF
 4716    9004   FORMAT(1H/, 'THE FINAL REACTANT CONCENTRATION WAS ',F8.5,/)
 4800           X=1
 4900           Y=1
 5000      1    READ(5,/)TMIN,NO,(CONCI(J),J=1,NO)
 5100     C     TEST FOR LAST CARD
```

```
5200          IF (NO)9,9,2
5300        2 TSEC(X)=TMIN*60.
5400          TOT=0.
5500          DO 3 I=1,NO
5600        3 TOT= CONCI(I)+TOT
5700          MEANI(X)=(TOT/NO)/TFACT
5800          X=X+1
5900          Y=Y+1
6000          GO TO 1
6100        9 N=Y-1
7000    C     This section calculates the parameters to be regressed.  MIOO
7100    C     is the mole fraction of product at infinity.  MIT is the mole
7200    C     fraction of product at some time.
7300          MIOO=MEANI(N)/(CRO-CRF)
7400          DO 6 X=1,N
7500          MIT(X)=MEANI(X)/CRO
7600        6 YPOINT(X)=ALOG(MIOO-MIT(X))
7700    C     This section calculates a regression line for YPOINT as
7800    C     a function of time. This provides a value for KR.
7900          SUMX=0.
8000          SUMX2=0.
8100          SUMY=0.
8200          SUMY2=0.
8300          SUMXY=0.
8400          DO 10 I=1,N
8500          SUMX=TSEC(I)+SUMX
8600          SUMX2=TSEC(I)*TSEC(I)+SUMX2
8700          SUMY=YPOINT(I)+SUMY
8800          SUMY2=YPOINT(I)*YPOINT(I)+SUMY2
8900       10 SUMXY=TSEC(I)*YPOINT(I)+SUMXY
9000    C     CC IS THE CORRELATION COEFFICIENT
9100          DENOM=((SUMX2-(SUMX*SUMX)/N)*(SUMY2-(SUMY*SUMY)/N))**.5
9200          CC=(SUMXY-(SUMX*SUMY)/N)/DENOM
9300    C     B IS THE INTERCEPT
9400          B=(SUMX2*SUMY-SUMX*SUMXY)/(N*SUMX2-SUMX*SUMX)
9500    C     M IS THE SLOPE
9600          M=(N*SUMXY-SUMX*SUMY)/(N*SUMX2-SUMY*SUMX)
9700    C     THIS SECTION FINDS THE CONFIDENCE INTERVAL OF THE SLOPE
9800          SSY=SUMY2-(SUMY*SUMY/N)
9900          SSX=SUMX2-(SUMX*SUMX/N)
10000         SSXY=SUMXY-(SUMX*SUMY/N)
10100         THETA=((SSY-M*SSXY)/N)**.5
10200   C     THIS IS A TABLE OF T VALUES AT THE 95% LEVEL
10300         T(1)=12.706
10400         T(2)=4.303
10500         T(3)=3.182
10600         T(4)=2.776
10700         T(5)=2.571
10800         T(6)=2.447
10900         T(7)=2.365
11000         T(8)=2.306
11100         T(9)=2.262
11200         T(10)=2.228
11300         T(11)=2.201
11400         T(12)=2.179
11500         T(13)=2.160
11600         T(14)=2.145
11700         T(15)=2.131
11800         T(16)=2.120
11900         T(17)=2.110
12000         T(18)=2.101
12100         T(19)=2.093
```

```
12200           T(20)=2.086
12300           ERROR=T(N-2)*THETA*((N/((N-2)*SSX))**.5)
12400     C     THIS CALCULATES THE REGRESSION CONTENTRATIONS
12500           DO 30 I=1,N
12600           CALC(I)=CRO*((MEANI(N)/(CRO-CRF))-TEXP(M*TSEC(I)+B)))
12700        30 DIFF(I)=MEANI(I)-CALC(I)
12710     C     This section calculates the rate of product appearance
12720           KI=-M*MEANI(N)
12800     C     THIS SECTION WRITES A TABLE OF TIMES AND CONCENTRATIONS
12900           WRITE(6,9006)
13000      9006 FORMAT('   SECONDS      CONCENTRATION      CALC. CONC.
13010          +DIFFERENCE ')
13100           WRITE(6,9007)(TSEC(I),MEANI(I),CALC(I),DIFF(I),I=1,N)
13200      9007 FORMAT(F10.1,3F15.6)
13300           WRITE(6,9008)M
13400      9008 FORMAT(1H/,'   THE SLOPE OF THE REGRESSION LINE IS',E12.4,/)
13500           WRITE(6,9009)ERROR
13600      9009 FORMAT(1H/,'THE 95%CONFIDENCE INTERVAL ON THE SLOPE IS',
13700          +E12.4,/)
13800           WRITE(6,9010)B
13900      9010 FORMAT(1H/,'THE INTERCEPT OF THE LINE IS',E12.4,/)
14000           WRITE(6,9011)CC
14100      9011 FORMAT(1H/,'THE CORRELATION COEFFIENT IS',F6.4,/)
14110           WRITE(6,9015)KI
14120      9015 FORMAT(1H/,'THE RATE OF PRODUCT APPEARANCE IS',E12.4,/)
14200     C     THIS SECTION GENERATES A FILE ON DISK CONTAINING YPOINT
14300     C     AS A FUNCTION OF TSEC.
14400           DO 12 I=1,N
14500      12   XPT(I)=TSEC(I)/1000
14600           WRITE(1,9012)(XPT(I),YPOINT(I),I=1,N)
14700      9012 FORMAT(2F10.4)
14800           STOP
14900           END
```

Program 4: MH/UNIVERSAL

```
100     $RESET FREE
200     C                  LINEAR REGRESSION PROGRAM
300     C            FOR ANALYSIS OF THE LAW OF UNIVERSAL
400     C                     REACTION RATES
500     C
600     C                        BY M. HENDERSON
700     C
800     C      THIS PROGRAM USES THE UNIVERSAL RATE EQUATION TO FIND THE
900     C      ACTIVATION ENERGY OF A REACTION.  THE INPUT CONSISTS OF
1000    C      RATE CONSTANT, TEMPERATURE (C) PAIRS, FOLLOWED BY
1100    C      A RECORD OF 0,0.  THE END RECORD THEN SPECIFIES THE
1200    C      TEMPERATURE FOR THE ENTROPY,ENTHALPY, AND FREE ENERGY.
1300    C      CALCULATIONS. THE DATA FILE IS DEFINED BY:
1400    FILE   5(KIND=DISK,FILETYPE=7, TITLE="DATA/KOA.")
1500    C
1600    C      THE OUTPUT CONSISTS OF A TABLE SHOWING EACH TEMPERATURE,
1700    C      THE OBSERVED RATE, THE CALCULATED (REGRESSION) RATE, AND
1800    C      THE DIFFERENCE BETWEEN THE RATES.  THE SLOPE, INTERCEPT,
1900    C      AND CORRELATION COEFFICIENT OF THE REGRESSION LINE ARE GIVEN.
2000    C      THE ENTHALPY, ENTROPY, AND FREE ENERGY OF ACTIVATION, AND
2100    C      THE ARRHENIUS ENERGY OF ACTIVATION ARE CALCULATED, WITH
2200    C      THEIR CONFIDENCE INTERVALS.
2300    C
2400    C      IF THE OUTPUT IS TO BE DIRECTED TO THE PRINTER,
2500    C      THEN REMOVE THE COMMENT CHARACTER FROM:
2600    FILE   6(KIND=PRINTER,MYUSE=OUT,MAXRECSIZE=22)
2700    C      AND COMPILE WITH FORTRAN.
2710    C      A DATA FILE CONTAINING THE DATA TO BE PLOTTED
2720    C      IS CREATED ON DISK.  IT IS DEFINED BY:
2730    FILE   1(KIND=DISK,TITLE="PLOT/KOA",PROTECTION=SAVE,AREAS=1,
2740           *AREASIZE=200)
2800    C
2900           INTEGER I,N
2910           REAL XAVE,YAVE,CISLP,CIINT,ERRORB,SSRESI,MEANSQ
3000           REAL SUMX,SUMXX,SUMY,SUMYY,SUMXY,SYX,SYY,SXY,T(20),H,A,S,F
3100           REAL M,B,DENOM,R2,Z,TEMP,K1,X(20),Y(20),SSR,SE,ERROR,TEM
3200           REAL YCALC(20),KCALC(20),DIFF(20),R(20),C(20),XVAL(20)
3210           REAL NUM,YUP(20),YLOW(20),YO(20),XO(20),XTEMP
3220           REAL SDEV,PDEV,SH,CIH,SS,LS
3300    C      THIS SECTION READS AND MANIPULATES THE INPUT DATA
3400           N=1
3500    1      READ (5,/) K1,TEMP
3600    9002   FORMAT(2F10.5)
3700    C      THIS TESTS FOR THE LAST DATA CARD
3800           IF(TEMP)9,9,2
3900    2      X(N)=1/(TEMP+273.)
4000           Y(N)=ALOG(K1*X(N))
4100           C(N)=TEMP
4200           R(N)=K1
4300           N=N+1
4400           GO TO 1
4500    9      N=N-1
4600           WRITE(6,9003)N
4700    9003   FORMAT(1H /,'   THE NUMBER OF DATA POINTS IS ',I5,/)
4800    C      THIS SECTION FINDS THE REGRESSION PARAMETERS
4900           SUMX=0.
5000           SUMY=0.
5100           SUMXY=0.
5200           SUMXX=0.
```

```
      SUMYY=0.
      DO 20 I=1,N
      SUMX=X(I)+SUMX
   20 SUMY=Y(I)+SUMY
      XAVE=SUMX/N
      YAVE=SUMY/N
      DO 50 I=1,N
      SXY=SXY + (X(I)-XAVE)*(Y(I)-YAVE)
      SXX=SXX + (X(I)-XAVE)**2
   50 SYY=SYY + (Y(I)-YAVE)**2
C     CALCULATE RESIDUALS
      S2XY=SXY*SXY
      SSREG=S2XY/SXX
      SSRESI=SYY-SSREG
      MEANSQ=(SSRESI/(N-2))**.5
C     M IS THE SLOPE
      M=SXY/SXX
C     B IS THE INTERCEPT
      B=YAVE-M*XAVE
C     R2 IS THE CORRELATION COEFFICIENT
      R2=SSREG/SYY
C     THIS IS A TABLE OF STUDENT'S T VALUES AT THE .095 LEVEL
      T(1)=12.706
      T(2)=4.303
      T(3)=3.182
      T(4)=2.776
      T(5)=2.571
      T(6)=2.447
      T(7)=2.365
      T(8)=2.306
      T(9)=2.262
      T(10)=2.228
      T(11)=2.201
      T(12)=2.179
      T(13)=2.160
      T(14)=2.145
      T(15)=2.131
      T(16)=2.120
      T(17)=2.110
      T(18)=2.101
      T(19)=2.093
      T(20)=2.086
C     THIS SECTION FINDS THE CONFIDENCE INTERVAL FOR THE SLOPE
      SS= SYY-(S2XY/SXX)
      LS = (SS/(N-2))**.5
      CISLP= (T(N-2)*LS)/(SXX**.5)
C     THIS FINDS THE CONFIDENCE INTERVAL FOR THE INTERCEPT
      CIINT=T(N-2)*(((SUMX**2)/(N*SXX))**.5)*LS
C     THIS WRITES THE SUMS AND MEANSQ
      WRITE(6,3000)MEANSQ,SXX,SUMX
 8000 FORMAT(1H/,'MEANSQ=',E12.4,'  SXX=',E14.4,' SUMX=',E12.4,/)
      WRITE(6,8005)SYY
 8005 FORMAT(1H/,'SYY=',E12.4,/)
C     THIS CALCULATES THE REGRESSION RATES
      DO 30 I=1,N
      YCALC(I)=(M*X(I)+B)
      KCALC(I)=EXP(YCALC(I))*(C(I)+273)
   30 DIFF(I)=R(I)-KCALC(I)
C     THIS SECTION WRITES THE OUTPUT DATA
      WRITE(6,9004)
 9004 FORMAT('    TEMP         RATE          CALC. RATE       DIFFERENCE '
      WRITE(6,9005)(C(I),R(I),KCALC(I),DIFF(I),I=1,N)
```

```
10200      9005 FORMAT(F9.1,E14.4,E15.4,E16.4)
10300           WRITE(6,9006)M
10400      9006 FORMAT(1H /,'   THE SLOPE OF THE REGRESSION LINE IS',E12.4,/)
10410           WRITE(6,9020)CISLP
10420      9020 FORMAT(1H /,'   THE SLOPES 95% CONFIDENCE INTERVAL IS',E12.4,/)
 1500           WRITE(6,9007)B
_1600      9007 FORMAT('  THE INTERCEPT OF THE LINE IS',E12.4,/)
10610           WRITE(6,9025)CIINT
10620      9025 FORMAT(1H /,' THE INTERCEPTS 95% CI IS',E12.4,/)
10700           WRITE(6,9008)R2
10800      9008 FORMAT('   THE CORRELATION COEFFICIENT IS  ',F6.4,/)
10900           READ(5,/)TEMP
11000           TEM=TEMP+273
11010      C    CALCULATE H, Ea, S, and F VALUES
11100           H=-M*1.9872
11200           Z=H*(1.9872*TEM)
11300           A=EXP(B)
11400            S=1.9872*(B-23.7600)
11500           F=H-TEM*S
11600           WRITE(6,9009)TEMP
11700      9009 FORMAT('   AT ',F5.1,' DEGREES C :',/)
11800           WRITE(6,9010)H
11900      9010 FORMAT('      THE ENTHALPY OF ACTIVATION IS',E12.5,/)
12000           WRITE(6,9011)Z
12100      9011 FORMAT('      THE ACTIVATION ENERGY IS',E12.5,/)
12200           WRITE(6,9012)F
12300      9012 FORMAT('      THE FREE ENERGY OF ACTIVATION IS',E12.5,/)
12310           SDEV=(CISLP*(N**.5))/(T(N-2))
12320           PDEV= SDEV/M
12330           SH= H*PDEV
12400           CIH=((T(N-2))*SH)/(N**.5)
  500           WRITE(6,9013)CIH
12600      9013 FORMAT('      THE CONFIDENCE INTERVAL ON H IS',E12.5,/)
12700           WRITE(6,9014)S
12800      9014 FORMAT('      THE ENTROPY OF ACTIVATION IS',E12.4,/)
13000           IDEV = (CIINT*(N**.5))/(T(N-2))
13020           PIDEV = IDEV/B
13040           SENT = S * PIDEV
13050           CIENT = ((T(N-2))*SENT)/(N**.5)
13100           WRITE(6,9015)CIENT
13200      9015 FORMAT('      THE CONFIDENCE INTERVAL ON THE ENTROPY IS',E12.4,/)
13210      C    THIS SECTION WRITES TO THE FILE ON DISK.
13212           DO 25 I=1,N
13214        25 XVAL(I)=X(I)*1000
13220           WRITE(1,9016)(XVAL(I),Y(I),I=1,N)
13230      9016 FORMAT(2F10.4)
13500      C    THIS SECTION CALCULATES Y-VALUES FOR THE 95% CI
13550           XTEMP=1.95E-03
13600           DO 70 I=1,10
13700           XO(I)=XTEMP+0.05E-03
13800           YO(I)=M*XO(I)+B
13900           NUM=(XO(I)-XAVE)**2
14000           YUP(I)=YO(I)+T(N-2)*9.612E-2*(1+(1/N)+((NUM/SXX)**.5))
14100           YLOW(I)=YO(I)-T(N-2)*9.612E-2*(1+(1/N)+((NUM/SXX)**.5))
14150        70 XTEMP=XO(I)
14200           WRITE(6,9030)
 4300      9030 FORMAT('    X VALUE      Y PREDICTED     Y UPPER    Y LOWER   ')
_4400           WRITE(6,9035)(XO(I),YO(I),YUP(I),YLOW(I),I=1,10)
14500      9035 FORMAT(4E15.4)
15000           STOP
15100           END
```

Program 5: TEMP/ADJ

```
$RESET FREE
C
C       RATE CONSTANT TEMPERATURE ADJUSTMENT
C
C            WRITTEN BY D. BLYTHE
C
C     THIS PROGRAM USES THE ARRENHIUS EQUATION TO ADJUST
C     A RATE CONSTANT FROM ONE TEMPERATURE TO ANOTHER.
C     THE INPUT CONSISTS OF RECORDS SPECIFYING THE OBSERVED
C     RATE OF REACTION AND TEMPERATURE (C), THE ACTIVATION
C     ENERGY OF THE REACTION (CAL), AND THE DESIRED TEMPERATURE.
C     THE END CARD IS 0.0,0.0,0.
C
C     THE OUTPUT SHOWS THE INPUT DATA AND THE CALCULATED
C     REACTION RATE AT THE DESIRED TEMPERATURE.
C     IF THE OUTPUT IS TO BE DIRECTED TO THE PRINTER,
C     THEN REMOVE THE COMMENT CARD FROM:
CFILE  6(KIND=PRINTER,MYUSE=OUT,MAXRECSIZE=22)
C     AND COMPILE WITH FORTRAN
C
      REAL TSET,K1,T1,KSET,ACTE
      WRITE(6,8887)
 8887 FORMAT(1H /,'   INPUT T     INPUT K        ACTV. E.       TSET
     *          KSET')
 1    READ(5,/)K1,T1,ACTE,TSET
 9999 FORMAT(2F10.5)
      IF(K1)4,4,3
 3    KSET=EXP(ALOG(K1)-(ACTE/1.9872)*(1/(TSET+273.)-1/(T1+273.)))
      WRITE(6,8888)T1,K1,ACTE,TSET,KSET
 8888 FORMAT(F10.2,E15.5,F14.0,F15.2,E15.5)
      GO TO 1
 4    STOP
      END
```

Program 6: ALL/AN

This HP-41 program converts peak areas obtained from the gc to concentrations according to the following equation:

$$M_{xi}=\left[\frac{M_{IS}\rho_x}{F_v\rho_{IS}}\right]\left[\frac{W_{IS}}{W_x A_{IS}}\right]\left[A_{xi} F_{xi}\right]$$

where M_{xi} = molarity of component i

M_{IS} = molarity of internal standard solution

F_V = expansivity factor

ρ_{IS} = density of internal standard solution

ρ_x = density of sample

W_{IS} = weight of internal standard added

W_x = wieght of sample

A_{IS} = area of internal standard

A_{xi} = area of component i

F_{xi} = response factor for component i

Registers used: 05 M_{IS} 06 ρ_x 07 ρ_{IS} 08 F_v 09 $\frac{M_{IS}\rho_x}{F_v\rho_{IS}}$ 10 $\frac{W_{IS}}{W_x A_{IS}}$ 11 F_{Mbitl} 12 F_{Mnitl} 13 F_{LM} 14 F_x

Program Steps:

```
[Prgm]
GTO ..
 LBL [Alpha] ALLAN [Alpha]
RCL 05
Enter
RCL 06
x
RCL 07
÷
RCL 08
÷
STO 09
[Alpha] WIS? [Alpha]
XEQ
[Alpha] Prompt [Alpha]
Enter
[Alpha] WX? [Alpha]
XEQ
[Alpha] Prompt [Alpha]
÷
[Alpha] AIS? [Alpha]
XEQ
[Alpha] prompt [Alpha]
÷
STO 10
LBL 01
[Alpha] AMBITL? [Alpha]
XEQ
[Alpha] Prompt [Alpha]
ENTER
X=0?
GTO 02
RCL 11
x
XEQ A
LBL 02
[Alpha] AMNITL? [Alpha]
XEQ
[Alpha] Prompt [Alpha]
ENTER
X=0?
GTO 03
RCL 12
X
XEQ A
LBL 03
[Alpha] ALM? [Alpha]
XEQ
[Alpha] Prompt [Alpha]
Enter
X=0?
GTO 04
RCL 13
x
```

```
XEQ A
LBL 04
[Alpha] AX? [Alpha]
XEQ
[Alpha] Prompt [Alpha]
Enter
X=0?
GTO 05
[Alpha] FX? [Alpha]
XEQ
[Alpha] Prompt [Alpha]
x
XEQ  A
GTO 05
LBL A
RCL 10
x
RCL 09
x
R/S
RTN
LBL 05
END
```

Program 7: O18AN.BAS

```
10 REM This program calculates the fraction of the mannitol
20 REM which forms from OA cleavage based on the amount
30 REM of O18 incorporated into it.
35 DIM A(25), T(25), U(25), V(25)
40 INPUT "Label for this degradation run ", LABEL$
50 'PRINT LABEL'
60 LPRINT "This is degradation "; LABEL$
70 REM This section calculates the fractions of the various
80 REM isotopes present in natural mannitol.
90 'Print Prompt'
100 PRINT "Enter ms counts for natural mannitol"
110 INPUT "No. counts at M=548 "; M548
120 INPUT "No. counts at M=549 "; M549
130 INPUT "No. counts at M=550 "; M550
140 INPUT "No. counts at M=551 "; M551
150 'Print Header and Label'
160 LPRINT "This is the natural MNT for degradation "; LABEL$
170 LPRINT "Pass      Alpha          M        MO17        MO18"
175 A(1)= .15
180 I=0
190 I=I+1
200 'Calculate MO17 and MO18'
205 M=M548
210 MO17=M549-(A(I)* M)
220 MO18=M550-(A(I)* MO17)
230 'Write values from this pass'
240 LPRINT USING "##        "; I;
250 LPRINT USING "#.####    "; A(I);
260 LPRINT USING "######.#  ";M, MO17, MO18
270 'Calculate new A'
280 A(I+1)= M551/MO18
290 'Compare last two A values'
300 IF I<25, GOTO 330
310 PRINT "25 passes, no convergence"
320 GOTO 1400
330 DIFA=ABS(A(I)-A(I+1))
340 IF DIFA > .0001, GOTO 190
345 ALPHA = A(I+1)
350 'Calculate Isotope Fractions'
360 MC13= ALPHA * M
370 MC13O17 = ALPHA * MO17
380 MC13O18 = ALPHA * MO18
390 MTOT = M+MO17+MO18+MC13+MC13O17+MC13O18
400 BETA = MO17/MTOT
410 GAMMA = MO18/MTOT
420 DELTA = M/MTOT
430 REM End of this section
440 REM Calculation of the numbers of various MBT species
450 RTOT = 100
460 RO17 = BETA * RTOT
470 RO18 = GAMMA * RTOT
480 R = DELTA * RTOT
490 RC13 = ALPHA * R
500 RC13O17 = ALPHA * RO17
```

```
510 RC13O18 = ALPHA * RO18
520 REM End of this Section
530 REM This section inputs the counts observed for the
540 REM experimentally observed mixture of natural and
550 REM enriched mannitol and normalizes them.
580 PRINT "Enter ms counts for product mannitol"
590 INPUT "No. counts at M=548"; M548P
600 INPUT "No. counts at M=549 "; M549P
610 INPUT "No. counts at M=55O "; M55OP
620 INPUT "No. counts at M=551 "; M551P
630 ETOT = RTOT
640 ETOTP = M548P+ M549P + M55OP + M551P
650 NORMF = ETOTP/ETOT
660 E548 = M548P/NORMF
670 E549 = M549P/NORMF
680 E55O = M55OP/NORMF
690 E551 = M551P/NORMF
700 REM End of this section
710 REM This section calculates the fractions of the various
720 REM isotopic species present in the liquor.
730 'Print Prompt'
740 PRINT "Enter ms counts for liquor"
750 INPUT "No. counts at M=16 "; M16
760 INPUT "No. counts at M=17 "; M17
770 INPUT "No. counts at M=18 "; M18
780 INPUT "No. counts at M=19 "; M19
790 INPUT "No. counts at M=20 "; M20
800 MTOT = M16 + M17 + M18 + M19 + M20
820 'Enter initial values for T, U, and V'
830 T(1) = .75
840 U(1) = .2
850 V(1) = .05
860 'Print header and label'
865 LPRINT
870 LPRINT "This is the liquor for deg. " LABEL$
880 LPRINT "Pass     T      U       V      O16       O17       O18 "
890 I=O
900 I=I+1
910 'Calculate O16, O17, and O18'
920 O18 = M2O/T(I)
930 O17 = (M19-(U(I)*O18))/T(I)
940 O16 = (M18-(U(I)*O17)-(V(I)*O18))/T(I)
950 'WRITE VALUES FROM THIS PASS'
960 LPRINT USING "##      ";I;
970 LPRINT USING "#.####    ";T(I), U(I), V(I);
980 LPRINT USING "#######.#  "; O16, O17, O18
990 'Calculate new T, U, and V'
1000 V(I+1) = M16/O16
1010 U(I+1) = (M17-(V(I+1)*O17))/O16
1020 T(I+1) = 1-U(I+1)-V(I+1)
1030 'Compare last two T, U, and V values'
1040 IF I<25, GOTO 1070
1050 PRINT "25 PASSES, NO CONVERGENCE"
1060 GOTO 1400
1070 DIFT = ABS(T(I)-T(I+1))
1080 IF DIFT > .0002, GOTO 900
1090 DIFU = ABS(U(I)-U(I+1))
1100 IF DIFU > .0002, GOTO 900
```

```
1110 DIFV = ABS(V(I)-V(I+1))
1120 IF DIFV > .0002, GOTO 900
1130 'Now calculate fractions of various species'
1140 C = O16/HTOT
1150 D = O17/HTOT
1160 E = O18/HTOT
1170 REM End of liquor calculation section
1180 REM This section calculates OA, the fraction of cleavage
1190 REM at the oxygen-aglycon bond.
1195 LPRINT
1200 LPRINT "These are OA fractions for Deg. ";LABEL$
1210 'Calculate OA from M548 measurement'
1220 OA548 = (E548-R)/(R * C - R)
1230 LPRINT "From M548, OA =";
1240 LPRINT USING "##.#### "; OA548
1250 'Calculate OA from M549 measurement'
1260 OA549 = (E549- (RC13 + RO17))/(RC13*C-RC13+R*D+RO17*C-RO17)
1270 LPRINT "From M549, OA = ";
1280 LPRINT USING "##.#### ";OA549
1300 'Calculate OA from M550 measurement'
1310 NUM = E550 - RO18-RC13O17
1320 DEN = R*E + RO18*C + RC13*D + RC13O17*C + RO17*D - RO18-RC13O17
1330 OA550 = NUM/DEN
1340 LPRINT "From M550, OA = ";
1350 LPRINT USING "##.#### "; OA550
1400 END
```

APPENDIX II

MASS SPECTRA

Table 17. CI mass spectrum of TFA derivative of 1,5-anhydro-D-mannitol, OV-1 column.

M/E	Intensity	Assignment
577	2.1	M+29
549	49.7	M+1
435	100.0	M-113
321	8.8	M-114-113
115	16.2	Protonated TFA

Table 18. CI mass spectrum of TFA derivative of product 1,5-anhydro-D-iditol, OV-1 column.

M/E	Intensity	Assignment
549	11.6	M+1
435	53.8	*,a
321	8.1	*,b
207	6.1	*,c
115	100.0	Protonated TFA

*Corresponds to the protonated molecular ion which has lost (a) one, (b), two, or (c) three TFA groups.

Table 19. NCI mass spectrum of TFA derivative of authentic 1,5-anhydro-D-iditol.

M/E	Intensity	Assignment
548	3.6	M
435	1.1	M-TFA anion
275	9.3	
227	100.0	TFA+TFA anion
113	37.0	TFA anion

Table 20. NCI mass spectrum of TFA derivative of product 1,5-anhydro-D-iditol.

M/E	Intensity	Assignment
548	3.1	M-1
275	10.8	
227	100.0	TFA+TFA anion
113	42.0	TFA anion

Table 21. EI mass spectrum of the TFA derivative of authentic 1,5-anhydro-D-iditol.

M/E	Intensity	Assignment
320	11.5	M-2TFAH
207	15.9	M-2TFAH-TFA
193	33.8	M-$CH_2OC(CF_3)O$
97	16.9	
69	100.0	CF_3+

Table 22. EI mass spectrum of the TFA derivative of product 1,5-anhydro-D-iditol.

M/E	Intensity	Assignment
320	7.6	M-2TFAH
207	10.4	M-2TFAH-TFA
193	23.8	M-$CH_2OC(CF_3)O$
97	15.7	
69	100.0	CF_3+

APPENDIX III

NUCLEAR MAGNETIC RESONANCE SPECTRA

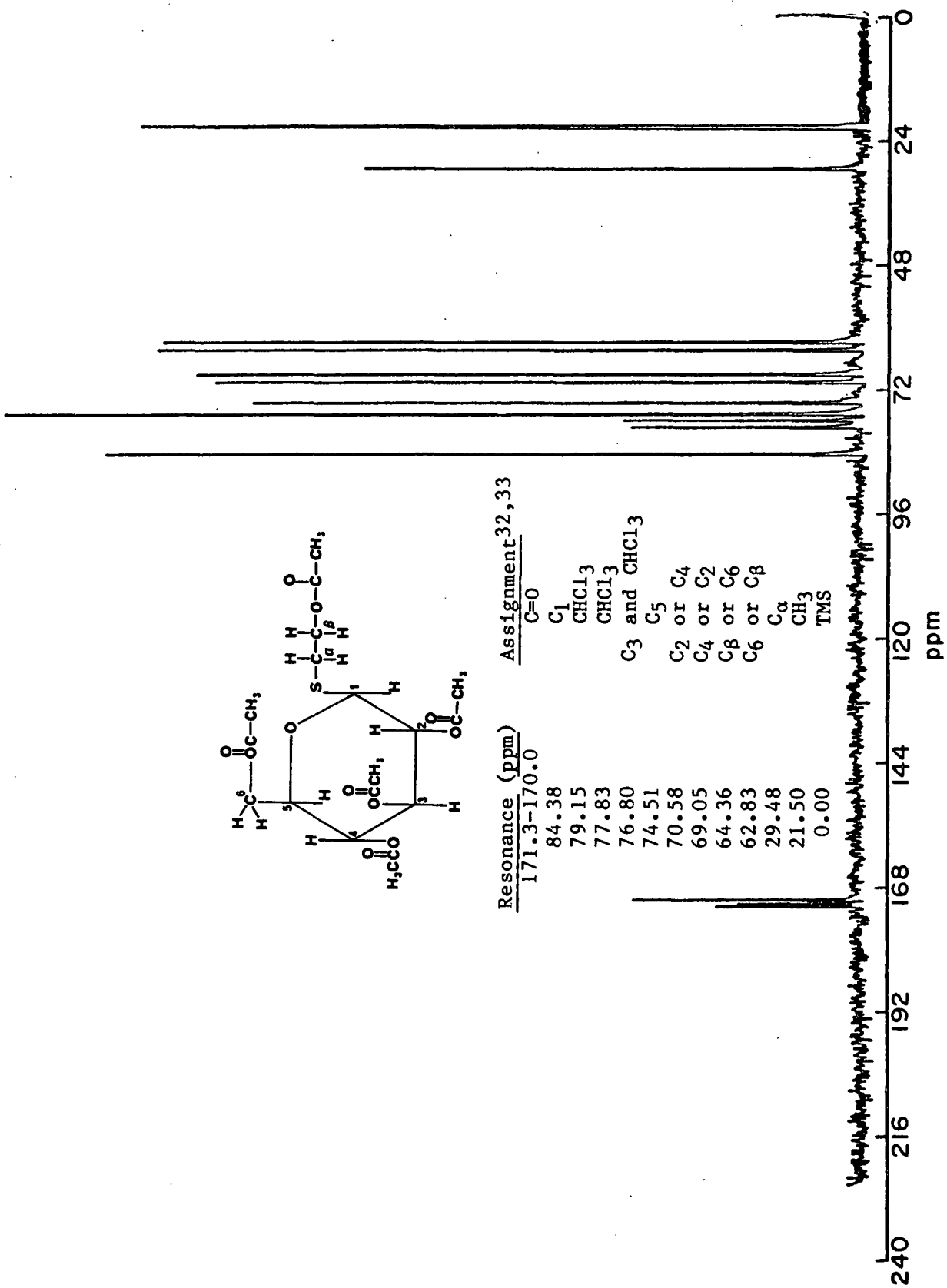

Figure 23. ^{13}C-NMR spectrum of 2-acetoxyethyl 2,3,4,6-tetra-O-acetyl-1-thio-β-D-glucopyranoside tetraacetate in $CDCl_3$.

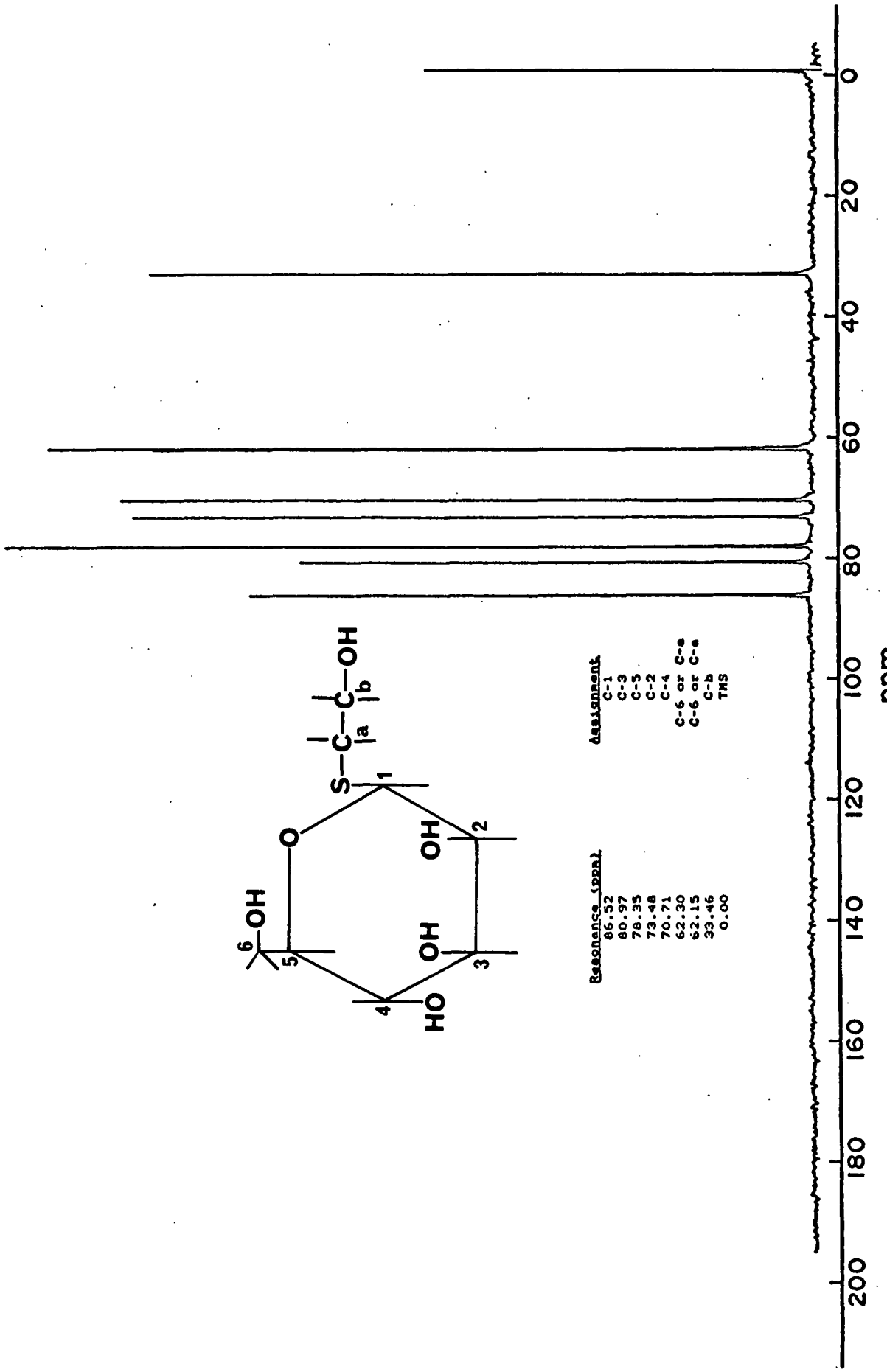

Figure 24. ^{13}C-NMR spectrum of 2-hydroxyethyl 1-thio-β-D-glucopyranoside in D_2O.

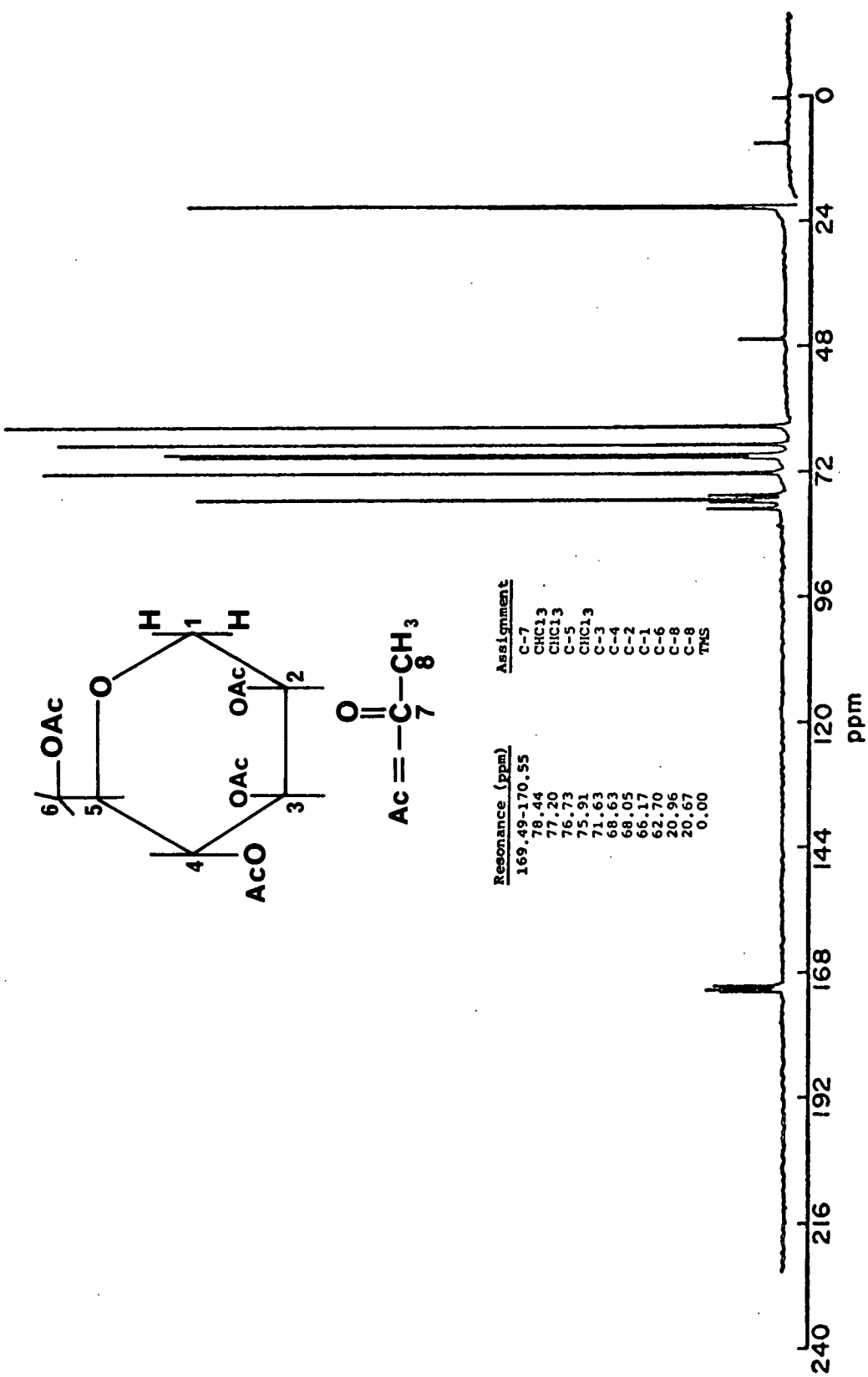

Figure 25. ^{13}C-NMR spectrum of 1,5-anhydro-2,3,4,6-tetra-O-acetyl-D-mannitol in $CDCl_3$.

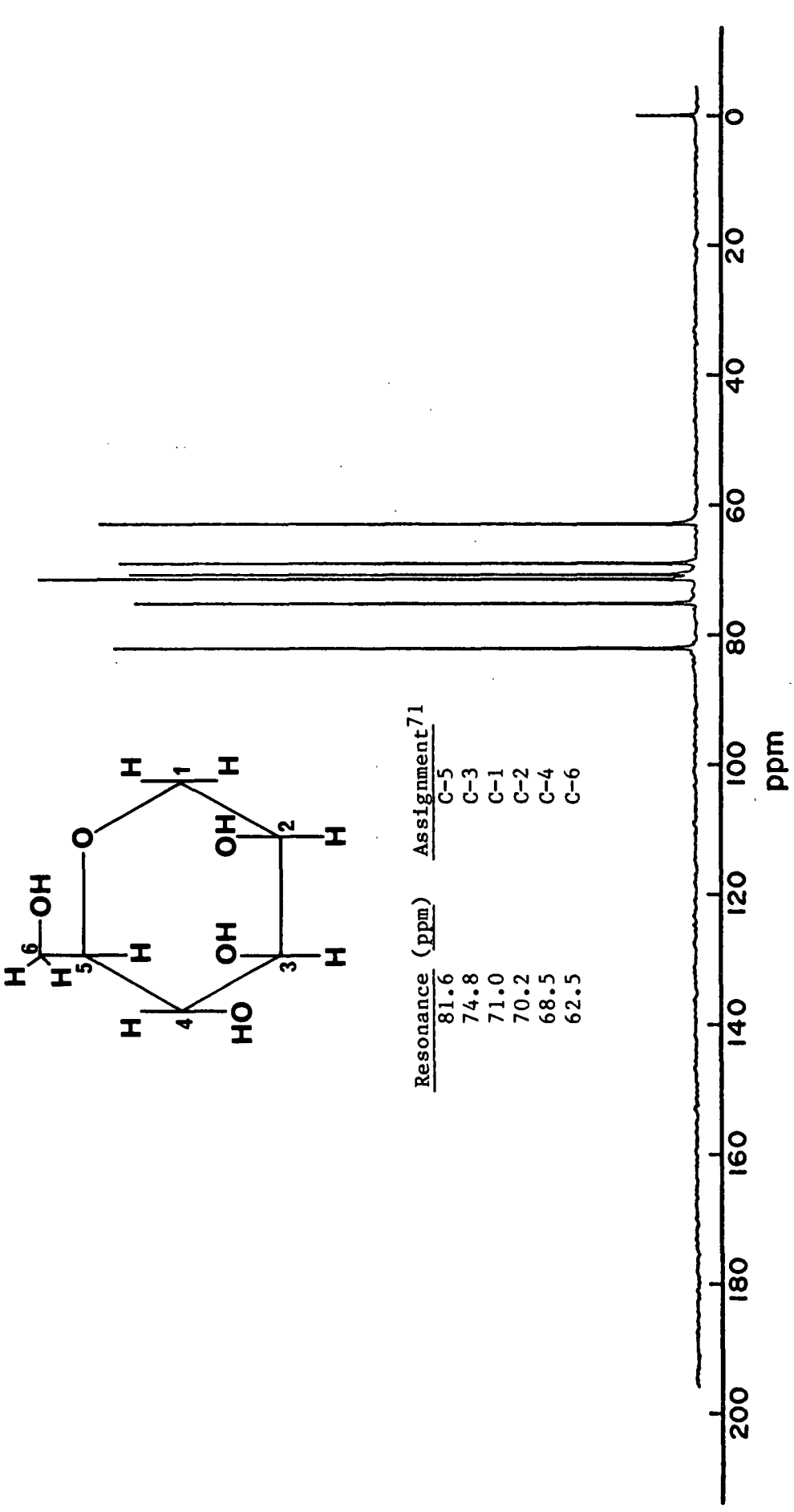

Resonance (ppm)	Assignment[71]
81.6	C-5
74.8	C-3
71.0	C-1
70.2	C-2
68.5	C-4
62.5	C-6

Figure 26. ^{13}C-NMR spectrum of 1,5-anhydro-D-mannitol in D_2O.

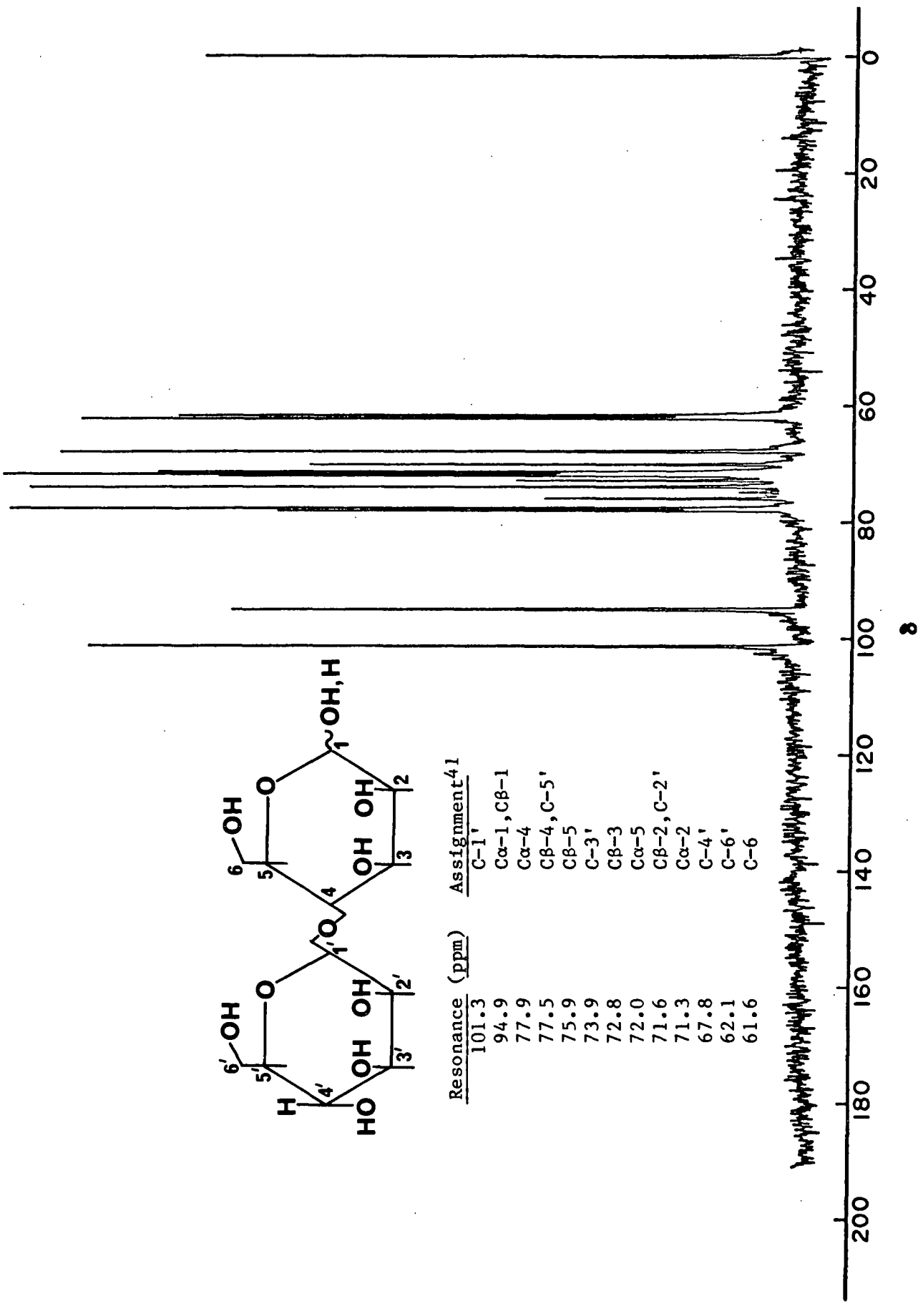

Figure 27. ^{13}C-NMR spectrum of mannobiose in D_2O.

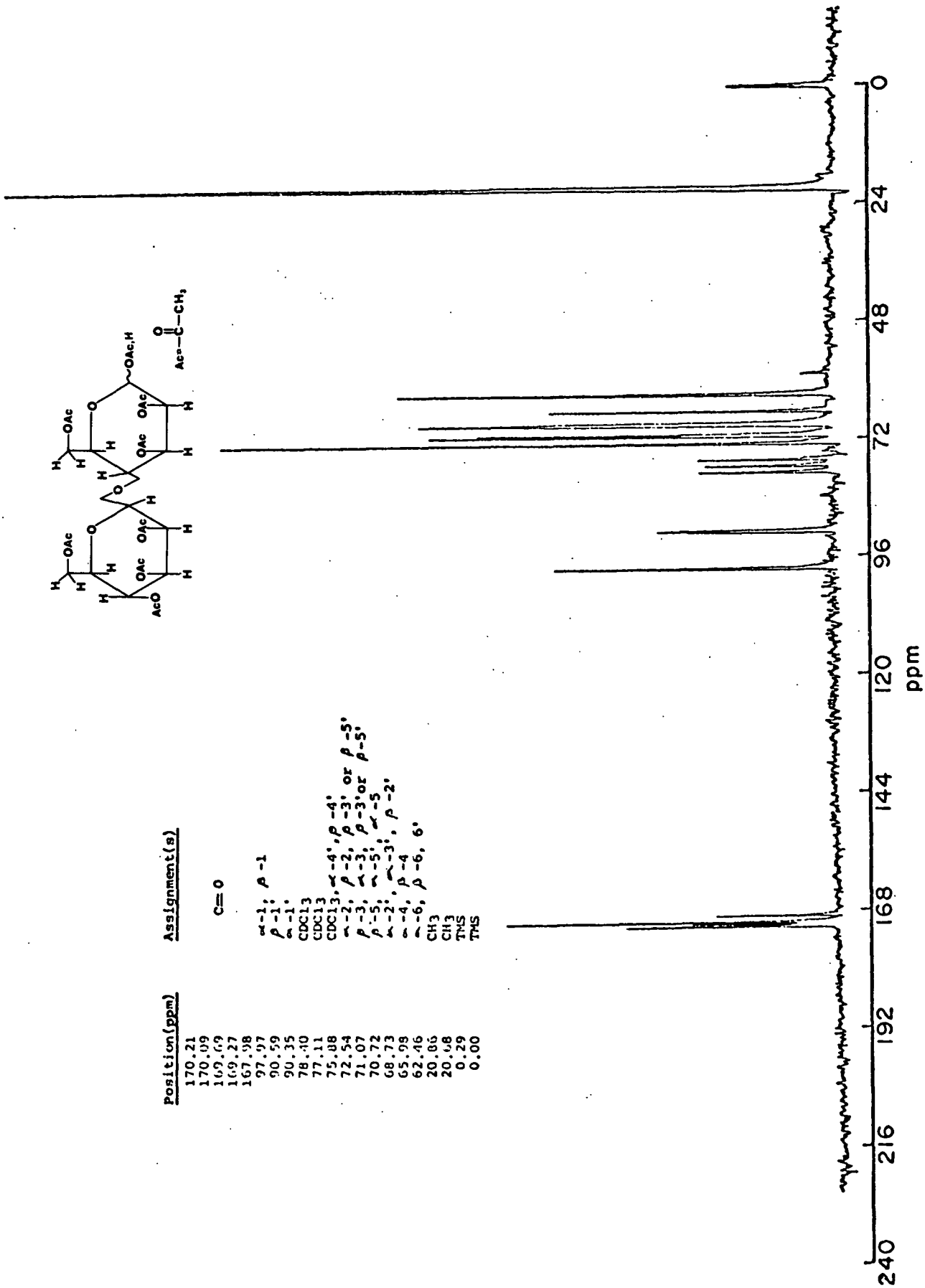

Figure 28. ^{13}C-NMR spectrum of mannobiose octaacetate in $CDCl_3$.

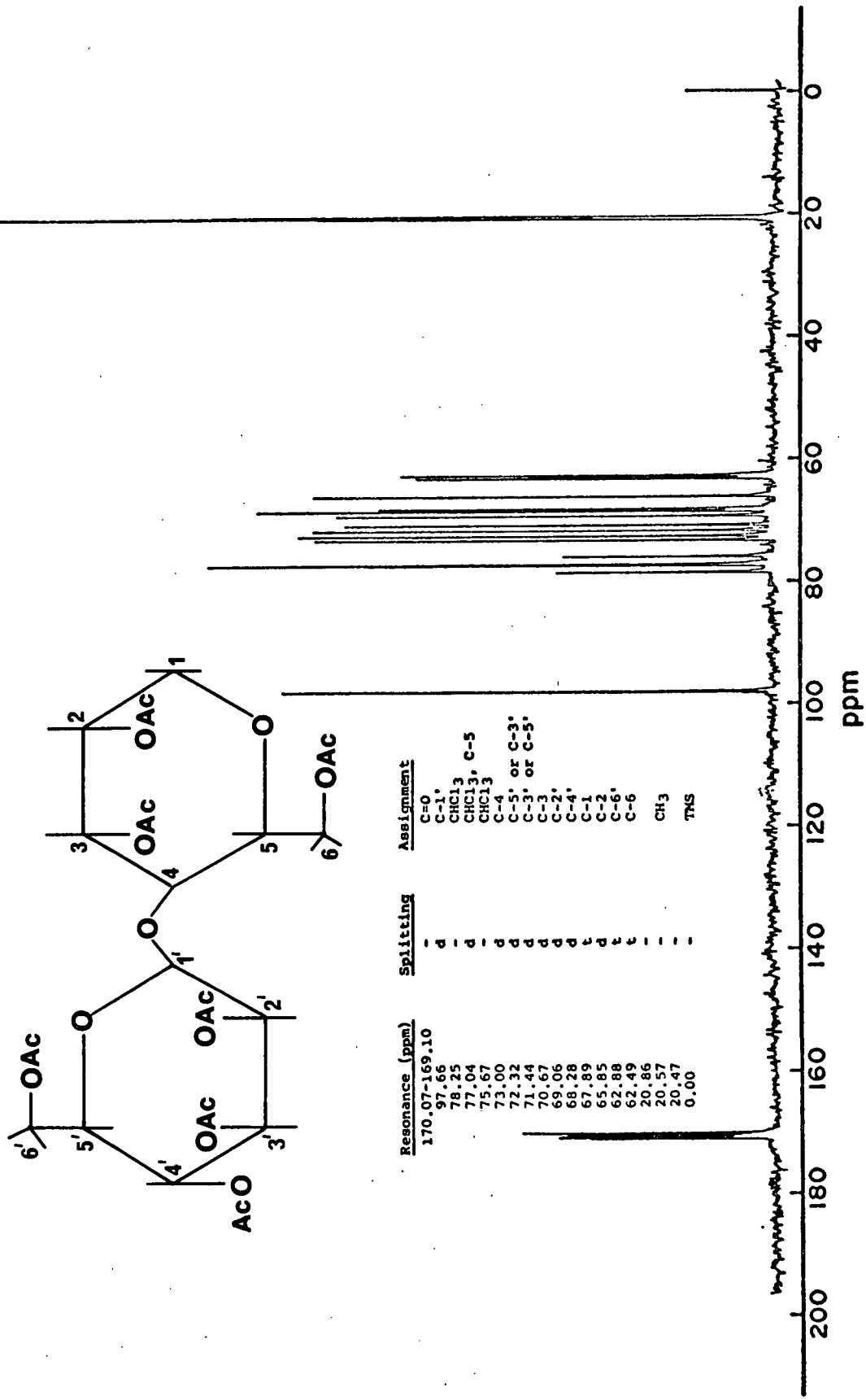

Figure 29. ^{13}C-NMR spectrum of 1,5-anhydro-2,3,6-tri-O-acetyl-4-O-(2,3,4,6-tetra-O-acetyl-mannopyranosyl)-D-mannitol.

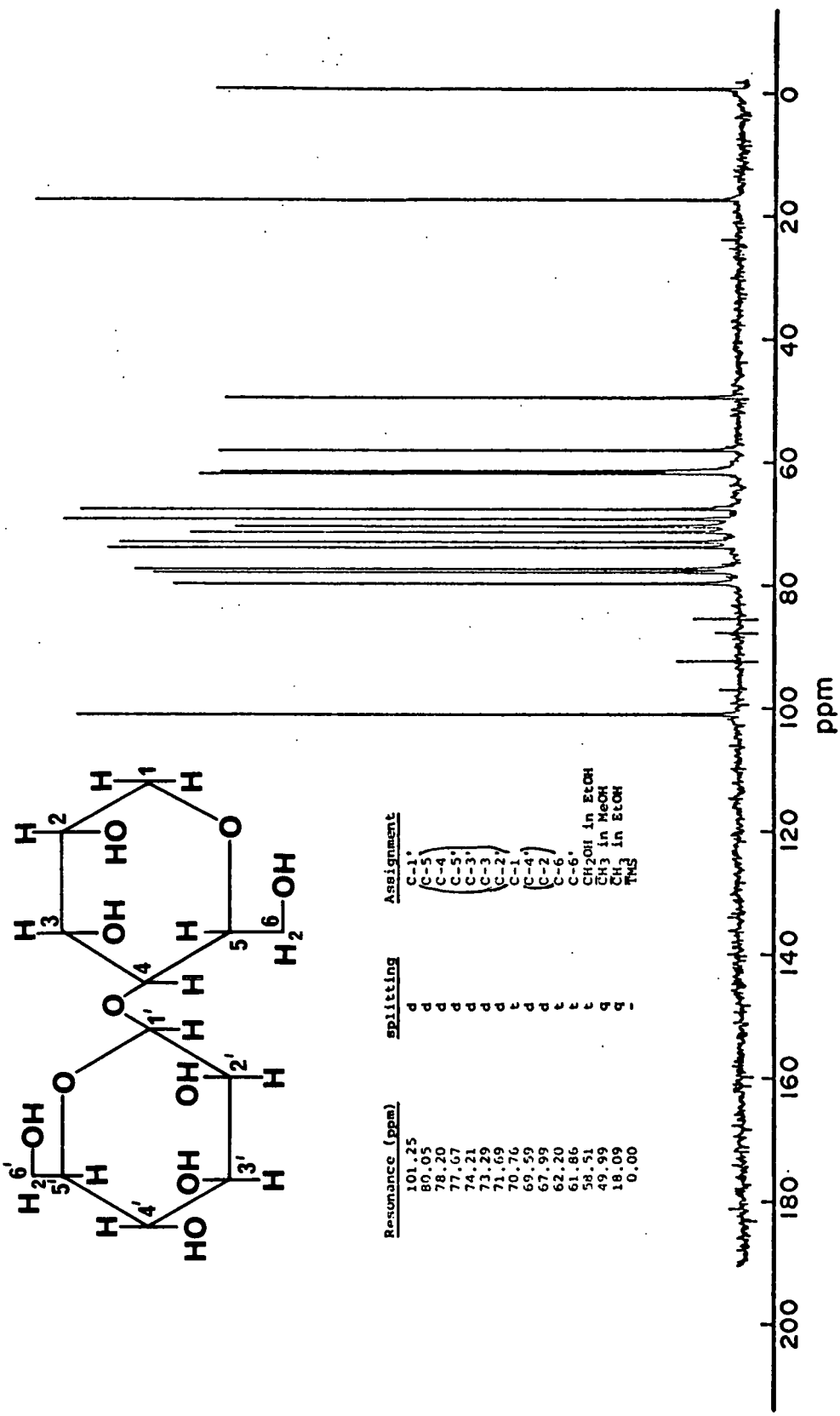

Figure 30. ^{13}C-NMR spectrum of 1,5-anhydro-4-O-β-mannopyranosyl-D-mannitol in D_2O.

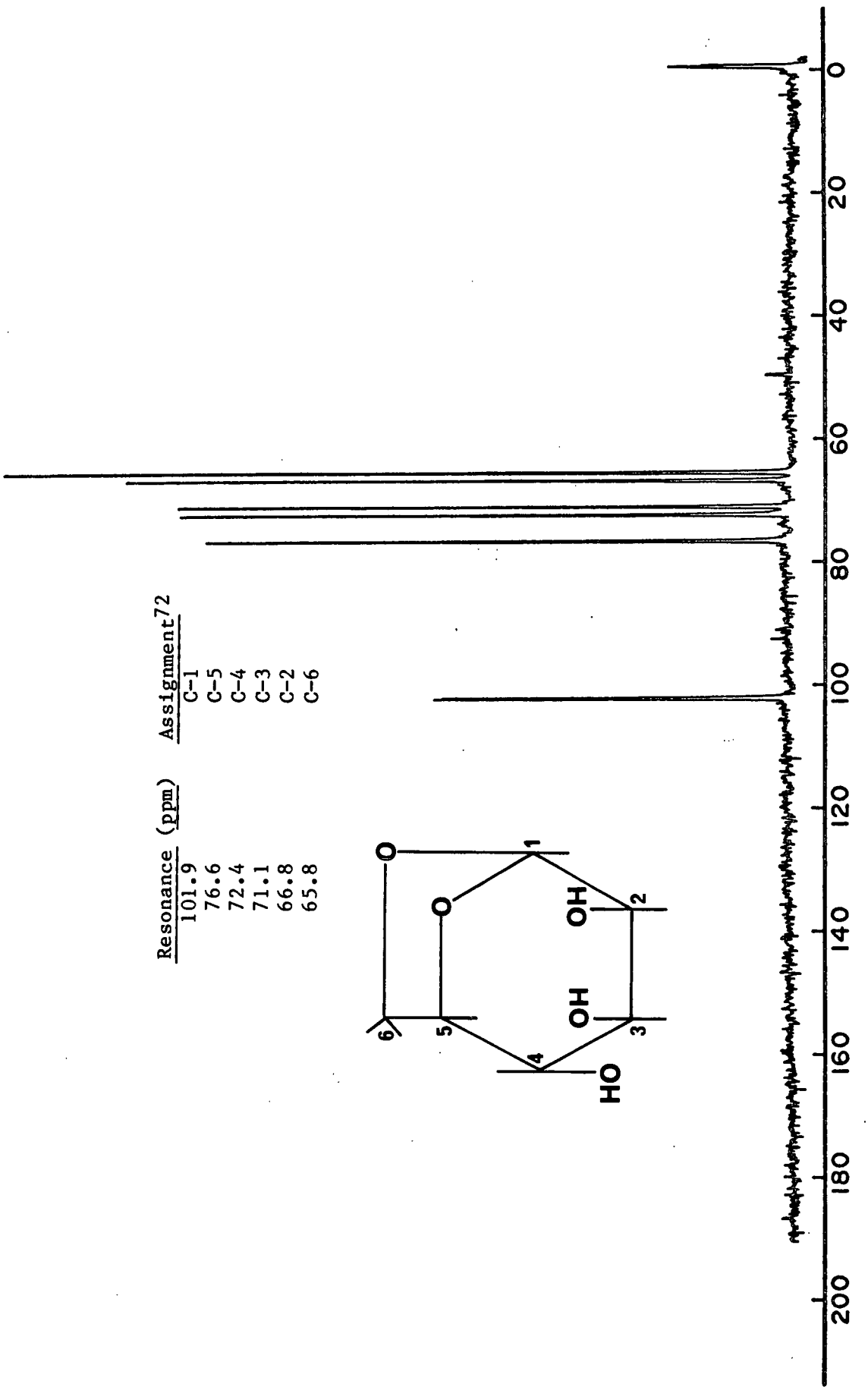

Figure 31. ^{13}C-NMR spectrum of 1,6-anhydro-β-D-mannopyranose in D_2O.

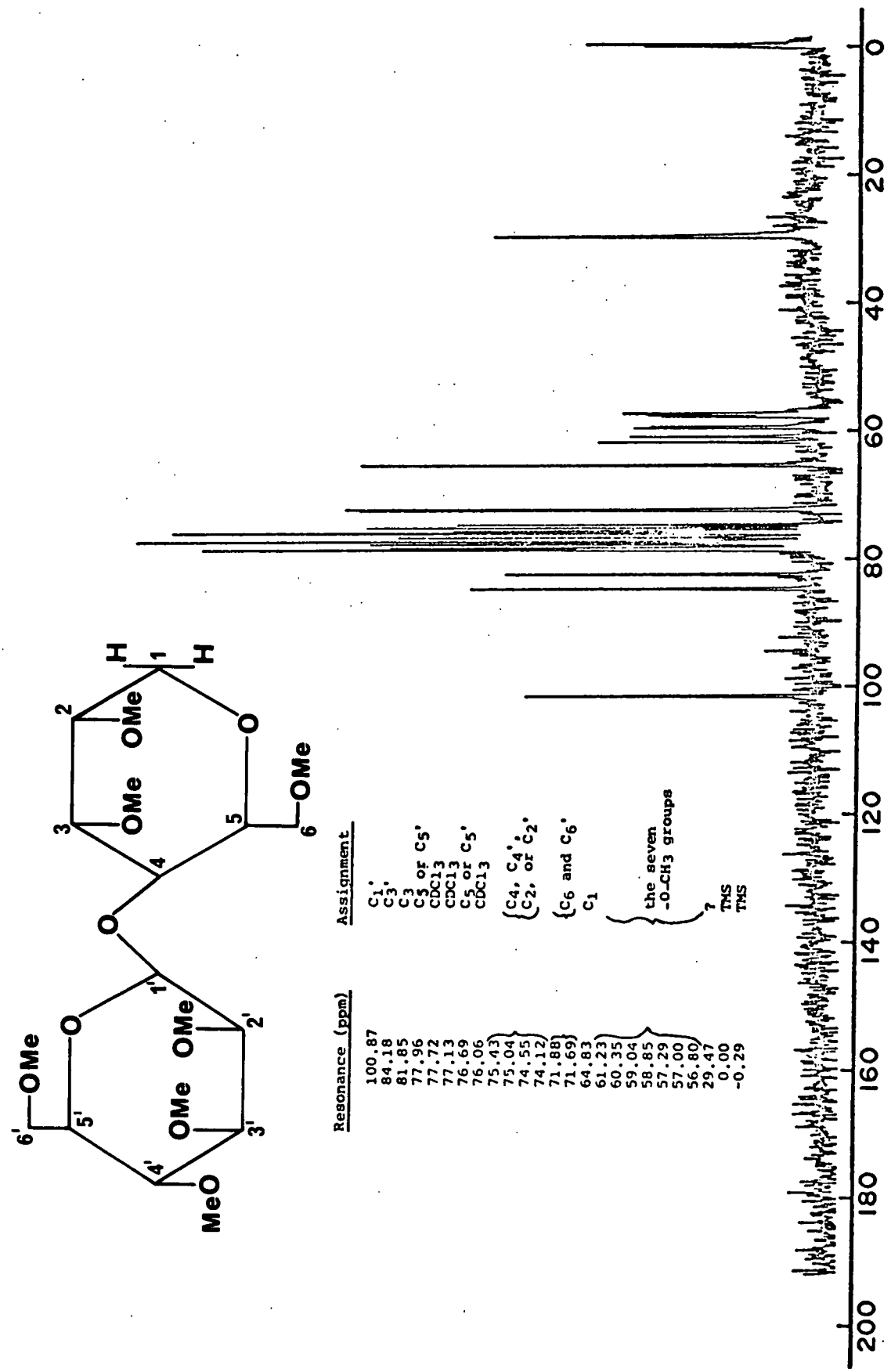

Figure 32. ^{13}C-NMR spectrum of 1,5-anhydro-2,3,6-tri-O-methyl-4-O-β-(2,3,4,6-tetra-O-methyl-mannopyranosyl)-D-mannitol in $CDCl_3$.

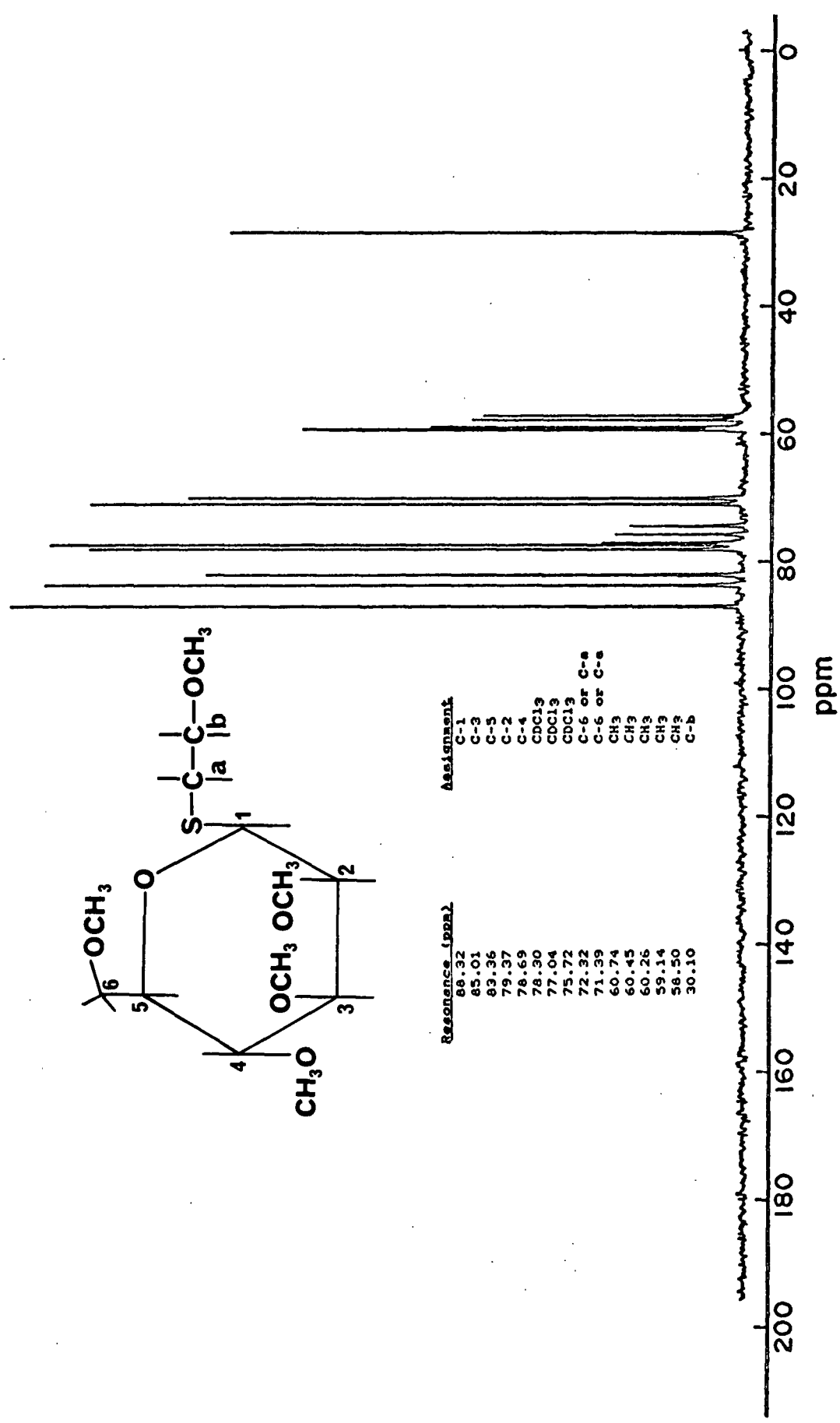

Figure 33. ^{13}C-NMR spectrum of 2-methoxyethyl 2,3,4,6-tetra-O-methyl-1-thio-β-D-glucopyranoside in $CDCl_3$.

APPENDIX IV

EXPERIMENTAL DATA

Table 23. Stability of 1,5-anhydro-D-mannitol (0.01M) in 2.553M sodium hydroxide at 180.36 ± 0.09°C.

Time, min	[MNT][a], M x 10^3
0.0	0.0105
1440.0	0.0100
2880.0	0.0100
4320.0	0.0102
5760.0	0.0101
7200.0	0.0097
8640.0	0.0103
10080.0	0.0101
11520.0	0.0099
12960.0	0.0094
14400.0	0.0097
15840.0	0.0100
17280.0	0.0096
18720.0	0.0096
21600.0	0.0095

[a][MNT] = concentration of 1,5-anhydro-D-mannitol at reaction temperature.

Table 24. Degradation of 1,5-anhydromannobiitol (0.01M) in 2.500M NaOH at 171.13 ± 0.1°C.

Time, min	[MBT][a]	[MBT][b]	[X4][c]
0.0	11.069	0.130	0.000
120.0	10.912	0.476	0.058
240.0	10.117	0.833	0.063
360.0	9.780	1.159	0.094
480.0	9.167	1.515	0.108
720.0	8.601	2.129	0.168
960.0	7.839	2.745	0.216
1440.0	6.631	3.585	0.256
1800.0	5.834	4.325	0.329
2160.0	5.076	4.834	0.382
2880.0	3.914	6.020	0.527
3600.0	3.010	6.418	0.524

$k_r = 6.05 \pm 0.10 \times 10^{-6}$, sec^{-1}.
$k_{MNT} = 4.81 \pm 0.13 \times 10^{-6}$, sec^{-1}.
$k_{X4} = 0.267 \pm 0.025 \times 10^{-6}$, sec^{-1}.
MNT from OA cleavage = 5.05%.
$k_{GO} = 4.57 \pm 0.13 \times 10^{-6}$, sec^{-1}.
$k_{OA} = 1.48 \pm 0.16 \times 10^{-6}$, sec^{-1}.

---

[a][MBT] = concentration of 1,5-anhydromannobiitol at reaction temperature, M x 10^3.
[b][MBT] = concentration of 1,5-anhydro-D-mannitol at reaction temperature, M x 10^3.
[c][X4] = concentration of 1,5-anhydro-D-iditol at reaction temperature, M x 10^3, calculated using MNT response factor.

Table 25. Degradation of 1,5-anhydromannobiitol (0.01M) in 2.508M NaOH at 162.18 ± 0.1°C.

Time, min	[MBT]a	[MBT]b	[X4]c
0.0	9.078	0.073	0.000
360.0	8.992	0.391	0.032
720.0	8.029	0.840	0.073
1080.3	7.702	1.172	0.100
1440.0	7.115	1.332	0.091
1800.3	7.053	1.698	0.136
2160.0	6.676	1.939	0.159
2880.0	5.985	2.734	0.206
3600.3	5.849	3.256	0.213
4320.0	4.864	3.615	0.286
5040.0	4.378	3.919	0.282
5760.3	3.828	4.105	0.332

$k_r = 2.42 \pm 0.19 \times 10^{-6}$, sec^{-1}.
$k_{MNT} = 1.99 \pm 0.11 \times 10^{-6}$, sec^{-1}.
$k_{X4} = 0.15 \pm 0.01 \times 10^{-6}$, sec^{-1}.
MNT from OA cleavage = 3.89%.
$k_{GO} = 1.91 \pm 0.11 \times 10^{-6}$, sec^{-1}.
$k_{OA} = 0.51 \pm 0.22 \times 10^{-6}$, sec^{-1}.

---

[a][MBT] = concentration of 1,5-anhydromannobiitol at reaction temperature, M x 10^3.
[b][MBT] = concentration of 1,5-anhydro-D-mannitol at reaction temperature, M x 10^3.
[c][X4] = concentration of 1,5-anhydro-D-iditol at reaction temperature, M x 10^3, calculated using MNT response factor.

Table 26. Degradation of 1,5-anhydromannobiitol (0.01M) in 2.501M NaOH at 181.29 ± 0.1°C.

Time, min	[MBT][a]	[MBT][b]	[X4][c]
0.0	10.886	0.173	0.000
60.4	10.364	0.601	0.036
120.4	9.636	1.026	0.075
180.0	9.201	1.382	0.095
240.0	8.877	1.825	0.138
360.4	7.860	2.549	0.195
480.0	6.898	3.022	0.234
600.4	6.234	3.783	0.298
720.0	5.537	4.232	0.298
960.0	4.729	4.871	0.377
1200.0	3.659	5.764	0.450
1440.0	2.882	6.079	0.475

k_r = 15.19 ± 0.43 x 10^{-6}, sec^{-1}.
k_{MNT} = 11.48 ± 0.34 x 10^{-6}, sec^{-1}.
k_{X4} = 0.92 ± 0.04 x 10^{-6}, sec^{-1}.
MNT from OA cleavage = 5.37%.
k_{GO} = 10.89 ± 0.34 x 10^{-6}, sec^{-1}.
k_{OA} = 4.30 ± 0.55 x 10^{-6}, sec^{-1}.

---

[a][MBT] = concentration of 1,5-anhydromannobiitol at reaction temperature, M x 10^3.
[b][MBT] = concentration of 1,5-anhydro-D-mannitol at reaction temperature, M x 10^3.
[c][X4] = concentration of 1,5-anhydro-D-iditol at reaction temperature, M x 10^3, calculated using MNT response factor.

Table 27. Degradation of 1,5-anhydromannobiitol (0.01M) in 2.507M NaOH at 191.86 ± 0.1°C.

Time, min	[MBT]a	[MBT]b	[X4]c
0.0	11.203	0.339	0.000
30.0	10.258	0.926	0.070
60.6	8.945	1.471	0.114
120.0	8.292	2.624	0.211
180.0	6.866	3.277	0.272
240.0	6.717	3.861	0.338
300.0	5.383	4.352	0.404
360.0	4.431	5.199	0.491
420.0	4.058	5.370	0.505
480.0	3.615	6.458	0.565
600.0	3.023	7.134	0.706
720.0	1.966	7.323	0.728

$k_r = 38.25 \pm 0.3 \times 10^{-6}$, sec^{-1}.
$k_{MNT} = 29.78 \pm 0.2 \times 10^{-6}$, sec^{-1}.
$k_{X4} = 3.00 \pm 0.20 \times 10^{-6}$, sec^{-1}.
MNT from OA cleavage = 5.51%.
$k_{GO} = 28.13 \pm 0.21 \times 10^{-6}$, sec^{-1}.
$k_{OA} = 10.12 \pm 0.34 \times 10^{-6}$, sec^{-1}.

---

a[MBT] = concentration of 1,5-anhydromannobiitol at reaction temperature, M x 10^3.
b[MBT] = concentration of 1,5-anhydro-D-mannitol at reaction temperature, M x 10^3.
c[X4] = concentration of 1,5-anhydro-D-iditol at reaction temperature, M x 10^3, calculated using MNT response factor.

Table 28. Degradation of 1,5-anhydromannobiitol (0.01M) in 1.5M NaOH and 1.0M NaOTs at 170.43°C.

Time, min	[MBT]a	[MBT]b	[X4]c
0.0	10.710	0.108	0.000
120.0	10.566	0.328	0.000
240.0	10.166	0.566	0.027
480.0	9.542	1.033	0.063
720.0	8.917	1.460	0.081
960.0	8.558	1.873	0.117
1440.0	7.552	2.547	0.166
2160.0	6.190	3.553	0.229
2880.0	5.234	4.452	0.291
3600.0	4.403	4.973	0.332

$k_r = 4.18 \pm 0.09 \times 10^{-6}$, sec^{-1}.
$k_{MNT} = 3.24 \pm 0.06 \times 10^{-6}$, sec^{-1}.
$k_{X4} = 0.226 \pm 0.008 \times 10^{-6}$, sec^{-1}.
MNT from OA cleavage = 4.14%.
$k_{GO} = 3.10 \pm 0.06 \times 10^{-6}$, sec^{-1}.
$k_{OA} = 1.08 \pm 0.11 \times 10^{-6}$, sec^{-1}.

---

a[MBT] = concentration of 1,5-anhydromannobiitol at reaction temperature, M x 10^3.
b[MBT] = concentration of 1,5-anhydro-D-mannitol at reaction temperature, M x 10^3.
c[X4] = concentration of 1,5-anhydro-D-iditol at reaction temperature, M x 10^3, calculated using MNT response factor.

Table 29. Degradation of 1,5-anhydromannobiitol (0.01M) in 1.0M NaOH and 1.5M NaOTs at 171.20°C.

Time, min	[MBT][a]	[MBT][b]	[X4][c]
0.0	10.506	0.084	0.000
120.0	10.067	0.288	0.031
240.0	9.892	0.500	--
480.0	9.212	0.904	0.057
720.0	8.850	1.366	0.081
1200.0	7.898	2.107	0.117
1680.0	6.923	2.606	0.175
2160.0	6.226	3.330	0.234
2880.0	5.404	4.223	0.283
3600.0	4.623	4.793	0.294
4320.0	3.890	5.373	0.317

$k_r = 3.79 \pm 0.1 \times 10^{-6}$, sec^{-1}.
$k_{MNT} = 2.95 \pm 0.07 \times 10^{-6}$, sec^{-1}.
$k_{X4} = 0.19 \pm 0.02 \times 10^{-6}$, sec^{-1}.
MNT from OA cleavage = 3.95%.
$k_{GO} = 2.83 \pm 0.07 \times 10^{-6}$, sec^{-1}.
$k_{OA} = 0.96 \pm 0.12 \times 10^{-6}$, sec^{-1}.

---

[a][MBT] = concentration of 1,5-anhydromannobiitol at reaction temperature, M x 10^3.
[b][MBT] = concentration of 1,5-anhydro-D-mannitol at reaction temperature, M x 10^3.
[c][X4] = concentration of 1,5-anhydro-D-iditol at reaction temperature, M x 10^3, calculated using MNT response factor.

Table 30. Degradation of 1,5-anhydromannobiitol (0.01M) in 0.5M NaOH and 2.0M NaOTs at 170.85°C.

Time, min	[MBT][a]	[MBT][b]	[X4][c]
0.0	9.407	0.081	0.000
180.0	9.178	0.261	0.000
360.0	8.899	0.454	0.000
720.0	8.585	0.818	0.031
1080.0	8.046	1.168	0.045
1440.0	7.650	1.541	0.094
2160.0	6.923	2.116	0.108
2880.0	6.190	2.749	0.148
3600.0	5.517	3.187	0.175
4320.0	5.013	3.670	0.198
5760.0	4.097	4.438	0.243
7200.0	3.148	5.079	0.296

$k_r = 2.49 \pm 0.06 \times 10^{-6}$, sec^{-1}.
$k_{MNT} = 2.01 \pm 0.02 \times 10^{-6}$, sec^{-1}.
$k_{X4} = 0.16 \pm 0.01 \times 10^{-6}$, sec^{-1}.
MNT from OA cleavage = 3.54%.
$k_{GO} = 1.94 \pm 0.02 \times 10^{-6}$, sec^{-1}.
$k_{OA} = 0.55 \pm 0.06 \times 10^{-6}$, sec^{-1}.

[a][MBT] = concentration of 1,5-anhydromannobiitol at reaction temperature, M x 10^3.
[b][MBT] = concentration of 1,5-anhydro-D-mannitol at reaction temperature, M x 10^3.
[c][X4] = concentration of 1,5-anhydro-D-iditol at reaction temperature, M x 10^3, calculated using MNT response factor.

Table 31. Degradation of 1,5-anhydromannobiitol (0.01M) in 0.5070M NaOH at 171.35 ± 0.1°C.

Time, min	[MBT]a	[MBT]b	[X4]c
0.0	10.809	0.099	0.000
360.0	10.422	0.431	0.000
720.0	9.883	0.845	0.040
1080.0	9.434	1.303	0.054
1440.0	9.012	1.712	0.076
2160.0	8.329	2.372	0.117
2890.0	7.412	3.028	0.148
3600.0	6.891	3.706	0.220
4320.0	6.155	4.187	0.252
5041.5	5.588	4.429	0.256
5760.0	5.310	5.171	0.270
6480.0	4.672	5.602	0.332
7200.0	4.205	5.894	0.364
7920.0	3.962	6.047	0.355

$k_r = 2.16 \pm 0.05 \times 10^{-6}$, sec^{-1}.
$k_{MNT} = 1.91 \pm 0.05 \times 10^{-6}$, sec^{-1}.
$k_{X4} = 0.122 \pm 0.009 \times 10^{-6}$, sec^{-1}.
MNT from OA cleavage = 3.81%.
$k_{GO} = 1.84 \pm 0.05 \times 10^{-6}$, sec^{-1}.
$k_{OA} = 0.32 \pm 0.07 \times 10^{-6}$, sec^{-1}.

---

a[MBT] = concentration of 1,5-anhydromannobiitol at reaction temperature, M x 10^3.
b[MBT] = concentration of 1,5-anhydro-D-mannitol at reaction temperature, M x 10^3.
c[X4] = concentration of 1,5-anhydro-D-iditol at reaction temperature, M x 10^3, calculated using MNT response factor.

Table 32. Degradation of 1,5-anhydromannobiitol (0.01M) in 1.506M NaOH and 1.10M SH^- at 171.65°C.

Time, min	[MBT][a], M x 10^3	[MNT][b], M x 10^3
0.0	10.069	0.102
120.0	9.721	0.377
240.0	9.200	0.668
480.0	8.598	1.155
720.0	7.844	1.617
960.0	7.245	2.046
1200.4	6.586	2.471
1440.4	6.222	2.808
2160.0	5.153	3.535
2880.0	4.111	4.465
3600.0	3.311	4.861
5040.0	2.192	5.753

$k_r = 5.03 \pm 0.1 \times 10^{-6}$, sec^{-1}.
$k_{MNT} = 3.59 \pm 0.1 \times 10^{-6}$, sec^{-1}.
MNT from OA cleavage = 0.07%.
$k_{GO} = 3.59 \pm 0.10 \times 10^{-6}$, sec^{-1}.
$k_{OA} = 1.44 \pm 0.18 \times 10^{-6}$, sec^{-1}.

---

[a][MBT] = concentration of 1,5-anhydromannobiitol at reaction temperature, M x 10^3.
[b][MBT] = concentration of 1,5-anhydro-D-mannitol at reaction temperature, M x 10^3.

APPENDIX V

CALCULATION OF THE FRACTIONS OF GLYCOSYL-OXYGEN AND OXYGEN-AGLYCON CLEAVAGE FROM THE AMOUNT OF OXYGEN-18 INCORPORATION IN 1,5-ANHYDRO-D-MANNITOL

The product mixture from the degradation of 1,5-anhydromannobiitol in ^{18}O-enriched liquors was derivatized with TFA and analyzed via NCI gc/ms. Molecular ion peaks were found for each isotopic species of 1,5-anhydro-D-mannitol and iditol. To calculate the fractions of GO and OA bond cleavage from these peak areas, it was necessary to take into account the natural isotopes present, the isotopic distribution of oxygen atoms in the liquor, and the isotopes present in the products. To do this, the problem was set up as shown in Scheme 1.

			OH	O17H	O18H
M		R	N	NO17	NO18
MC13		RC13	NC13	NC13O17	NC13O18
MO17	$\xleftarrow{b}$	RO17	NO17	NO17O17	NO17O18
MO18		RO18	NO18	NO18NO17	NO18O18
MC13O17		RC13O17	NC13O17	NC13O17O17	NC13O17O18
MC13O18		RC13O18	NC13O18	NC13O18O17	NC13O18O18
MTOT		RTOT		NTOT	

where R = number of mannobiitol molecules which degrade to mannitol.
M = number of mannitol molecules resulting from GO bond cleavage.
N = number of mannitol molecules resulting from OA bond cleavage.
C13, O17, and O18 represent the presence of a carbon-13, oxygen-17, or oxygen-18 atom, respectively.
a = fraction of OA bond cleavage.
b = fraction of GO bond cleavage.
TOT = total number of molecules.

Some reactant molecules naturally contain ^{13}C, ^{17}O, and ^{18}O atoms. Cleavage of the GO bond will produce 1,5-anhydro-D-mannitol with the same

isotopic distribution present in 1,5-anhydromannobiitol. This can be expressed by Eq. (35a-f).

$$b * R = M \tag{35a}$$

$$b * RC13 = MC13 \tag{35b}$$

$$b * RO17 = MO17 \tag{35c}$$

$$b * RO18 = MO18 \tag{35d}$$

$$b * RC13O17 = MC13O17 \tag{35e}$$

$$b * RC13O18 = MC13O18 \tag{35f}$$

Those 1,5-anhydromannobiitol molecules which cleave at the OA bond must react with a hydroxide ion from solution to form mannitol. Depending upon whether the mannobiitol intermediate happens to react with a hydroxide ion which contains ^{16}O, ^{17}O, or ^{18}O, the mannitol formed may be enriched in ^{17}O or ^{18}O, as shown in Scheme 1. The fractions of $^{16}OH^-$, $^{17}OH^-$, and $^{18}OH^-$ present (c, d, and e, respectively), determine the chance that an intermediate will react with a given species. For example, an unlabelled mannobiitol molecule, R, could react with $^{16}OH^-$ to give unlabelled mannitol (N), with $^{17}OH^-$ to give mannitol containing one ^{17}O atom (NO17), or with $^{18}OH^-$ to give mannitol containing one ^{18}O atom (NO18). The chance of each of these reactions occurring is expressed by Eq. (36a-c).

$$a * R * c = N \tag{36a}$$

$$a * R * d = NO17 \tag{36b}$$

$$a * R * e = NO18 \tag{36c}$$

Similar equations can be written for each isotopic mannobiitol species.

In the mass spectra, peaks were found at M/E values of 548, 549, 550, and 551. These are due to a mixture of M and N species as shown in Eq. (37a-d).

$$M548' = M + N \tag{37a}$$

$$M549' = MC13 + MO17 + NC13 + NO17 \tag{37b}$$

$$M550' = MO18 + MC13O17 + NO18 + NC13O17 + NO17O17 \tag{37c}$$

$$M551' = MC13O18 + NC13O18 + NO18O17 \tag{37d}$$

Values for the M and N quantities cannot be measured separately. When Eq. (35) and (36) are substituted into Eq. (37), the following set of equations results.

$$M548' = (b*R) + (a*R*c) \tag{38a}$$

$$M549' = (a*RC13*c) + (a*R*d) + (a*RO17*c) + (b*RC13) + (b*RO17) \tag{38b}$$

$$M550' = (a*R*e) + (a*RO18*c) + (a*RC13*d) + (a*RC13O17*c) + (a*RO17*d) + (b*RO18) + (b*RC13O17*c) \tag{38c}$$

$$M551' = (a*RC13*e) + (a*RC13O18*c) + (A*RO17*d) + (b*RC13O18) \tag{38d}$$

To solve these equations for a and b, it is necessary to determine the values of c, d, and e, the fractions of each isotopic oxygen species present in the liquor, and the isotopic distribution in the reactant, 1,5-anhydromannobiitol.

Liquor

To determine the fractions of the various isotopic hydroxide ions present in the liquor, the liquors were analyzed on the mass spectrometer. Ions were found at masses of 16 through 20. These must be due to the species shown:

$$M16 = O \tag{39a}$$

$$M17 = OH + O17 \tag{39b}$$

$$M18 = H_2O + O17H + O18 \tag{39c}$$

$$M19 = H_2O17 + O18H \tag{39d}$$

$$M20 = H_2O18 \tag{39e}$$

where M16 through M20 = number of counts observed at that mass.

O, OH, H_2O, etc. = number of molecules of that type.

To solve for the fractions of the various species, let:

X = number of all O16 containing species

Y = number of all O17 containing species

Z = number of all O18 containing species

α = fraction present as H_2O

β = fraction present as OH

δ = fraction present as O

Substituting these values into (39a-e) gives:

$$M16 = \delta * X \tag{40a}$$

$$M17 = \beta * X + \delta * Y \tag{40b}$$

$$M18 = \alpha * X + \beta * Y + \delta * Z \tag{40c}$$

$$M19 = \alpha * Y + \beta * Z \tag{40d}$$

$$M20 = \alpha * Z \tag{40e}$$

By definition:

$$\alpha + \beta + \delta = 1 \tag{41}$$

This is a system of 6 equations and 6 unknowns and can therefore be solved by successive approximation.

Now the fraction of each isotopic species of oxygen present can be calculated:

$$HTOT = X + Y + Z \tag{42}$$

$$\frac{X}{HTOT} = c = \text{fraction of unlabelled molecules} \tag{43}$$

$$\frac{Y}{HTOT} = d = \text{fraction of O17 labelled molecules} \tag{44}$$

$$\frac{Z}{HTOT} = e = \text{fraction of O18 labelled molecules} \qquad (45)$$

Unenriched (Natural) Mannitol

The natural isotopic distribution in 1,5-anhydromannobiitol could not be measured because no molecular ions were found in its mass spectrum. Instead, the isotopic distribution of natural mannitol was measured in a separate experiment and assumed to be the same as that of mannobiitol.

The mass spectrum of natural mannitol contained four molecular ion peaks. These come from the species shown in Eq. (46a-d).

$$M548 = M \qquad (46a)$$

$$M549 = MC13 + MO17 \qquad (46b)$$

$$M550 = MO18 + MC13O17 \qquad (46c)$$

$$M551 = MC13O18 \qquad (46d)$$

where M548 through M551 = number of counts observed at that mass

M = number of MNT molecules containing no isotopes

MO17 = number of MNT molecules containing one O17 atom

MO18 = number of MNT molecules containing one O18 atom

MC13 = number of MNT molecules containing one C13 atom

MC13O17 = number of MNT molecules which contain a C13 and O17 atom

MC13O18 = number of MNT molecules which contain a C13 and O18 atom

To solve this set of equations, let

α = the fraction of molecules containing a carbon-13 atom,

$$\alpha = \frac{MC13}{M} = \frac{MC13O17}{MO17} = \frac{MC13O18}{MO18} \qquad (47)$$

Substituting (47) into Eq. (46) gives:

$$M548 = M \tag{48a}$$

$$M549 = \alpha * M + M017 \tag{48b}$$

$$M550 = M018 + \alpha * M017 \tag{48c}$$

$$M551 = \alpha * M018 \tag{48d}$$

This is a system of 4 equations and 4 unknowns so it can be solved by successive approximation.

Once values for variables in Eq. (48) have been determined, the distribution of oxygen isotopes can be calculated.

$$MTOT = M + MC13 + M017 + M018 + MC13017 + MC13018 \tag{49}$$

$$= \text{total number of mannitol molecules}$$

and

$$\frac{M017}{MTOT} = \beta = \text{fraction of MNT molecules which naturally contain an O17 atom} \tag{50}$$

$$\frac{M018}{MTOT} = \Phi = \text{fraction of MNT molecules which naturally contain an O18 atom} \tag{51}$$

$$\frac{M}{MTOT} = \delta = \text{fraction of MNT molecules which naturally contain no isotopes} \tag{52}$$

Isotopic Distribution in 1,5-Anhydromannobiitol

This same isotopic distribution can be applied to 1,5-anhydromannobiitol. To do this, choose an arbitrary total number of 1,5-anhydromannobiitol molecules (i.e., 100) to use as a basis.

$$RTOT = 100 = \text{total number of mannobiitol molecules}$$

$$= R + RC13 + R017 + R018 + RC13017 + RC13018 \tag{53}$$

The isotope fractions determined for natural mannitol can now be used to calculate the relative number of each species of mannobiitol present.

$$\frac{RO17}{RTOT} = \beta = \text{fraction of mannobiitol molecules which contain an O17 atom} \quad (54)$$

or

$$RO17 = \beta * RTOT \quad (54b)$$

Likewise

$$RO18 = \Phi * RTOT \quad (55)$$

$$R = \delta * RTOT \quad (56)$$

$$RC13 = \alpha * R \quad (57)$$

$$RC13017 = \alpha * RO17 \quad (58)$$

$$RC13018 = \alpha * RO18 \quad (59)$$

Overall

Except for a and b, the fractions of cleavage at the OA and GO bond, the variables in Eq. (38a-d) have all been calculated. Since a + b equals 1, it is possible to solve any of these equations for a or b. This yields the fraction of cleavage occurring at each bond. Program 7 (Appendix I) performs these calculations.

APPENDIX VI

DERIVATION OF RECIPROCAL HYDROXIDE-RATE RELATIONSHIP FOR GLYCOSYL-OXYGEN BOND CLEAVAGE IN 1,5-ANHYDROMANNOBIITOL VIA A MIXED $S_N1cB(2')$-RO/S_N1 MECHANISM

The reaction scheme for cleavage of the glycosyl-oxygen bond in 1,5-anhydromannobiitol via a mixed $S_N1cB(2')$-ro/S_N1 mechanism is shown in Eq. (60).

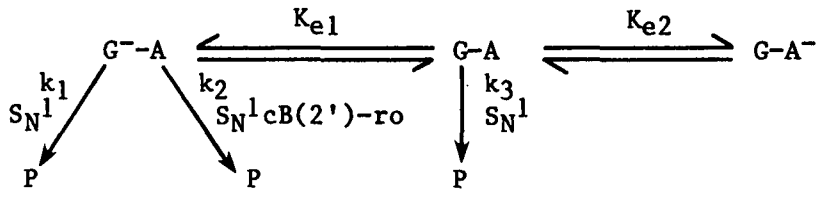

(60)

where G-A = unionized mannobiitol which undergoes glycosyl-oxygen bond cleavage
G^--A = mannobiitol with an ionized hydroxyl on the glycon which undergoes glycosyl-oxygen bond cleavage
G-A^- = mannobiitol with an ionized hydroxyl on the aglycon which undergoes glycosyl-oxygen bond cleavage
k_1 = rate constant for cleavage of G^--A via an S_N1 mechanism
k_2 = rate constant for cleavage of G^--A via an $S_N1cB(2')$-ro mechanism
k_3 = rate constant for cleavage of G-A via an S_N1 mechanism
P = products from glycosyl-oxygen bond cleavage
K_{e1} = equilibrium constant between G-A and G^--A
K_{e2} = equilibrium constant between G-A and G-A^-

The equilibrium constants can be expressed as:

$$K_{e1} = \frac{[G^-\text{-A}]}{[\text{G-A}][OH^-]} \tag{61a}$$

$$[\text{G-A}] = K_{e1}[\text{G-A}][OH^-] \tag{61b}$$

$$K_{e2} = \frac{[\text{G-A}^-]}{[\text{G-A}][OH^-]} \tag{62a}$$

$$[\text{G-A}^-] = K_{e2}[\text{G-A}][OH^-] \tag{62b}$$

where $[OH^-]$ = concentration of hydroxide ion.

The appearance of products is described by Eq. (63):

$$\frac{d[P]}{dt} = k_1[G^-\text{-}A] + k_2[G^-\text{-}A] + k_3[G\text{-}A] \qquad (63)$$

where [P] = concentration of products at time, t.

The concentration of glycoside at any time can be expressed as:

$$[G\text{-}A]_t = [G\text{-}A]_o - [G^-\text{-}A]_t - [G\text{-}A^-]_t - [P]_t \qquad (64)$$

where $[G\text{-}A]_t$ = concentration of neutral glycoside which degrades via glycosyl-oxygen bond cleavage at any time, t

$[G\text{-}A]_o$ = initial concentration of glycoside which undergoes glycosyl-oxygen bond cleavage

$[G^-\text{-}A]_t$, $[G\text{-}A^-]_t$ = concentrations of conjugate bases of the glycoside at any time, t

$[P]_t$ = concentrations of products of glycosyl-oxygen bond cleavage at any time, t

Substituting Eq. (61) and (62) into (64) gives:

$$[G\text{-}A]_t = [G\text{-}A]_o - (K_{e1}[G\text{-}A][OH^-]) - (K_{e2}[G\text{-}A][OH^-]) - [P]_t \qquad (65)$$

Solving Eq. (65) for [G-A] yields:

$$[G\text{-}A] = \frac{[G\text{-}A]_o - [P]_t}{\{1 + K_{e1}[OH^-] + K_{e2}[OH^-]\}} \qquad (65b)$$

When (61) is substituted into (63), Eq. (66) results.

$$\frac{d[P]}{dt} = k_1K_{e1}\,[G\text{-}A][OH^-] + k_2K_{e1}\,[G\text{-}A][OH^-] + k_3\,[G\text{-}A] \qquad (66)$$

Rearranging gives:

$$\frac{d[P]}{dt} = [G\text{-}A]\,\{k_1K_{e1}[OH^-] + k_2K_{e1}\,[OH^-] + k_3\} \qquad (66b)$$

An expression for [G-A] is given by Eq. (65b). Use this in Eq. (66b) to obtain an integratable expression for product formation.

$$\frac{d[P]}{dt} = \frac{([G\text{-}A]_o - [P]_t}{(1 + K_{e1}[OH^-] + K_{e2}[OH^-])} * (k_1K_{e1}[OH^-] + k_2K_{e1}[OH^-] + k_3 \quad (67)$$

To simplify Eq. (67), let:

$$N = k_1K_{e1}[OH^-] + k_2K_{e1}[OH^-] + k_3 \quad (68)$$

and

$$D = 1 + K_{e1}[OH^-] + K_{e2}[OH^-] \quad (69)$$

Substituting (68) and (69) into (67) simplifies it to:

$$\frac{d[P]}{dt} = \frac{N}{D} * ([G\text{-}A]_o\text{-}[P]) \quad (70)$$

Equation (70) can be rearranged to:

$$\frac{d[P]}{([G\text{-}A]_o - [P])} = \frac{N}{D}\, dt \quad (70b)$$

Integrating yields:

$$-\log([G\text{-}A]_o - [P]) = \frac{N}{D} * t + C \quad (71)$$

When t = o, [P] = 0, so:

$$C = -\log([G\text{-}A]_o) \quad (72)$$

Plugging (72) into (71) and rearranging gives:

$$\log \frac{[G\text{-}A]_o - [P]}{[G\text{-}A]_o} = -\frac{N}{D} * t \quad (73)$$

Letting $[R]' = [G\text{-}A]_o - [P]$ and substituting into Eq. (73) gives:

$$\log \frac{[R]'}{[G\text{-}A]_o} = -\frac{N}{D} * t \tag{74}$$

and

$$\log \frac{[R]'}{[G\text{-}A]_o} = -k_r t \tag{75}$$

Comparing Eq. (74) and (75) and expanding N and D according to Eq. (68) and (69) shows that:

$$k_r = \frac{\{k_1 K_{e1}[OH^-] + k_2 K_{e1}[OH^-] + k_3\}}{\{1 + K_{e1}[OH^-] + K_{e2}[OH^-]\}} \tag{76}$$

Assuming that $k_3 <<< k_1$ and k_2 reduces Eq. (76) to:

$$k_r = \frac{(k_1 + k_2)\ K_{e1}[OH^-]}{1 + (K_{e1} + K_{e2})[OH^-]} \tag{77}$$

Which when inverted gives:

$$\frac{1}{k_r} = \frac{1}{K_{e1}\ (k_1 + k_2)} * \frac{1}{[OH^-]} + \frac{(K_{e1} + K_{e2})}{(k_1 + k_2)K_{e1}} \tag{78}$$

Equation (78) predicts a linear relationship between $1/k_r$ and $1/[OH^-]$.